PHYSICAL REVIEW
LETTERS

VOLUME 4 APRIL 1, 1960 NUMBER 7

APPARENT WEIGHT OF PHOTONS*

R. V. Pound and G. A. Rebka, Jr.
Lyman Laboratory of Physics, Harvard University, Cambridge, Massachusetts
(Received March 9, 1960)

As we proposed a few months ago,[1] we have now measured the effect, originally hypothesized by Einstein,[2] of gravitational potential on the apparent frequency of electromagnetic radiation by using the sharply defined energy of recoil-free γ rays emitted and absorbed in solids, as discovered by Mössbauer.[3] We have already reported[4] a detailed study of the shape and width of the line obtained at room temperature for the 14.4-kev, 0.1-microsecond level in Fe^{57}. Particular attention was paid to finding the conditions required to obtain a narrow line. We found that the line had a Lorentzian shape with a fractional full-width at half-height of 1.13×10^{-12} when the source was carefully prepared according to a prescription developed from experience. We have also investigated the 93-kev, 9.4-microsecond level of Zn^{67} at liquid helium and liquid nitrogen temperatures using several combinations of source and absorber environment, but have not observed a usable resonant absorption. That work will be reported later. The fractional width and intensity of the absorption in Fe^{57} seemed sufficient to measure the gravitational effect in the laboratory.

As a preliminary, we sought possible sources of systematic error that would interfere with measurements of small changes in frequency using this medium. Early in our development of the instrumentation necessary for this experiment, we concluded that there were asymmetries in, or frequency differences between, the lines of given combinations of source and absorber which vary from one combination to another. Thus it is absolutely necessary to measure a change in the relative frequency that is produced by the perturbation being studied. Observation of a frequency difference between a given source and absorber cannot be uniquely attributed to this perturbation. More recently, we have discovered and explained a variation of frequency with temperature of either the source or absorber.[5] We conclude that the temperature difference between the source and absorber must be accurately known and its effect considered before any meaning can be extracted from even a change observed when the perturbation is altered.

The basic elements of the apparatus finally developed to measure the gravitational shift in frequency were a carefully prepared source containing 0.4 curie of 270-day Co^{57}, and a carefully prepared, rigidly supported, iron film absorber. Using the results of our initial experiment, we requested the Nuclear Science and Engineering Corporation to repurify their nickel cyclotron target by ion exchange to reduce cobalt carrier. Following the bombardment, in a special run in the high-energy proton beam of the high-current cyclotron at the Oak Ridge National Laboratory, they electroplated the separated Co^{57} onto one side of a 2-in. diameter, 0.005-in. thick disk of Armco iron according to our prescription. After this disk was received, it was heated to 900°-1000°C for one hour in a hydrogen atmosphere[6] to diffuse the cobalt into the iron foil about 3×10^{-5} cm.

The absorber made by Nuclear Metals Inc., was composed of seven separate units. Each

unit consisted of about 80 mg of iron, enriched in Fe^{57} to 31.9%, electroplated onto a polished side of a 3-in. diameter, 0.040-in. thick disk of beryllium. The electroplating technique required considerable development to produce films with absorption lines of width and strength that satisfied our tests. The films finally accepted, resonantly absorbed about 1/3 the recoil-free γ rays from our source. Each unit of the absorber was mounted over the 0.001-in. Al window of a 3 in. $\times$ 1/4 in. NaI(Tl) scintillation crystal integrally mounted on a Dumont 6363 multiplier phototube. The multiplier supply voltages were separately adjusted to equalize their conversion gains, and their outputs were mixed.

The required stable vertical baseline was conveniently obtained in the enclosed, isolated tower of the Jefferson Physical Laboratory.[7] A statistical argument suggests that the precision of a measurement of the gravitational frequency shift should be independent of the height. Instrumental instability but more significantly the sources of systematic error mentioned above are less critical compared to the larger fractional shifts obtained with an increased height. Our net operating baseline of 74 feet required only conveniently realizable control over these sources of error.

The absorption of the 14.4-kev γ ray by air in the path was reduced by running a 16-in. diameter, cylindrical, Mylar bag with thin end windows and filled with helium through most of the distance between source and absorber. To sweep out small amounts of air diffusing into the bag, the helium was kept flowing through it at a rate of about 30 liters/hr.

The over-all experiment is described by the block diagram of Fig. 1. The source was moved sinusoidally by either a ferroelectric or a moving-coil magnetic transducer. During the quarter of the modulation cycle centered about the time of maximum velocity the pulses from the scintillation spectrometer, adjusted to select the 14.4-kev γ-ray line, were fed into one scaler while, during the opposite quarter cycle, they were fed into another. The difference in counts recorded was a measure of the asymmetry in, or frequency-shift between, the emission and absorption lines. As a precaution the relative phase of the gating pulses and the sinusoidal modulation were displayed continuously. The data were found to be insensitive to phase changes much larger than the drifts of phase observed.

A completely duplicate system of electronics, controlled by the same gating pulses, recorded

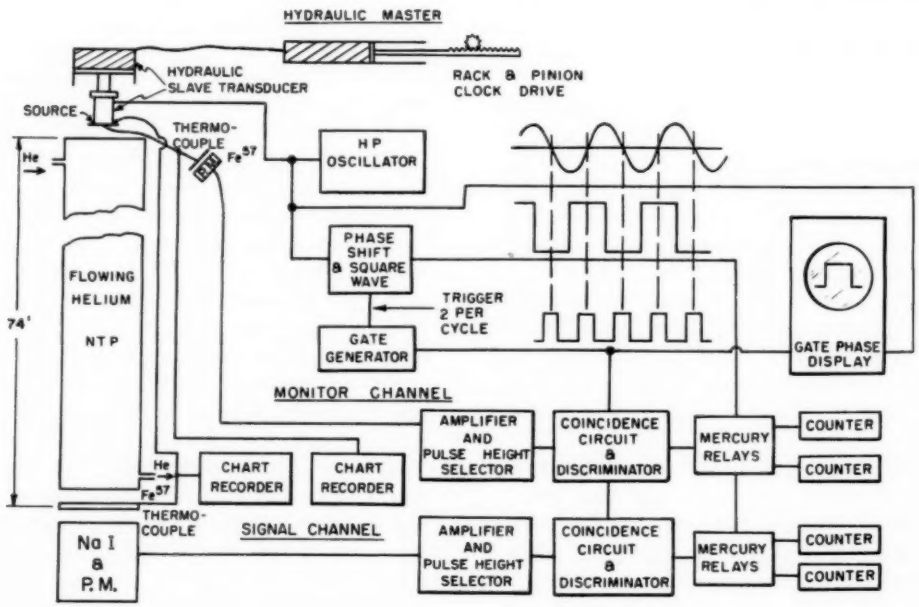

FIG. 1. A block diagram of the over-all experimental arrangement. The source and absorber-detector units were frequently interchanged. Sometimes a ferroelectric and sometimes a moving-coil magnetic transducer was used with frequencies ranging from 10 to 50 cps.

data from a counter having a 1-in. diameter, 0.015-in. thick NaI(Tl) scintillation crystal covered by an absorber similar to the main absorber. This absorber and crystal unit was mounted to see the source from only three feet away. This monitor channel measured the stability of the over-all modulation system, and, because of its higher counting rate, had a smaller statistical uncertainty.

The relation between the counting rate difference and relative frequency shifts between the emission and absorption lines was measured directly by adding a Doppler shift several times the size of the gravitational shift to the emission line. The necessary constant velocity was introduced by coupling a hydraulic cylinder of large bore carrying the transducer and source to a master cylinder of small bore connected to a rack-and-pinion driven by a clock.

Combining data from two periods having Doppler shifts of equal magnitude, but opposite sign, allowed measurement of both sensitivity and relative frequency shift. Because no sacrifice of valuable data resulted, the sensitivity was calibrated about 1/3 of the operating time which was as often as convenient without recording the data automatically. In this way we were able to eliminate errors due to drifts in sensitivity such as would be anticipated from gain or discriminator drift, changes in background, or changes in modulation swing.

The second order Doppler shift resulting from lattice vibrations required that the temperature difference between the source and absorber be controlled or monitored. A difference of 1°C would produce a shift as large as that sought, so the potential difference of a thermocouple with one junction at the source and the other at the main absorber was recorded. An identical system was provided for the monitor channel. The recorded temperature data were integrated over a counting period, and the average determined to 0.03°C. The temperature coefficient of frequency which we have used to correct the data, was calculated from the specific heat of a lattice having a Debye temperature of 420°K. Although at room temperature this coefficient is but weakly dependent on the Debye temperature, residual error in the correction for, or control of, the temperature difference limits the ability to measure frequency shifts and favors the use of a large height difference for the gravitational experiment.

Data typical of those collected are shown in Table I. The right-hand column is the data after correction for temperature difference. All data are expressed as fractional frequency shift $\times 10^{15}$. The difference of the shift seen with γ rays rising and that with γ rays falling should be the result of gravity. The average for the two directions of travel should measure an effective shift of other origin, and this is about four times the difference between the shifts. We confirmed that this shift was an inherent property of the particular combination of source and absorber by measuring the shift for each absorber unit in turn, with temperature correction, when it was six inches from the source. Although this test was not exact because only about half the area of each absorber was involved, the weighted mean shift from this test for the combination of all absorber units agreed well with that observed in the main experiment. The individual fractional frequency shifts found for these, for the monitor absorber, as well as for a 11.7-mg/cm^2 Armco iron foil, are displayed in Table II. The considerable variation among them is as striking as the size of the weighted mean shift. Such shifts could result from differences in a range of about 11% in effective Debye temperature through producing differences in net second order Doppler effect. Other explanations based on hyperfine structure including electric quadrupole interactions are also plausible. Although heat treatment might be expected to change these shifts for the iron-plated beryllium absorbers, experience showed that the line width was materially increased by such treatment, probably owing to interdiffusion. The presence of a significant shift for even the Armco foil relative to the source, both of which had received heat treatments, suggests that it is unlikely one would have, without test, a shift of this sort smaller than the gravitational effect expected in even our "two-way" baseline of 148 feet. The apparently fortuitous smallness of the shift of the monitor absorber relative to our source corresponds to the shift expected for about 30 feet of height difference.

Recently Cranshaw, Schiffer, and Whitehead[8] claimed to have measured the gravitational shift using the γ ray of Fe^{57}. They state that they believe their 43% statistical uncertainty represents the major error. Two much larger sources of error apparently have not been considered: (1) the temperature difference between the source and absorber, and (2) the frequency difference inherent in a given combination of source and absorber. From the above discussion, only 0.6°C of temperature difference would produce a shift

Table I. Data from the first four days of counting. The data are expressed as fractional frequency differences between source and absorber multiplied by 10^{15}, as derived from the appropriate sensitivity calibration. The negative signs mean that the γ ray has a frequency lower than the frequency of maximum absorption at the absorber.

Period	Shift observed	Temperature correction	Net shift
	Source at bottom		
Feb. 22, 5 p.m.	-11.5 ± 3.0	-9.2	-20.7 ± 3.0
	-16.4 ± 2.2[a]	-5.9	-22.3 ± 2.2
	-13.8 ± 1.3	-5.3	-19.1 ± 1.3
	-11.9 ± 2.1[a]	-8.0	-19.9 ± 2.1
	-8.7 ± 2.0[a]	-10.5	-19.2 ± 2.0
Feb. 23, 10 p.m.	-10.5 ± 2.0	-10.6	-21.0 ± 2.0
		Weighted average =	-19.7 ± 0.8
	Source at top		
Feb. 24, 0 a.m.	-12.0 ± 4.1	-8.6	-20.6 ± 4.1
	-5.7 ± 1.4	-9.6	-15.3 ± 1.4
	-7.4 ± 2.1[a]	-7.4	-14.8 ± 2.1
	-6.5 ± 2.1[a]	-5.8	-12.3 ± 2.1
	-13.9 ± 3.1[a]	-7.5	-21.4 ± 3.1
	-6.6 ± 3.0	-5.7	-12.3 ± 3.0
Feb. 25, 6 p.m.	-6.5 ± 2.0[a]	-8.9	-15.4 ± 2.0
	-10.0 ± 2.6	-7.9	-17.9 ± 2.6
		Weighted average =	-15.5 ± 0.8
		Mean shift =	-17.6 ± 0.6
		Difference of averages =	-4.2 ± 1.1

[a]These data were taken simultaneously with a sensitivity calibration.

Table II. Data on asymmetries of various absorbers in apparent fractional frequency shift multiplied by 10^{15}. In the third column we tabulate the Debye temperature increase of the absorber above that of the source which could account for the shift.

Absorber	$(\Delta\nu/\nu)\times 10^{15}$	$\Delta\theta_D$ in °K
No. 1	-8.4 ± 2.5	$+15 \pm 4$
No. 2	-24 ± 3.5	$+41 \pm 6$
No. 3	-28 ± 3.5	$+48 \pm 6$
No. 4	-19 ± 3.5	$+33 \pm 6$
No. 5	-24 ± 3.5	$+41 \pm 6$
No. 6	-17 ± 2.5	$+29 \pm 4$
No. 7	-19 ± 3.5	$+33 \pm 6$
Weighted mean of No. 1-No. 7	-19 ± 3.0	$+33 \pm 5$
Monitor absorber	$+0.55 \pm 0.15$	-0.95 ± 0.26
Armco foil	$+10 \pm 3.5$	-17 ± 6

as large as the whole effect observed. Their additional experiment at the shortened height difference of three meters does not, without concomitant temperature data, resolve the question of inherent frequency difference. Their stated disappointment with the over-all line width observed would seem to add to the probability of existence of such a shift. They mention this broadening in connection with its possible influence on the sensitivity, derived rather than measured, owing to a departure from Lorentzian shape. Clearly such a departure is even more important in allowing asymmetry.

Our experience shows that no conclusion can be drawn from the experiment of Cranshaw et al.

If the frequency-shift inherent in our source-absorber combination is not affected by inversion of the relative positions, the difference between shifts observed with rising and falling γ rays measures the effect of gravity. All data collected since recognizing the need for temperature correction, yield a net fractional shift, $-(5.13 \pm 0.51) \times 10^{-15}$. The error assigned is the rms statistical deviation including that of independent sensitivity calibrations taken as representative of their respective periods of operation. The shift observed agrees with -4.92×10^{-15}, the predicted gravitational shift for this "two-way" height difference.

Expressed in this unit, the result is

$$(\Delta\nu)_{exp}/(\Delta\nu)_{theor} = +1.05 \pm 0.10,$$

where the plus sign indicates that the frequency increases in falling, as expected.

These data were collected in about 10 days of operation. We expect to continue counting with some improvements in sensitivity, and to reduce the statistical uncertainty about fourfold. With our present experimental arrangement this should result in a comparable reduction in error in the measurement since we believe we can take adequate steps to avoid systematic errors on the resulting scale. A higher baseline or possibly a narrower γ ray would seem to be required to extend the precision by a factor much larger than this.

We wish to express deep appreciation for the generosity, encouragement, and assistance with details of the experiment accorded us by our colleagues and the entire technical staff of these laboratories during the three months we have been preoccupied with it.

---

*Supported in part by the joint program of the Office of Naval Research and the U. S. Atomic Energy Commission and by a grant from the Higgins Scientific Trust.

[1]R. V. Pound and G. A. Rebka, Jr., Phys. Rev. Letters 3, 439 (1959).

[2]A. Einstein, Ann. Physik 35, 898 (1911).

[3]R. L. Mössbauer, Z. Physik 151, 124 (1958); Naturwissenschaften 45, 538 (1958); Z. Naturforsch. 14a, 211 (1959).

[4]R. V. Pound and G. A. Rebka, Jr., Phys. Rev. Letters 3, 554 (1959).

[5]R. V. Pound and G. A. Rebka, Jr., Phys. Rev. Letters 4, 274 (1960).

[6]We wish to thank Mr. F. Rosebury of the Research Laboratory of Electronics, Massachusetts Institute of Technology, for providing his facilities for this treatment.

[7]See E. H. Hall, Phys. Rev. 17, 245 (1903), first paragraph.

[8]T. E. Cranshaw, J. P. Schiffer, and A. B. Whitehead, Phys. Rev. Letters 4, 163 (1960).

TEMPERATURE-DEPENDENT SHIFT OF γ RAYS EMITTED BY A SOLID

B. D. Josephson
Trinity College, Cambridge, England
(Received March 11, 1960)

Recent experiments by Mössbauer[1] have shown that when low-energy γ rays are emitted from nuclei in a solid a certain proportion of them are unaffected by the Doppler effect. It is the purpose of this Letter to show that they are nevertheless subject to a temperature-dependent shift to lower energy which can be attributed to the relativistic time dilatation caused by the motion of the nuclei.

Let us regard the solid as a system of interacting atoms with the Hamiltonian

$$H = \sum p_i^2/2m_i + V(r_1, r_2, \cdots).$$

The Mössbauer effect is due to those processes in which the phonon occupation numbers do not change. It might appear that in such cases the energy of the solid is unaltered, but this is not so, as the nucleus which emits the γ ray changes its mass, and this affects the lattice vibrations. Suppose the nucleus of the ith atom emits a γ ray of energy E, its mass changing by $\delta m_i = -E/c^2$.

The change in energy, δE, of the solid is given by

$$\delta E = \langle \Delta H \rangle = \delta \langle p_i^2/2m_i \rangle = -\delta m_i \langle p_i^2/2m_i^2 \rangle$$
$$= (\delta m_i/m_i) T_i = (E/m_i c^2) T_i,$$

where T_i is the expectation value of the kinetic energy of the ith atom. The energy of the γ ray must accordingly be reduced by δE so there is a shift of relative magnitude $\delta E/E = T_i/m_i c^2$. The same formula can be deduced by regarding the shift as due to a relativistic time dilatation.

To estimate T_i we make the following assumptions: (i) The atoms all have the same mass, and the kinetic energy is equally distributed among them. (ii) The kinetic energy is half the total lattice energy, i.e., we assume that the forces coupling the atoms are harmonic. Under these assumptions $T_i/m_i = \frac{1}{2}U$, where U is the lattice energy per unit mass. The relative shift is thus given by $\delta E/E = U/2c^2$. For Fe at 300°K

this has the value 8×10^{-13}. Clearly a compensating shift would occur for absorption provided source and absorber were identical and at the same temperature. A small difference in temperature between source and absorber leads to a relative shift per degree given by $\delta E/E = C_p/2c^2$ where C_p is the specific heat. For Fe at 300°K this is 2.2×10^{-15}/°K. This is sufficient for it to be necessary to take it into account in accurate experiments using the resonance absorption of γ rays, such as those to measure the gravitational red shift.[2,3]

I would like to thank Dr. Ziman, Professor O. R. Frisch, and Dr. W. Marshall for helpful discussions.

[1]R. L. Mössbauer, Z. Physik 151, 124 (1958).
[2]R. V. Pound and G. A. Rebka, Phys. Rev. Letters 3, 554 (1959).
[3]T. E. Cranshaw, J. P. Schiffer, and A. B. Whitehead, Phys. Rev. Letters 4, 163 (1960).

UPPER LIMIT FOR THE ANISOTROPY OF INERTIAL MASS FROM NUCLEAR RESONANCE EXPERIMENTS*

V. W. Hughes, H. G. Robinson, and V. Beltran-Lopez
Gibbs Laboratory, Yale University, New Haven, Connecticut
(Received March 2, 1960)

Mach's principle states that the inertial mass of a body is determined by the total distribution of matter in the universe; if the matter distribution is not isotropic, it is conceivable that the mass of a body depends on its direction of acceleration and is a tensor rather than a scalar quantity. Thus the matter in our galaxy is not distributed isotropically with respect to the earth, and hence the mass of a body on the earth may depend on the direction of its acceleration with respect to the direction towards the center of our galaxy. Cocconi and Salpeter[1] have proposed that the total inertial mass of a body on the earth be considered the sum of an isotropic part m and an anisotropic part Δm, and that the contribution to the mass of a body on the earth due to a mass $\mathfrak{M}$ a distance r away from the body is proportional to $\mathfrak{M}/r^{\nu}$ $(0 \leq \nu \leq 1)$. The ratio of Δm, due to a mass $\mathfrak{M}$ a distance r away, to m, due to the total mass in the universe, is

$$\frac{\Delta m}{m} = \frac{\mathfrak{M}}{r^{\nu}} \frac{3-\nu}{4\pi\rho R^{(3-\nu)}}, \qquad (1)$$

in which ρ = average density of matter in the universe (10^{-29} g/cm^3) and R = radius of the universe (3×10^{27} cm).[2] If Δm is ascribed to our own galaxy, then $r = 2.5\times10^{22}$ cm and $\mathfrak{M} = 3\times10^{44}$ g, where the total mass of the galaxy is considered concentrated at its center. Hence for $\nu = 1$, $\Delta m/m = 2\times10^{-5}$ and for $\nu = 0$, $\Delta m/m = 3\times10^{-10}$.

Cocconi and Salpeter have suggested several experiments to test for this anisotropy of mass based on the observation that the contribution to the binding energy of a particle in a Coulomb potential due to the anisotropic mass term Δm is

$$\Delta E = (\Delta m/m)\overline{T}\,\overline{P}_2(\cos\theta). \qquad (2)$$

Here $\overline{T}$ is the average kinetic energy of the particle, P_2 is the Legendre polynomial of order 2, and θ is the angle between the direction of acceleration of the particle (determined by the direction of an external magnetic field $\vec{H}$ and by the magnetic quantum state) and the direction to the galactic center. This equation is based on the assumption that Δm varies as $P_2(\cos\theta)$. The first experiment suggested was to observe the Zeeman splitting in an atom[1] and the second was to observe the Zeeman splitting in the excited nuclear state of Fe^{57} by use of the Mössbauer effect.[3] [The change in binding energy due to Δm will not be given exactly by Eq. (2) in the nuclear case, but if the nucleus is idealized as a single particle in a spherically symmetric square well potential a similar type of equation applies.] For both experiments effects are to be measured as a function of the angle θ. The models used for the atom and the nucleus are adequate for the order of magnitude estimate we require for ΔE.

In this Letter we report an experiment using nuclear magnetic resonance in the ground state of nuclei to test for the anisotropy of mass. This method gives a sensitivity some factor of 10^6 greater than could be achieved in the experiment suggested by Cocconi and Salpeter using the Mössbauer effect. In addition, we report experiments on the Zeeman effect in atoms of the first type suggested by Cocconi and Salpeter.

We discuss first the atomic Zeeman experiments. There are at least two methods of searching for the effect of mass anisotropy in an atomic state with orbital angular momentum quantum number $L \geq 1$ and with total angular momentum quantum number $J \geq 3/2$. One method is to observe, for example, the frequency of the Zeeman transition $M_J = +3/2 \rightarrow M_J = +1/2$ in the $^2P_{3/2}$ state as a function of the relative orientation of the direction of the magnetic field and the direction to the galactic center. In our experiment with our electromagnet fixed to the earth and with the magnetic field pointing approximately in the north-south direction, the change in relative orientation is achieved as a function of time due to the rotation of the earth. In New Haven at 41° latitude at a certain time in the sidereal day the south direction in the horizontal plane points within 22 degrees towards the center of our galaxy; 12 hours later this same direction along the earth's horizontal plane points 104 degrees away from the galactic center. It is important, of course, that the frequency standard with respect to which the Zeeman transition frequency is compared shall itself exhibit no mass anisotropy effect. Most Zeeman transition frequency measurements such as those quoted by Cocconi and Salpeter[1] have been referred to crystal oscillator secondary standards calibrated occasionally against the signal from WWV, and hence because of possible mass anisotropy effects in the crystal oscillator are not suitable for the present purpose. In our experiment a frequency derived from the cesium atomic frequency standard (National Company Atomichron) was used. The transition $(F, M_F) = (4, 0) \rightarrow (3, 0)$ used in this frequency standard[4] will not exhibit any mass anisotropy effect. The magnetic field is maintained constant with a proton resonance probe whose resonance frequency is compared with the Atomichron frequency. For a constant magnetic field the proton resonance frequency will exhibit no mass anisotropy effect. The transition $M_J = +3/2 \rightarrow M_J = +1/2$ with $M_I = +3/2$ in the $^2P_{3/2}$ state of Cl^{35} was observed over a twelve-hour period. No variation with time of the Zeeman transition frequency occurring at about 9190 Mc/sec in a magnetic field of 4730 gauss was observed within the experimental error of 30 kc/sec. If the electronic structure of chlorine, which is an atom lacking one electron to complete the outer $3p$ shell, is treated as a hole moving in a Coulomb potential due to the nucleus and electrons, the upper limit to $\Delta m/m$ of 10^{-10} is obtained.

A second method is to observe the frequencies of two Zeeman transitions where the intervals would be affected differently by any mass anisotropy. It is only necessary to observe the two transitions at the time at which the direction to the galactic center is such as to maximize the mass anisotropy effect. Simple experimental data of this type are available from the Zeeman transitions $\Delta M_J = \pm 1, \pm 2$ in the $^3P_2$ state of atomic oxygen.[5] From these data it can be deduced that $\Delta m/m \leq 10^{-10}$.

By far the most sensitive test is obtained from a nuclear magnetic resonance experiment on an appropriate nucleus in its ground state. Consider the Li^7 nucleus in its ground state which has nuclear spin $I = 3/2$. In a magnetic field there will be four energy levels corresponding to the allowed values of the magnetic quantum number M_I. In the absence of any mass anisotropy, adjacent levels are equally spaced and a single nuclear resonance line will be observed. If the mass anisotropy effect is present, there will be three different intervals which will lead to a triplet nuclear resonance line, if the structure is resolved, or to a single broadened line if the structure is unresolved. Over a twelve-hour period, the resonance line for Li^7 was observed in a $1N$ water solution of $FeCl_3$ saturated with LiCl. The magnetic field of about 4700 gauss was stabilized against the proton resonance frequency with the Atomichron as a frequency standard. Only a single line was observed. The line width of 4.3 parts per million is due primarily to the inhomogeneity of the magnetic field and from the width of the proton resonance line should be (5.0 ± 1) parts per million. Hence a broadening of no greater than 8 cps could be due to the effect of mass anisotropy. If the nuclear structure of Li^7 is treated as a single $P_{3/2}$ proton in a central nuclear potential,[6] the limit $\Delta m/m \leq 10^{-20}$ is obtained. The increase in sensitivity over that which one could obtain from the Mössbauer effect is due to the far narrower line width obtainable for a transition with a nucleus in its ground state as compared with a nucleus in an excited state.

The limit here obtained of $\Delta m/m \leq 10^{-20}$ is far less than the value of 3×10^{-10} obtained by setting $\nu = 0$ in Eq. (1). Hence it seems that within the framework of the Mach theory as discussed by Cocconi and Salpeter one should conclude that there is no anisotropy of mass of the type which varies as $P_2(\cos\theta)$ associated with effects of mass in our galaxy.

In the interest of completeness we intend to improve the sensitivity of the nuclear resonance experiment at least one order of magnitude by obtaining a narrower line width. We shall study the nuclear resonance signal of nuclei consisting of closed shells plus or minus one nucleon. Also we shall search for an anisotropic mass which varies other than as $P_2(\cos\theta)$ by studying nuclear resonance signals of nuclei with spin greater than 3/2. Finally, since in the spirit of this investigation it is not necessarily excluded that mass anisotropy could be associated with a point in the universe other than the center of our galaxy, we shall study the nuclear resonance signal with respect to any arbitrary direction.

It is a pleasure to thank Professor H. Smith and Professor R. Wildt of the Yale Astronomy Department and Professor E. E. Salpeter for helpful and enlightening discussions.

---

*This research has been supported in part by the National Aeronautics and Space Administration.

[1]G. Cocconi and E. E. Salpeter, Nuovo cimento 10, 646 (1958).

[2]C. W. Allen, Astrophysical Quantities (The Athlone Press, London, 1955).

[3]G. Cocconi and E. E. Salpeter, Phys. Rev. Letters 4, 176 (1960).

[4]P. Kusch and V. W. Hughes, Encyclopedia of Physics (Springer-Verlag, Berlin, 1959), Vol. 37, Part 1.

[5]H. E. Radford and V. W. Hughes, Phys. Rev. 114, 1274 (1959).

[6]M. G. Mayer and J. H. D. Jensen, Elementary Theory of Nuclear Shell Structure (John Wiley & Sons, Inc., New York, 1955).

SIGNIFICANCE OF ELECTROMAGNETIC POTENTIALS IN THE QUANTUM THEORY IN THE INTERPRETATION OF ELECTRON INTERFEROMETER FRINGE OBSERVATIONS

Frederick G. Werner
Physics Department, University of Cincinnati, Cincinnati, Ohio

and

Dieter R. Brill
Palmer Physical Laboratory, Princeton University, Princeton, New Jersey

(Received March 7, 1960)

The effects of electromagnetic potentials in quantum theory recently discussed by Aharonov and Bohm[1] and also by Furry and Ramsey,[2] and a decade ago by Ehrenberg and Siday,[3] have been the subject of some lively discussion[4] regarding experimental observations. Interference fringes have been observed[5,6] in electron interferometers in which electron beams are split into separate component beams which travel along spatially separated paths before being recombined to produce the interference. One of the effects in question would be an observable shift of interference fringes produced by a quite small amount of magnetic flux passing between the two component beams, but confined completely to regions not penetrated by the beams, for example by means of a long solenoid. The presence of such a magnetic field would thus be detected in spite of the fact that none of the detecting apparatus ever actually entered any of the region of that field.

The question has arisen whether the existence of such an effect can be ruled out already, in the light of the fact that electron interference fringes have actually been observed. Marton has informed us that stray 60-cycle magnetic fields were present in his electron interferometer such that the magnetic flux passing between the beams was quite large in comparison with the very small amount of flux predicted to be needed to change the relative phase of the two component beams by 2π. It was thought at first that if the effect predicted by quantum theory referred to above had indeed been present, the interference fringes would have been shifted back and forth sixty times each second during the exposure by such large amounts that they could not possibly have been seen.[7] After considerable discussion at Princeton, National Bureau of Standards, Swarthmore, New York, and elsewhere, it was finally realized, during the New York meetings of the American Physical Society, that the change in length of the two component electron beams, due to their being bent in actually passing through

a magnetic field of this sort, surely must be taken into account. Furthermore, order of magnitude calculations at that time led to the conclusion that the effect of magnetic potential, rather than being absent, actually contributed significantly to the stability of the fringe pattern in spite of such beam bending.[8] A detailed treatment follows.

In the Marton-type interferometer schematically indicated in Fig. 1(a) the incoming beam at the top (solid line) is amplitude-split by a very thin crystal C_1, into a zero-order beam (vertical dashed line) continuing in the same direction, and a first order beam (slanting dotted line) which makes an angle θ with the original beam direction. After travel distances l_1 and m_1, respectively, these beams meet another very thin crystal C_2, where both beams are diffracted, partly into beams (slanting dashed line and vertical dotted line) which come together at a third very thin crystal C_3 after travelling additional distances l_2 and m_2, respectively. At C_3 the beams are again diffracted, each partly into the vertical direction of the outgoing beams at the bottom (dash-dotted vertical line). If the geometry and the crystals were ideal, these two component beams would superpose constructively with no angle between them. However, due to nonideal geometry and crystal warp the two beams fail to coincide exactly, differing not only in phase, but also in direction by the very small angle ϕ. In contrast to the first diffraction angle θ, this angle of deviation from parallelism ϕ can be made sufficiently small so that fringes resulting from interference of these two nearly parallel component beams can be observed.

In the presence of a weak uniform magnetic field H coming out from the plane of the paper in Fig. 1(b) the component beams will follow circle arcs, l_1', m_1', l_2', and m_2'. These circles all have the same radius,

$$R = \frac{cp}{|-e|H} = \frac{2\pi\hbar c}{e}\,\frac{1}{H\lambda},$$

where $(-e)$ is the electron charge, p the magnitude of momentum of the electrons, and λ the wavelength. The angle through which a beam is bent after travelling an arc length L is $\tau = L/R$. The angle between m_1 and the chord joining the ends of m_1' is

$$\tfrac{1}{2}\tau_1 = \tfrac{1}{2}m_1'/R \doteq \tfrac{1}{2}m_1/R$$

to first order in the magnetic field strength $H = 2\pi(\hbar c/e)/(\lambda R)$. As shown in more detail in the enlargement of Fig. 1(c), the line m_1' exceeds in length the line m_1 by the amount

$$\Delta m_1 \equiv m_1' - m_1 \doteq [m_1(\tfrac{1}{2}\tau_1)]\tan\theta \doteq \tfrac{1}{2}(m_1^2/R)\tan\theta.$$

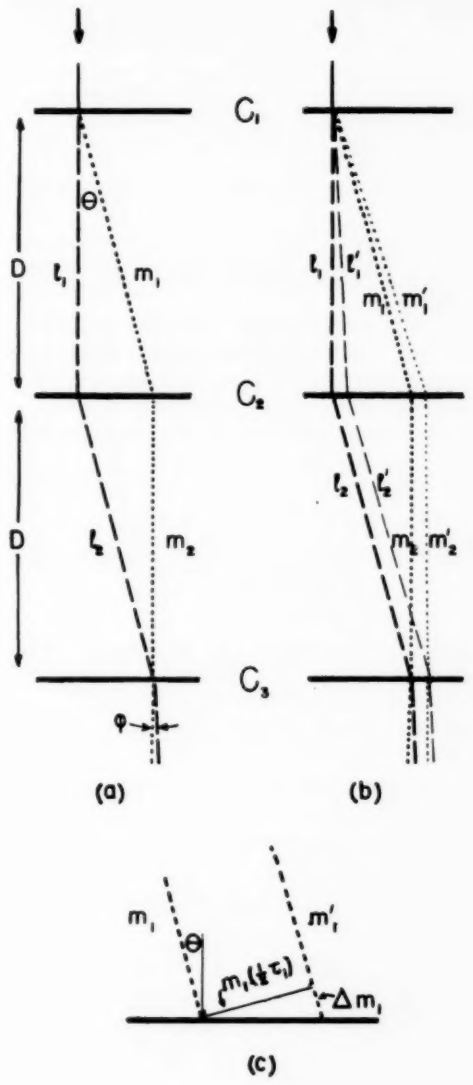

FIG. 1. Schematic diagram of component beam paths (dashed and dotted lines) in a Marton-type three-crystal electron interferometer: (a) in the absence of magnetic field; (b) with beams being bent by a uniform magnetic field coming out from the page. (c) Shown in enlarged detail is the region in (b) where original and displaced beam components m_1 and m_1' meet the second thin crystal C_2.

Since the angle of diffraction between l_1' and l_2' is the same as it was between l_1 and l_2, the angle between l_2 and the chord joining the ends of l_2' is

$$\frac{l_1'}{R}+\tfrac{1}{2}\frac{l_2'}{R}\doteq\frac{l_1+\frac{1}{2}l_2}{R}.$$

The excess of l_2' over l_2 is then

$$\Delta l_2\doteq\frac{l_1+\frac{1}{2}l_2}{R}l_2\tan\theta.$$

The differences in length between l_1' and l_1, and between m_2' and m_2 are both smaller by another order in H.

Substituting the distance D between the thin crystals for l_1 and $D/\cos\theta$ for m_1 and l_2, we have the change in the difference between path-lengths of the two component beams from C_1 through C_2 to C_3, resulting from bending of the beams by the uniform magnetic field H,

$$\Delta l_2-\Delta m_1\doteq\frac{1}{R}\left(D+\tfrac{1}{2}\frac{D}{\cos\theta}\right)\frac{D}{\cos\theta}\tan\theta-\frac{1}{2R}\frac{D^2}{\cos^2\theta}\tan\theta$$

$$\doteq\frac{e}{2\pi\hbar c}H\lambda D^2\frac{\tan\theta}{\cos\theta}.$$

As pointed out by Aharonov and Bohm[1] and by Ehrenberg and Siday,[3] the change in phase difference between the two component beams from their differences in magnetic potential in the presence of magnetic flux passing between the two component beams is

$$\frac{(-e)}{\hbar c}\oint\vec{A}\cdot d\vec{x}=\frac{(-e)}{\hbar c}H\,(\text{area between beams})$$

$$\doteq\frac{(-e)}{\hbar c}HD^2\tan\theta.$$

Taking into account the negative sign of the charge of the electron and combining this effect with the change in phase difference due to length change from beam bending, we have the net change in relative phase,

$$\delta\doteq\frac{e}{\hbar c}HD^2\left(\frac{1}{\cos\theta}-1,\right)\tan\theta,$$

to first order in H. For small diffraction angle θ, this is approximated by

$$\delta\cong(e/\hbar c)HD^2\theta^3/2.$$

In terms of the distance of maximum separation d, and the difference in length ϵ between l_1 and m_1, this is

$$\delta\cong(e/\hbar c)H\epsilon d/2.$$

This is just $(e/\hbar c)$ times the magnetic flux through the very small triangle of base d and altitude ϵ in contradistinction to that through the very much larger parallelogram between the component beams. For practically perfect geometry, where the fringe width is very large, this means that for a uniform magnetic field the change in phase due to the integral of the magnetic potential is almost perfectly compensated by the change in phase due to the change in length of the component beams resulting from bending.

In fact, for proper adjustment of the geometry, the small angle of deviation from parallelism of outcoming component beams ϕ can be made such that this small relative phase change just compensates for the sidewise displacement (due to bending) of the place where the component beams join to form the interference fringes. In this case, when the magnetic field strength has reached the value H_C which results in bending the beams into arcs of radius R_C so that the point of recombination at C_3 is displaced by one whole fringe spacing, the net change in the relative phase of the beams δ, due to both beam length change and the magnetic vector potential integral, will reach the value 2π. Here the positions of the maxima and minima of the fringes are undisplaced to first order in H by the presence of the uniform magnetic field, which in this case only changes the relative intensity of illumination of the fringes.

Far from being absent, the effect of the change of relative phase from magnetic potentials is essential for the observation of fringes in a Marton-type electron interferometer in the presence of uniform magnetic fields which vary slowly with time.

We are grateful to E. P. Wigner, R. Brill, L. Marton, W. H. Furry, N. F. Ramsey, and R. N. Euwema for very stimulating discussions on this point.

---

[1] Y. Aharonov and D. Bohm, Phys. Rev. 115, 485 (1959).

[2] W. H. Furry and N. F. Ramsey, Bull. Am. Phys. Soc. 5, 66 (1960); Phys. Rev. (to be published).

[3] W. Ehrenberg and R. E. Siday, Proc. Phys. Soc. (London) B62, 8 (1949), especially p. 21.

[4] E. P. Wigner, in his colloquium of December 3, 1959, at Palmer Physical Laboratory, Princeton, and in private discussion pointed out that such effects should be observable according to "orthodox" quantum theory, and that if such effects are found absent under conditions where they are predicted, it would necessi-

tate an "unorthodoxy" or break from present quantum theory.

[5]L. Marton, J. Arol Simpson, and J. A. Suddeth, Rev. Sci. Instr. 25, 1099 (1954).

[6]G. Möllenstedt and H. Düker, Naturwissenschaften 42, 41 (1954).

[7]This was discussed by Dr. H. Mendlowitz in a post-deadline paper at the January, 1960 New York Meeting of the American Physical Society.

[8]After the presentation of the paper of Furry and Ramsey at the meeting in New York we were pleased to learn, in discussion with Professor Ramsey, that he had also reached the same conclusion independently in discussion with Dr. H. Mendlowitz. Dr. Marton kindly sent us comments by Dr. Mendlowitz on a preliminary draft of this Letter, indicating that in calculations carried out at the National Bureau of Standards Dr. Z. Bay and he also arrived (from a slightly different approach) at essentially the same conclusion.

MICROWAVE WHISTLER MODE PROPAGATION IN A DENSE LABORATORY PLASMA*

R. M. Gallet, J. M. Richardson, B. Wieder, and G. D. Ward
Boulder Laboratories, National Bureau of Standards, Boulder, Colorado

and

G. N. Harding
Atomic Energy Research Establishment, Harwell, England

(Received February 12, 1960)

If plane wave solutions which retain constant polarization are sought to the wave equation applicable to propagation at angular frequency ω in a homogeneous plasma in a magnetic field $\vec{H}_0$, one finds the indices of refraction for the characteristic ordinary and extraordinary wave given by Appleton's equation,[1,2]

$$n^2 = 1 - \frac{X}{1-\frac{1}{2}Y_T^2/(1-X) \pm \left[\frac{1}{4}Y_T^4/(1-X)^2 + Y_L^2\right]^{1/2}}, \quad (1)$$

where $X = \omega_p^2/\omega^2$; $Y = \omega_H/\omega$; $Y_L = Y\cos\theta$; $Y_T = Y\sin\theta$; $\omega_p = (4\pi Ne^2/\epsilon_0 m)^{1/2}$, the plasma frequency for electron density N; $\omega_H = \mu_0 H_0 e/m$, the electron gyro frequency; and θ is the angle between $\vec{H}_0$ and the wave normal. Here the collision frequency ν is neglected, and the ion plasma and ion gyro frequencies are assumed negligibly small. Propagation occurs for real positive n. The usual modes used for diagnostics are for $\omega > \omega_p$, requiring inconveniently large ω for even moderately dense plasmas. Another propagating mode occurs when $\omega < \omega_H$, for right-hand circular polarization, and $\cos\theta$ near unity. This mode has recently been used to explain extraterrestrial very low frequency propagation associated with lightning discharges[3] and very low frequency emissions in the exosphere of the earth[4] and has been called the "whistler" mode. It is characterized by an index of refraction greater than unity and confinement of the radiated energy to a narrow cone along $\vec{H}_0$.

One of us (R. M. G.) pointed out at the 1958 summer International School of Physics, Varenna, Italy, the usefulness of the whistler mode for plasma diagnostics particularly under conditions such that the refractive index becomes very large (of the order of 100 or more) and suggested that a large, slow thermonuclear machine such as the ZETA[5] at Harwell, England, would offer the best initial laboratory medium for observation of this mode. Through the efforts of Thonemann and Pease an invitation was extended by the Atomic Energy Research Establishment, Harwell, to the American authors to attempt such experiments on ZETA.

In ZETA, $\omega_p/2\pi \approx 100$ kMc/sec, $\omega_H/2\pi \approx 3$ to 40 kMc/sec, and $\nu \approx 10^7$ sec^{-1}. If we choose $\omega/2\pi \approx 3$ kMc/sec, then $X \approx 1600$, $Y \approx 1$ to 10, and ν is satisfactorily small. Under these conditions we can simplify the expression for n^2. For propagation along $\vec{H}_0$,

$$n^2 \approx \frac{\omega_p^2/\omega^2}{(\omega_H/\omega)-1}, \quad (2)$$

provided $\nu \ll \omega_H - \omega$.

Measurement of n at two frequencies permits solution for ω_p and ω_H and hence N and H_0. As the propagation is sharply beamed, two receiving antennas may be used to define direction so that in fact $\vec{H}_0$ is measured. This technique could be used to map the magnetic field in a dense plasma. Both N and $\vec{H}_0$ are obtained as a function of time.

The index, n, may be measured by pulse transit time or interferometric methods. The highly dispersive qualities of the medium permit the use of FM interferometric techniques to obtain phase information to good accuracy.

For small losses, described by a complex index of refraction $n_c = n - iq$, the attenuation rate (for field amplitude) may be shown to be

$$\alpha = \omega q/c = \nu\omega n/2c\omega_H(1-\omega/\omega_H). \quad (3)$$

Spitzer[6] gives

$$\nu = 3.74\, NT^{-3/2}(15.92 - \ln N^{1/2}T^{-3/2}). \quad (4)$$

Measurement of α yields ν and leads to T.

Propagation in the whistler mode near 3000 Mc/sec for $\omega_H/\omega \simeq 2$ was observed between cross-polarized short electric dipole antennas over paths up to 24 cm along the ZETA torus axis as in Fig. 1, where $\vec{H}_0$ is expected to be axial. Figure 2 shows an example of the received signal. It is cut off at the onset of ionization as ω_p becomes greater than ω; it remains absent until the mode opens by virtue of the gyro frequency exceeding the applied frequency; then a saturated signal is recorded until the mode closes. The current through the gas is shown on the lower trace. With the transmitter off, there is no signal greater than the noise level, for this discharge condition in which the current decays smoothly. The reproducibility of the propagation in a series of discharges under the same conditions is often excellent.

Emission of strong bursts of noise of non-thermal origin is observed under other discharge conditions, in which the current through the gas decays almost discontinuously. This occurrence is displayed in Fig. 3(a), taken with the transmitter off. Other less intense bursts appear often associated with small but rapid fluctuations in the gas current. While these emissions are clearly related to the occurrence of instabilities in the plasma, their mechanism is still unknown. One possibility is the Čerenkov radiation due to

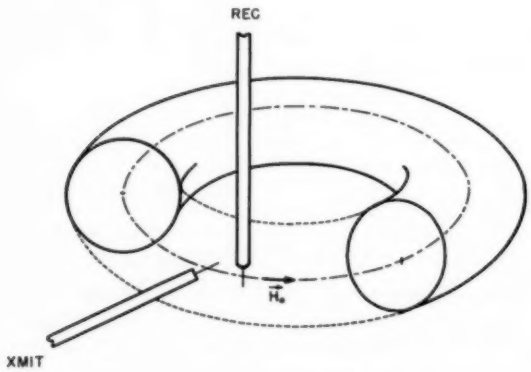

FIG. 1. Orientation of antennas.

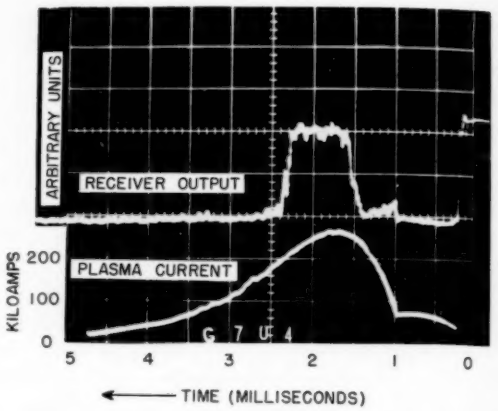

FIG. 2. Onset and extinction of 3300-Mc/sec transmission along ZETA torus axis ($\omega_p/\omega \simeq 50$ and $\omega_H/\omega \simeq 2$ at current peak).

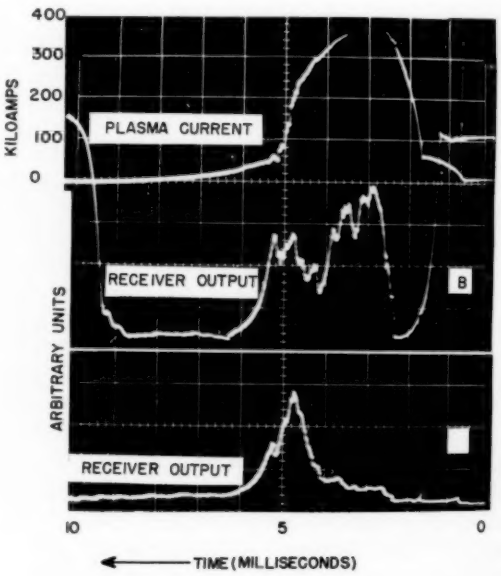

FIG. 3. (a) 2800-Mc/sec noise emission from ZETA plasma; transmitter off. (b) Superposition of signal and of noise emission, 2800 Mc/sec ($\omega_p/\omega \simeq 40$ and $\omega_H/\omega \simeq 2$ at current peak).

the runaway electrons, when the phase velocity at the observed frequency becomes equal to or smaller than the velocity of the electrons. This occurs because the refractive index has typical values of the order of 100 in the present conditions, and goes to much larger values when ω/ω_H approaches unity due to changes in the value of the magnetic field.

The superposition of the emissions and the propagated microwaves with the transmitter on is exhibited in Fig. 3(b), taken exactly in the same conditions as Fig. 3(a) during the shot immediately preceding. The two maxima have a completely different origin, but it is easy to understand the structure of this signal which is more complex than Fig. 2. The signal recovers at long times as ω_p becomes small by recombination.

Preservation of coherence of the radiation during transmission was observed by allowing the outputs of two antennas, spaced along different paths from a transmitting antenna, to interfere at the i.f. frequency. Each of the two detected receiver outputs separately resembles Fig. 1. When allowed to interfere, the detected output of the resultant showed clearly recognizable fringes caused by relative variations in the optical paths during the pulse. These fringes occur rapidly compared to the pulse duration for some discharge conditions. The preservation of coherence indicates that the scattering of the propagating wave by plasma irregularities is relatively unimportant.

Quantitative measurements are in progress. Measurement of n and α simultaneously on two frequencies will be attempted.

The short wavelength and low phase velocity due to the high refractive index imply certain characteristics which may be adaptable for diagnostic use. Transmission paths may be short thus providing good spatial resolution in measurement. Diffraction is less severe. Eventually directive antennas may be designed to facilitate scattering experiments to explore distribution of the sizes of local inhomogeneities.

---

*Supported by the Air Force Cambridge Research Center.

[1]E. V. Appleton, J. Inst. Elec. Engrs. Japan 71, 642 (1932).

[2]J. A. Ratcliffe, The Magneto-Ionic Theory and Its Application to the Ionosphere (University Press, Cambridge, 1959).

[3]L. R. O. Storey, Phil. Trans. Roy. Soc. (London) A246, 113 (1953).

[4]R. M. Gallet, Proc. Inst. Radio Engrs. 47, 211 (1959).

[5]P. C. Thonemann, E. P. Butt, R. Carruthers, A. N. Dellis, D. W. Fry, A. Gibson, G. N. Harding, D. J. Lees, R. W. P. McWhirter, R. S. Pease, S. A. Ramsden, and S. Ward, Nature 181, 217 (1958).

[6]L. Spitzer, Physics of Fully Ionized Gases (Interscience Publishers, Inc., New York, 1956), p. 78.

SUPERFLUIDITY AND SUPERCONDUCTIVITY IN ELECTRON GASES

G. Wentzel
Enrico Fermi Institute for Nuclear Studies, University of Chicago, Chicago, Illinois
(Received February 26, 1960)

Lately, several investigations[1-3] have been devoted to the moment of inertia of Fermion gases, with interactions treated by perturbation or random-phase approximations. We want to point out that the main results of these papers might have been anticipated on the basis of Schafroth's paper,[4] in conjunction with what is known about the magnetic behavior of charged Fermion gases, admitting similar interactions and approximation methods.

As in a preceding paper by Blatt, Butler, and Schafroth,[5] Schafroth discusses "rotating buckets" in thermal equilibrium. In the rest frame of the bucket, the boundary conditions on the wave functions at the walls of the container (perfect reflection) are assumed to be independent of the angular velocity ω. The moment of inertia I is then defined as

$$I = \lim_{\omega=0} (\partial L/\partial\omega),$$

where L is the angular momentum in the canonical ensemble average. [We can here always regard ω as infinitesimally small and thereby avoid the complications discussed by Blatt and Butler.[6]] It is to be noted that the rotating bucket model, in the limit of zero temperature, becomes identical with the "cranking model" which is employed in the papers[1-3] cited at the beginning, provided the same boundary conditions are

imposed.

The "classical" or rigid-body value of I is called I_0. For instance, in the case of a cylindrical container of radius R, rotating about the symmetry axis,

$$I_0 = \tfrac{1}{2}R^2Nm,$$

where Nm is the total mass. The liquid is "superfluid" if I is (significantly) smaller than I_0. The salient point in Schafroth's paper[4] is the proof of a general relationship between $I_0 - I$ and the magnetization produced in the (charged) liquid by a homogeneous magnetic field H, directed along the axis of rotation, e.g., the symmetry axis of the cylinder. As in earlier papers by Schafroth,[7] H is considered as a given "external" or "impressed" field, arising for instance out of a nuclear spin polarization. All particles of the liquid are thought to carry a "test charge" ϵ, but no intrinsic (spin) magnetic moment (this is the simplest case); in other words, the whole magnetization originates in the electric currents $\sum\epsilon\vec{v}$. The particles are allowed to interact through arbitrary potentials depending on the space coordinates. In the special case that all particles are identical (Bosons or Fermions, mass m), Schafroth's "connection theorem" may be formulated as follows. Let M be the total magnetic moment induced by H in the sample; then[8]

$$\lim_{H=0}\frac{\partial M}{\partial H} = \left(\frac{\epsilon}{2mc}\right)^2 (I - I_0).$$

If the liquid is superfluid (as defined above), the apparent susceptibility $\chi' = V^{-1}(\partial M/\partial H)_{H=0}$ of a cylinder has the order of magnitude

$$\chi' \propto -\frac{\epsilon^2}{8mc^2}\times R^2 \times \frac{N}{V},$$

where N/V is the number density. The dependence on R is the same as for a superconductor obeying London's equation [see Schafroth,[4] Eq. (12)].

We shall now apply the connection theorem to electron gases (ignoring the ionic lattice).

(1) Free electrons show an ordinary diamagnetism. The Landau value of the susceptibility is

$$\chi = -\frac{\epsilon^2}{4mc^2}\times\lambda_F{}^2\times\frac{N}{V},$$

where λ_F = de Broglie wavelength of an electron at the Fermi surface. We conclude

$$(I_0 - I)/I_0 = O(\lambda_F/R)^2.$$

This conforms with the direct calculation by Amado and Brueckner[1] who found $I = I_0$ for a cranked cubic volume (at zero temperature). This result must remain valid if weak interactions are introduced as perturbations[1] since these do not radically alter the diamagnetic behavior of the gas (they can not cause χ' to increase as R^2).

(2) We admit Coulomb interactions between the electrons and treat their ground state in the high-density approximation which is equivalent to a certain random-phase approximation.[9] It is known[10] that, in this approximation, the Landau diamagnetism is not affected by the interactions, and the same must then be true for the moment of inertia. This has indeed been found by Rockmore,[2] for the cranked cube.

(3) The same author[3] studied the Bardeen-Cooper-Schrieffer-Bogoliubov model of a superconductor, introducing the energy gap in the spectrum of excitations, and using as a tool again a random-phase approximation. For the cranked ground state he finds that I/I_0 goes to zero ($\sim V^{-1/3}$) as the cubic volume V becomes very large. This amounts to an extreme superfluidity. If we now invoke Schafroth's connection theorem and accept the statement $I = 0$ for a cylindrical container (R large), we then find that the magnetic moment M is the same as for a superconductor which obeys the London equation, with the "London value" for the London constant [see Schafroth,[4] Eqs. (7) and (11)]:

$$\operatorname{curl}\vec{I} = -\left(\frac{\epsilon^2}{mc}\frac{N}{V}\right)\vec{B}.$$

This, however, is precisely what one would have expected on the basis of those theories of the Meissner effect which employ the random-phase approximation.[11] [Refining the London equation for nonlocal effects (Pippard or BCS) is of no relevance here.]

In this context, it should be borne in mind that the random-phase approximation, when applied to the BCS model, is by no means guaranteed to be a good approximation. But whatever the answer to this question may be, it is interesting to note that "extreme superfluidity" ($I = 0$) entails, for charged identical Fermions or Bosons, "extreme superconductivity," namely, the London value for the London constant.

Another point to emphasize is that in real fluids, as opposed to idealized models, there exists a maximum correlation distance Λ beyond which all correlations are wiped out by disordered collisions. For $R \gg \Lambda$, Blatt, Butler, and Schafroth[5] have proved that the moment of inertia necessarily approaches the rigid-body value: $I = I_0[1 + O(\Lambda/R)]$. How this affects the London equation (at large wavelengths) has been discussed by Schafroth and Blatt.[12] The results quoted above under (3) illustrate the fact that, for the BCS model, Λ is infinite. A realistic computation of Λ would be desirable, not only for superconductors but even more so for systems like He II and heavy nuclei.

[1]R. D. Amado and K. A. Brueckner, Phys. Rev. 115, 778 (1959).

[2]R. M. Rockmore, Phys. Rev. 116, 469 (1959).

[3]R. M. Rockmore (to be published).

[4]M. R. Schafroth, Phys. Rev. 100, 502 (1955).

[5]J. M. Blatt, S. T. Butler, and M. R. Schafroth, Phys. Rev. 100, 481 (1955).

[6]J. M. Blatt and S. T. Butler, Phys. Rev. 100, 476 (1955).

[7]M. R. Schafroth, Helv. Phys. Acta 24, 645 (1951).

[8]Unfortunately, Schafroth's paper[4] contains several bothersome misprints. On p. 504, all expressions for the magnetic moment should be divided by 2. Accordingly, in Eq. (13), $2\chi'$ should be replaced by $4\chi'$.

[9]M. Gell-Mann and K. A. Brueckner Phys. Rev. 106, 364 (1957); K. Sawada, Phys. Rev. 106, 372 (1957); K. Sawada, K. A. Brueckner, N. Fukuda, and R. Brout, Phys. Rev. 108, 507 (1957).

[10]G. Wentzel, Phys. Rev. 108, 1593 (1957).

[11]P. W. Anderson, Phys. Rev. 112, 1900 (1958); G. Rickayzen, Phys. Rev. 115, 795 (1959).

[12]M. R. Schafroth and J. M. Blatt, Phys. Rev. 100, 1221 (1955), and Nuovo cimento 4, 786 (1956).

ISOTOPIC COMPOSITION OF PRIMORDIAL XENON*

J. H. Reynolds
Department of Physics, Miller Institute for Basic Research in Science
University of California, Berkeley, California
(Received March 7, 1960)

In a previous Letter,[1] we reported a large excess of Xe^{129} in a chondritic stone meteorite, Richardton. We also reported secondary anomalous abundaces for many of the other isotopes in this xenon. We have now found similar secondary anomalies in xenon from a carbonaceous chondrite, Murray. Since the ratio of xenon to the cosmic-ray-produced nuclides Ne^{21} and He^3 is very different for these two meteorites, we conclude that the anomalies in question are not due to nuclear reactions induced by cosmic rays. There appears to be an isotopic difference between primordial xenon—or at least xenon incorporated in stone meteorites—and xenon in the atmosphere. To our knowledge, xenon is unique among the elements in exhibiting an effect of this kind and magnitude.

We have made a comprehensive analysis by isotope dilution of all the rare gases in the two stones. The results are presented in Tables I, II, and III. The nuclides He^3 and Ne^{21} are almost entirely cosmic-ray produced in both stones. We note from the abundances of these isotopes in Table I that the integrated cosmic-ray exposure for Richardton exceeds that for Murray by a factor of about 5. Data for argon and for the other isotopes of He and Ne show clearly that there is primordial gas in Murray. The isotopes A^{36} and A^{38} are more abundant in Murray than in Richardton by factors 30 and 9, respectively. The ratio A^{36}/A^{38} in Murray is 5.39 which is very close to that for the atmosphere (5.35) and very unlike that produced by cosmic rays in iron meteorites (0.6); for Richardton, A^{36}/A^{38} is 1.62 which is intermediate. That little of the argon in Murray can be from atmospheric contamination is seen from the A^{40}/A^{36} ratio which is 8.5, in contrast with 296 for the atmosphere. (The A^{40}/A^{36} ratio for Murray is the lowest that has been seen thus far in a stone meteorite.) Clearly argon was incorporated in the Murray stone at the time of its formation. Neon from Murray can be resolved into a cosmic-ray component ($Ne^{20} \cong Ne^{21} \cong Ne^{22}$) plus a primordial component with Ne^{21}/Ne^{20} assumed to be that for the atmosphere and $Ne^{22}/Ne^{20} = 0.111 \pm 0.005$ as compared with $Ne^{22}/Ne^{20} = 0.097$ for atmospheric neon. It is very unlikely that this neon is from atmospheric contamination because Ne/A in Murray is 0.1 [which means that $Ne/(A)_{atmos}$ in Murray is considerably greater than 0.1] while Ne/A in the atmosphere is 0.002. He^4 is also in

Table I. Rare gas analyses of the meteorites. (All gas contents are in cc STP/g.)

	Richardton	Murray	Pesyanoe
Sampling	Reduced to minus 20 m in diamond mortar. (Large malleable grains rejected.) 20-100 m used for analysis.	Samples crushed by several blows in diamond mortar. All material used.	...
He^3	$(2.88^b \pm 0.15)\times10^{-7}$ (3.30^c)	$(0.68 \pm 0.03)\times10^{-7}$	$<18^f\times10^{-7}$
He^4	$(12.0^b \pm 2.5)\times10^{-6}$ (15.1^c)	$(142 \pm 7)\times10^{-6}$	$7300^f\times10^{-6}$
Ne^{20}	$(9.88^b \pm 0.6)\times10^{-8}$	$(65.2 \pm 3.2)\times10^{-8}$	$1900^f\times10^{-8}$
Ne^{21}	$(11.52^b \pm 0.7)\times10^{-8}$	$(2.22 \pm 0.11)\times10^{-8}$	$19^f\times10^{-8}$
Ne^{22}	$(11.82^b \pm 0.7)\times10^{-8}$	$(9.07 \pm 0.45)\times10^{-8}$	$171^f\times10^{-8}$
A^{36}	$(2.59^b \pm 0.4)\times10^{-8}$ (2.83^d)	$(76.5 \pm 3.8)\times10^{-8}$	$168^f\times10^{-8}$
A^{38}	$(1.60^b \pm 0.06)\times10^{-8}$ (1.16^d)	$(14.2 \pm 0.7)\times10^{-8}$	$36^f\times10^{-8}$
A^{40}	$(53.2^b \pm 2.1)\times10^{-6}$ (54.0^d)	$<6.53\times10^{-6}$	$47.1^f\times10^{-6}$
Total Kr	Within factor 3 of total Xe	$(27.3 \pm 1.3)\times10^{-9}$	...
Total Xe	$(1.04 \pm 0.05)\times10^{-9}$	$(43 \pm 4)\times10^{-9}$	...
Anomalous Xe^{129}	$(0.13 \pm 0.01)\times10^{-9}$	$(1.09 \pm 0.11)\times10^{-9}$	...
Anomalous Xe other than Xe^{129}	$(0.029 \pm 0.002)\times10^{-9}$	$(1.24 \pm 0.12)\times10^{-9}$	...
K content	$(0.073^b \pm 0.009)$ % (0.083^d)	$(0.026^b \pm 0.010)$ % (0.038^e)	?
K-A age[a]	$(4.47 \pm 0.2)\times10^9$ years	$<2.77\times10^9$ years	$4.2^f\times10^9$ years

[a]Using $\lambda_K = 0.585\times10^{-10}$ yr^{-1}; $\lambda = 5.30\times10^{-10}$ yr^{-1} for K^{40} decay.
[b]Correction for blank run has been made.
[c]P. Eberhardt and D. Hess (to be published), with different sampling.
[d]J. Geiss and D. Hess, Astrophys. J. 127, 224 (1958), with different sampling.
[e]G. Edwards, Geochim. et Cosmochim. Acta 8, 285 (1955).
[f]E. Gerling and L. Levskii, Doklady Akad. Nauk S.S.S.R. 110, 750 (1956).

Table II. Isotope abundance data for krypton.

Isotope ratio	78/84	83/84	86/84
Richardton	...	0.211 ± 0.007	0.318 ± 0.003
Murray	0.0062 ± 0.0006	0.201 ± 0.0025	0.311 ± 0.006
Atmosphere	0.00622	0.203	0.305

Table III. Percentage composition of anomalous xenon.

Isotope	Richardton	Murray	Murray/Richardton
124	0.33 ± 0.09	0.64 ± 0.05	1.94 ± 0.54
126	0.23 ± 0.02	0.56 ± 0.10	2.43 ± 0.50
128	2.51 ± 0.32	6.52 ± 0.25	2.60 ± 0.35
129	81.5 ± 3.5	46.6 ± 3.4	(0.572 ± 0.048)
130	2.27 ± 0.39	7.33 ± 0.81	3.23 ± 0.66
131	8.18 ± 2.0	25.12 ± 2.7	3.07 ± 0.81
132	3.63 ± 2.3	11.59 ± 3.4	3.19 ± 2.21
134	1.35 ± 1.0	1.69 ± 1.3	1.25 ± 1.36
136	≡0	≡0	...
		Average	2.53
		Weighted average	2.53

excess abundance in Murray. If the uranium content of Murray is 0.01 ppm, as for Richardton and other chondrites,[2] then the large difference in He^4 content between Murray and Richardton must be attributed to primordial helium in the former. Richardton may contain a little primordial A^{36}. We calculate an upper limit of 1.8×10^{-8} cc STP/g primordial A^{36} in Richardton by assuming that A^{36} and A^{38} in this stone is a mixture of primordial argon with $A^{36}/A^{38} = 5.35$ and cosmogenic argon with $A^{36}/A^{38} = 0.6$. Thus Murray has more primordial argon than Richardton by a factor of at least 42. There is one other stone meteorite known to contain primordial gas. This is Pesyanoe, which is variously described as a howardite or aubrite achondrite and which has been studied by Gerling and Levskii.[3] Their data are included in Table I for comparison.

K-A ages for the stones are given in Table I. The upper limit for the K-A age of Murray of 2.8×10^9 years results from assuming that all of the A^{40} is radiogenic. This low K-A age probably means that Murray has lost much (about 2/3) of its radiogenic argon. There may have been loss of primordial gas as well, although such loss would not alter markedly any of the conclusions reached in this Letter. Los of cosmic-ray-produced gas should be much less since these gases were produced in the last few tens of millions of years and, furthermore, cannot be concentrated at grain boundaries. A partial isotopic analysis of the krypton from the stones is presented in Table II. These data are averages from about 16 krypton runs. Other isotopes could not be studied due to memory problems in the mass spectrometer. It is seen that krypton in the stones is of normal isotopic composition except for a slight excess of Kr^{86} in Richardton.

Turning to the xenon data, we first assume, rightly or wrongly as in the previous Letter,[1] that Xe^{136} is an index to the xenon of terrestrial composition in the sample; this is assumed so as to be able to resolve the xenon into a terrestrial and an anomalous component. The isotopic compositions of the anomalous components for Richardton and Murray are compared in Table III. For every isotope other than Xe^{129} the ratio of the Murray percent abundance to the Richardton percent abundance is consistent within experimental error with the average value for this quantity. In other words, within experimental error the isotopic composition of the secondary anomalous component—i.e., excluding mass 129—is the same for both meteorites. The anomalous Xe^{129} is, on the other hand, very definitely an independent component, in agreement with our assignment of the origin of most of it to extinct I^{129} decay.[1]

The secondary anomalous component is more abundant in Murray than in Richardton by a factor $1.24/0.029 = 43$. We have already seen that contrasted with Richardton, Murray is poorer by a factor 5 in cosmic-ray-produced nuclides and richer by a factor of at least 42 in a primordial nuclide. We take these ratios to be strong evidence that the secondary anomalous xenon component in the meteorites is primordial in origin—i.e., was incorporated in the stones at the time of their formation. The only alternative possibility, seemingly, is that Murray is uniformly richer in the heavy nuclides serving as cosmic-ray targets for Xe production by a fac-

tor $5\times43=215$, which seems most unlikely.

There seems to be no simple explanation for the secondary anomalies. If there is more than one mechanism responsible, it is going to require xenon analyses for other meteorites to distinguish among the mechanisms, since the anomalies in Richardton and Murray are so similar. In the meantime, the following speculative comments are offered.

The xenon in meteorites may have been augmented by nuclear processes between the time it was separated from the xenon now on earth and the time the meteorites were formed. The mass spectrum of the added xenon peaks at mass 131. The contribution at mass 129 is most probably comparable to the nearly equal contributions at masses 128 and 130. This means that Xe^{129} from I^{129} decay is more abundant in Murray than in Richardton by a factor 7.4. If the stones have the same I^{127} content, this would imply that Murray cooled 2.9 half-lives of I^{129} or 50 million years before Richardton.

On the other hand a strong mass-dependent fractionation may be responsible for most of the anomalies. This is suggested by the regular nature of the isotope abundances of meteoritic xenon when plotted normalized to terrestrial abundances as in Fig. 1. Except at masses 129, 134, and 136, the normalized abundances conform well to a straight line on a logarithmic plot against mass. With this interpretation, there is excess Xe^{134} and Xe^{136} in meteoritic xenon which we cannot explain in any really satisfactory manner. If, nonetheless, the mass fractionation is real, Murray is deficient in Xe^{129}. This would mean that I^{129} decay has contributed to Xe^{129} in the terrestrial atmosphere, as suggested by Katcoff, Schaeffer, and Hastings.[4] For illustrative purposes we assume that the meteorites were all formed 200 million years after the last nuclear synthesizing event.[5] Then we find from differences between Murray and Richardton that (I^{129}/I^{127}) immediately after the event was 0.0021 and that $(Xe^{129}/Xe^{132})_{cosmic}$ is 0.93. This means that about five percent of terrestrial Xe^{129} is due to I^{129} decay. Repeating the calculation of Katcoff, Schaeffer, and Hastings,[4] we find that the earth was isolated from cosmic xenon 250 million years after the last nuclear synthesis. The 50-million year interval thus found for the period between meteorite and earth formation does not depend upon the 200-million year value assumed for $(\Delta t)_{meteorites}$.

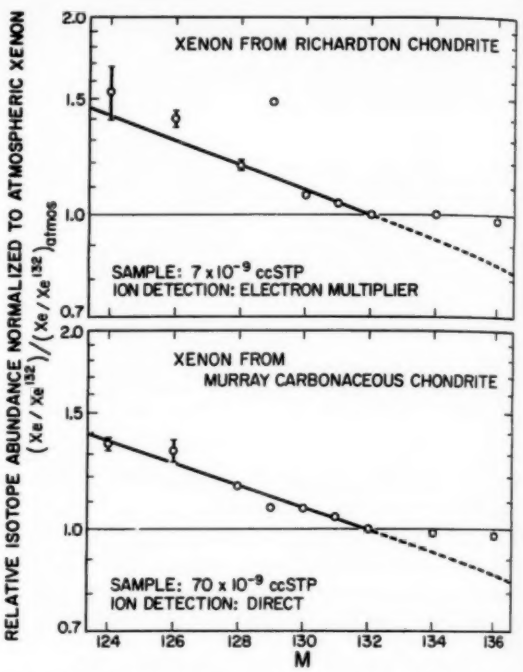

FIG. 1. Isotopic composition of xenon from the meteorites.

I wish to thank Mr. S. Putnam for assistance with the gas extraction apparatus and Mr. L. Kovich for making the flame photometric potassium determinations. The samples of Murray were from the U. S. National Museum, Washington. I wish to thank Mr. E. P. Henderson of that institution for his cooperation. I am grateful to Professor Calvin of this University for providing samples of Murray for our first measurements.

*Work supported in part by the U. S. Atomic Energy Commission.

[1]J. H. Reynolds, Phys. Rev. Letters 4, 8 (1960).

[2]H. Hamaguchi, G. Reed, and A. Turkevich, Geochim. et Cosmochim. Acta 12, 337 (1957).

[3]E. K. Gerling and L. K. Levskii, Doklady Akad. Nauk S.S.S.R. 110, 750 (1956).

[4]S. Katcoff, O. A. Schaeffer, and J. M. Hastings, Phys. Rev. 82, 688 (1951).

[5]G. J. Wasserburg, W. A. Fowler, and F. Hoyle, Phys. Rev. Letters 4, 112 (1960).

GENERALIZATION OF THE APPLETON-HARTREE MAGNETO-IONIC FORMULA

H. K. Sen and A. A. Wyller
Geophysics Research Directorate, Air Force Cambridge Research Center, Bedford, Massachusetts
(Received March 1, 1960)

The classical Appleton-Hartree formula describes the magneto-ionic dispersion of electromagnetic waves in the ionosphere. The effects of electron-neutral collisions are taken into account by a "friction" term, ν, in the equation of propagation. This term, a collisional frequency term, is assumed to be independent of the electron velocities. Such an assumption is not valid in view of the recent laboratory results of Phelps and Pack.[1] They found that to a good approximation the above collision frequency is proportional to the electron energy in nitrogen gas.

Several workers[2-5] have previously tried to generalize suitably the classical Appleton-Hartree formula taking into account the effect of the electron velocity distribution function. In our opinion the most successful attempt so far, has been achieved by Jancel and Kahan[5] in a treatment based upon the Chapman-Enskog method of solving the Boltzmann transport equation. However, at the time of their study the laboratory results quoted above were not known. Consequently the theory was not pushed to a practical limit in its application.

In the present communication we will briefly report on a generalization which incorporates in applicable form these recent laboratory results. A further account will be published elsewhere.

The generalization of the Appleton-Hartree formula essentially involves a generalization of the conductivity tensor, σ, and subsequently the dielectric tensor, ϵ. We have solved the Boltzmann transport equation for a uniform Lorentz gas in a magnetic field, adopting the Chapman-Enskog method of expansion for the velocity distribution function. The method is identical to that of Jancel and Kahan, but the resultant expressions are formally simpler. In this particular case the Chapman-Enskog method and the method used by Allis[6] of expanding the velocity distribution function, yield identical results as expected.

The solution of the resulting determinantal equation from Maxwell's equations and the generalized dielectric tensor yields the following expression for the complex refractive index:

$$\frac{c^2}{u^2}=\left(n-i\frac{c\kappa}{\omega}\right)^2 = \frac{A+B\sin^2\phi\pm(B^2\sin^4\phi-C^2\cos^2\phi)^{1/2}}{D+E\sin^2\phi}, \quad (1)$$

where $A=2\epsilon_I(\epsilon_I+\epsilon_{III})$, $B=\epsilon_{III}(\epsilon_I+\epsilon_{III})+\epsilon_{II}^2$, $C=2\epsilon_I\epsilon_{III}$, $D=2\epsilon_I$, $E=2\epsilon_{III}$, and ϕ is the angle between the direction of propagation and the magnetic field. The principal axes of the generalized dielectric tensor are ϵ_I, ϵ_{II}, and ϵ_{III} and will be evaluated later.

This expression is identical with that derived originally by Jancel and Kahan.[5] They were able to show that in the case where $\nu \ll \omega$ the expression degenerates into the classical Appleton-Hartree formula.[7]

The close relationship between the generalized expression and the classical form is brought out better by rearranging the above expression into the following:

$$\frac{c^2}{u^2}=\left(n-i\frac{c\kappa}{\omega}\right)^2 = 1+\frac{1+A'\sin^2\phi}{B'+C'\sin^2\phi\pm(D'\sin^4\phi+E'\cos^2\phi)^{1/2}}, \quad (2)$$

where

$$A'=\frac{[\epsilon_{III}(1-\epsilon_I-\epsilon_{III})-\epsilon_{II}^2]}{\epsilon_I[(1-\epsilon_I-\epsilon_{III})^2+\epsilon_{II}^2]}, \qquad B'=\frac{-(1-\epsilon_I-\epsilon_{III})}{[(1-\epsilon_I-\epsilon_{III})^2+\epsilon_{II}^2]}, \qquad C'=\frac{-[\epsilon_{III}+\epsilon_{III}(1-\epsilon_I-\epsilon_{III})-\epsilon_{II}^2]}{2\epsilon_I[(1-\epsilon_I-\epsilon_{III})^2+\epsilon_{II}^2]},$$

$$D'=\frac{[\epsilon_{III}(\epsilon_I+\epsilon_{III})+\epsilon_{II}^2]^2}{4\epsilon_I^2[(1-\epsilon_I-\epsilon_{III})^2+\epsilon_{II}^2]^2}, \qquad E'=\frac{-\epsilon_{II}^2}{[(1-\epsilon_I-\epsilon_{III})^2+\epsilon_{II}^2]^2}.$$

In contrast, the classical Appleton-Hartree expression is of the form[8]:

$$\frac{c^2}{u^2}=\left(n-i\frac{c\kappa}{\omega}\right)^2$$

$$=1+\frac{1}{B''+C''\sin^2\phi\pm(D''\sin^4\phi+E''\cos^2\phi)^{1/2}}, \quad (3)$$

where

$$s=\frac{eH_0}{m}, \quad B''=\frac{-(\omega^2+i\nu\omega)}{\omega_0^2},$$

$$C''=\frac{-\omega^2 s^2}{2\omega_0^2(\omega_0^2-\omega^2+i\nu\omega)},$$

$$D''=\frac{\omega^4 s^4}{4\omega_0^4(\omega_0^2-\omega^2+i\nu\omega)^2}, \quad E''=\frac{\omega^2 s^2}{\omega_0^4}.$$

It is important to note that when the classical dielectric tensor elements are substituted into the coefficients A', B', C', D', and E', the generalized expression reduces to the classical Eq. (3). Then the new term $A'\sin^2\phi$ introduced into the generalized expression vanishes as A' goes identically to zero.

We have studied some numerical applications of the above generalized expression (1). The coefficients A, B, C, D, and E are complex quantities, which for arbitrary ϕ are somewhat complicated in structure. Fortunately, it is now possible quite simply to evaluate the dielectric tensor elements ϵ_{I}, ϵ_{II}, and ϵ_{III} in terms of recently tabulated $\mathfrak{G}$ integrals.[9] These have been applied by Phelps and Pack[1] to the problem of electron collision frequencies to the ionospheric D layer.

The following quantities are defined:

$$a=\frac{\omega_0^2}{\nu_m^2}\,\mathfrak{G}_{3/2}\left(\frac{\omega}{\nu_m}\right), \quad b=\frac{5\omega_0^2}{2\omega\nu_m}\,\mathfrak{G}_{5/2}\left(\frac{\omega}{\nu_m}\right),$$

$$c=\frac{\omega_0^2(\omega-s)}{\omega\nu_m^2}\,\mathfrak{G}_{3/2}\left(\frac{\omega-s}{\nu_m}\right), \quad d=\frac{5\omega_0^2}{2\omega\nu_m}\,\mathfrak{G}_{5/2}\left(\frac{\omega-s}{\nu_m}\right),$$

$$e=\frac{\omega_0^2(\omega+s)}{\omega\nu_m^2}\,\mathfrak{G}_{3/2}\left(\frac{\omega+s}{\nu_m}\right), \quad f=\frac{5\omega_0^2}{2\omega\nu_m}\,\mathfrak{G}_{5/2}\left(\frac{\omega+s}{\nu_m}\right),$$

where

$$\mathfrak{G}_p(x)\equiv\frac{1}{p!}\int_0^\infty\frac{\epsilon^p e^{-\epsilon}d\epsilon}{\epsilon^2+x^2}, \quad \nu=\nu_m\epsilon, \quad \epsilon=\frac{mv^2}{2kT},$$

v being the electron velocity. Then the principal axes of the generalized dielectric tensor are expressed as follows:

$$\epsilon_{\mathrm{I}}=(1-a)-ib, \quad \epsilon_{\mathrm{II}}=\tfrac{1}{2}(f-d)+\tfrac{1}{2}(c-e)i,$$

$$\epsilon_{\mathrm{III}}=[a-\tfrac{1}{2}(c+e)]+[b-\tfrac{1}{2}(f+d)]i.$$

The generalization is of little interest when $\nu_m \ll \omega$. In that case we can retain the classical Appleton-Hartree formula provided the friction term, ν, is multiplied by a factor $\frac{4}{5}$ (see Pfister[3] and Westfold[4]). However, in recent years an interest has developed in transmission of low-frequency radio waves with application to the ionospheric D layer and in telemetry. In both cases the condition $\nu_m \approx \omega$ is of considerable interest.

We have therefore studied a longitudinal and a transversal propagation ($\phi=0$ and $\phi=\pi/2$, respectively), where ω, ν_m, and s are of the same order of magnitude. These angles of propagation should give, respectively, minimum and maximum effects in n and $c\kappa/\omega$. The following representative values were adopted from Goubau[10]:

$$\omega=3.86\times10^6, \quad \nu_m=\omega/2=1.93\times10^6, \quad s=8.69\times10^6.$$

The results of the calculations are shown in Figs. 1 and 2. In both cases we notice that the generalized and classical expressions for n and

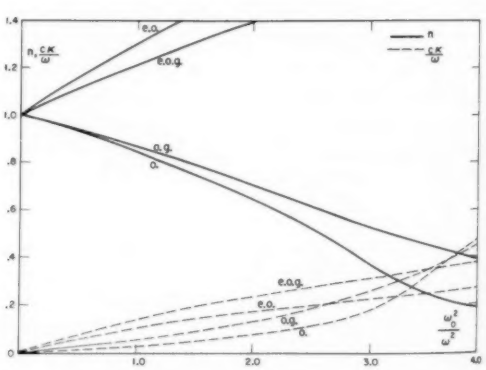

FIG. 1. The real refractive index, n, and the absorptivity, $c\kappa/\omega$, as a function of the square of the ratio of the plasma frequency, ω_0, to the wave frequency, ω, for longitudinal propagation ($\phi=0$). Here o. = ordinary ray (classical theory), e.o. = extraordinary ray (classical theory), o.g. = ordinary ray (generalized theory), e.o.g. = extraordinary ray (generalized theory).

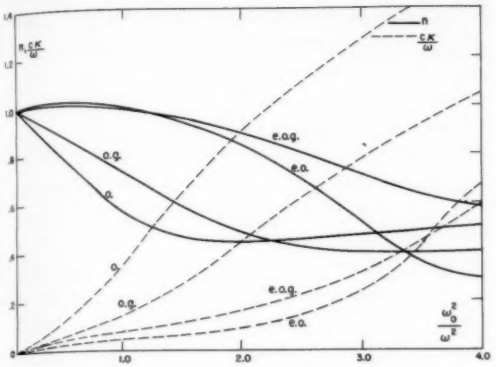

FIG. 2. The real refractive index, n, and the absorptivity, $c\kappa/\omega$, as a function of the square of the ratio of the plasma frequency, ω_0, to the wave frequency, ω, for transversal propagation ($\phi=\pi/2$). Here o. = ordinary ray (classical theory), e.o. = extraordinary ray (classical theory), o.g. = ordinary ray (generalized theory), e.o.g. = extraordinary ray (generalized theory).

$c\kappa/\omega$ may differ up to 100% or by a factor of 2. The effects are pronounced for the attenuation factor, $c\kappa/\omega$, over most wave frequencies, and for the real refractive index when $\omega \ll \omega_0$.

We have also studied the case when $\nu_m = 2\omega$ and find results similar to the above. We, therefore, conclude that for any precise work involving attenuation effects, use should be made of the generalized expression when $\nu_m \gtrsim \omega$. For arbitrary ϕ it appears most convenient to retain the form of Eq. (1), as it provides simpler algebraic means for separating the real and imaginary parts of the expression.

[1]A. V. Phelps and J. L. Pack, Phys. Rev. Letters 3, 340 (1959).
[2]L. G. H. Huxley, Phil. Mag. 23, 210, 442 (1937); 25, 148, 388 (1938).
[3]W. Pfister, The Physics of the Ionosphere (Cambridge University Press, New York, 1954), p. 394.
[4]K. C. Westfold, Phil. Mag. 44, 711 (1953).
[5]R. Jancel and T. Kahan, J. phys. radium 16, 136 (1955); Nuovo cimento 12, 573 (1954).
[6]W. P. Allis, Handbuch der Physik (Springer Verlag, Berlin, 1956), Vol. 21, p. 413.
[7]R. Jancel and T. Kahan, J. phys. radium 15, 696 (1954).
[8]S. K. Mitra, The Upper Atmosphere (The Royal Asiatic Society of Bengal, Calcutta, 1952), p. 629.
[9]R. B. Dingle, D. Arndt, and S. K. Roy, Appl. Sci. Research 6B, 155 (1957).
[10]G. Goubau, Hochfrequenztechn. u. El. Akustik 45, 179 (1935).

PHOTON MOMENTUM EFFECTS IN THE MAGNETO-OPTICS OF EXCITONS

J. J. Hopfield and D. G. Thomas
Bell Telephone Laboratories, Murray Hill, New Jersey
(Received February 26, 1960)

The optical selection rules and energy levels for exciton and band-to-band transitions as ordinarily calculated ignore the small but finite wave vector of visible light. No effects due to the finite wave vector have previously been noticed except the occasional observation of weak forbidden lines.[1] We describe here two pronounced magneto-optic effects (on excitons) due to the finite wave vector of light. The first effect is the drastic alteration of the magneto-optic absorption spectrum when the magnetic field is reversed; the second effect arises from the quasi-electric field $(1/c)\vec{v}\times\vec{H}$ due to the motion of the exciton in a uniform magnetic field. Only the first effect has been positively identified. These effects were investigated while determining effective masses and g values from exciton magneto-optic effects in CdS.

Observations were made on the $n=2$ P states of excitons formed from the top valence band in hexagonal CdS. Magneto-absorption experiments were performed at 1.6°K on platelets 5-10 μ thick mounted to minimize strains. The plane of the platelet contained the c axis. The incident light was polarized parallel to the c axis and normally incident on the platelets. The magnetic field was perpendicular to both the c axis and the direction of propagation of the light. The states of interest are six "P" states, $P_{x\pm}, P_{y\pm}, P_{z\pm}$, corresponding to the three P orbitals and the two electron spin orientations (- parallel and + antiparallel to the magnetic field). The sign of the electron g value is assumed to be negative. This assumption influ-

ences only the nomenclature. The g value of the hole is zero for magnetic fields perpendicular to the c axis. S states, both longitudinal and transverse (denoted S_L and S_T), are also observed.[2]

Figure 1(c) shows the absorption spectrum for $H = 0$. Figure 1(b) shows the absorption spectrum for $H = 31\,000$ gauss. Figure 1(a) shows the absorption spectrum in an experiment identical to that of 1(b) except that H is in the opposite direction. One sees that in 1(a) lines P_{x-}, P_{y-}, and P_{z-} are strong, while P_{x+}, P_{y+}, and P_{z+} are weak. (In the present notation, x is parallel to H, and z parallel to the c axis.) When the magnetic field is reversed in 1(b), the previously weak lines become stronger and the strong lines become weaker. Rotation of the crystal by 180° around the c axis does not affect the observed spectrum. Rotation of the crystal by 180° around the direction of propagation of the light reverses the intensity distribution (i.e., this rotation plus field reversal leaves the absorption unchanged). The same effect has been observed in four samples.

Since time reversal reverses the sign of the magnetic field, but leaves the selection rules for infinite wavelength plane polarized light unchanged, the experimental results must be due to the finite wave vector of light and the excitons with which the light interacts. It can easily be shown that if the crystal had inversion symmetry (which wurtzite does not) the effect could not occur even with finite wave vectors.

With no magnetic field, the four states $P_{x\pm}$ and $P_{y\pm}$ (eight states including hole spin) can be considered to be degenerate. Group theory, taking into account the finite wave vector of light and the experimental geometry, indicates that one linear combination of these eight states (derived from Γ_1) has an optical matrix element in the limit $k \to 0$, and that one linear combination (derived from Γ_{5y}) has an optical matrix element proportional to k_y. Utilizing these known linear combinations, the optical matrix elements for states $P_{x\pm}$ can be computed (omitting terms of order k^2). One finds for the states having spins in the plus and minus x directions, respectively,

$$\text{matrix element for spin } +x = A + k_y B,$$

$$\text{matrix element for spin } -x = A - k_y B.$$

In general, the absolute magnitudes of these two optical matrix elements are different as long as both A and B are nonzero. Reversing the direction of k_y reverses the relative magnitude of the two matrix elements. One state (say with spin in the plus x direction) has an energy corresponding to P_{x+} or P_{x-} according to the direction of H. Reversing H therefore interchanges the energy levels of the two spin orientations without altering the optical matrix elements.

The same qualitative behavior is expected of the states $P_{y\pm}$, which are separated from $P_{x\pm}$

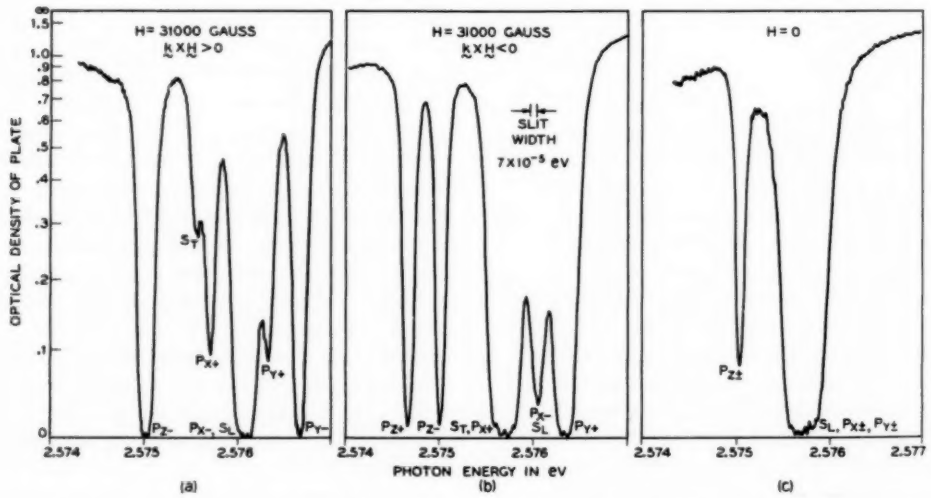

FIG. 1. Microphotometer trace of Zeeman effects in CdS of the $n = 2$ exciton state at 1.6°K. The geometry is $\vec{c} \perp \vec{H}$, $\vec{H} \parallel \vec{x}$, $\vec{k} \perp \vec{H}$, and $\vec{k} \perp \vec{c}$ (approximately).

by a diamagnetic shift and by magnetic mixing with $P_{z\pm}$. Brevity requires the omission of the discussion of the effect of this mixing on the strengths of $P_{y\pm}$ (where the effect is small) and $P_{z\pm}$ (where the effect is large).

The theory indicates that the sign of $(\vec{k}\times\vec{H})\cdot\vec{z}$ should determine which lines are strong. (One should note that $\vec{z}$ and $-\vec{z}$ are not equivalent directions in wurtzite.) The rotation experiments agree with this theoretical conclusion.

The peculiar band structure[3] of CdS makes A rather small and k_yB unexpectedly large for the states under study. Independent evidence in experiments with H parallel to the c axis indicates that $|k_yB/A| \approx \frac{1}{2}$. If A and B have the same phase, this could lead to a 9:1 intensity ratio of strong $P_{x\pm}$ or $P_{y\pm}$ to weak $P_{x\pm}$ or $P_{y\pm}$ lines, in at least qualitative agreement with experiment.

A second effect, independent of the effect just described, should be observable in magneto-optic experiments because of the finite wave vector of light. A quasi-electric field $(1/c)\vec{v}\times\vec{H}$ should act on excitons in a uniform magnetic field due to the exciton center-of-mass velocity (finite wave vector). In CdS, this field should be approximately 150 volts/cm for $H = 30\,000$ gauss. This small electric field is capable of producing observable effects on excitons of large radius (say > 100 A) if the excitons can exhibit a linear Stark effect. We have compared experimental results for $\vec{H}\perp\vec{k}$ and $\vec{H}\parallel\vec{k}$ to look for this effect. Unfortunately we have not yet been able to isolate this effect due to other complications which arise. It should be possible, however, to perform exciton mass spectrometry experiments with crossed electric and magnetic fields. By balancing the quasi-electric field with a real field, $\vec{v}$ (and thus the exciton mass) can be determined.

We wish to thank Dr. W. W. Piper of the General Electric Company Research Laboratory for providing the crystals.

[1]D. G. Thomas, J. Phys. Chem. Solids (to be published).

[2]J. J. Hopfield and D. G. Thomas, J. Phys. Chem. Solids (to be published).

[3]D. G. Thomas and J. J. Hopfield, Phys. Rev. 116, 573 (1959).

PHOTOSENSITIVE ULTRASONIC ATTENUATION IN CdS

Harmon D. Nine
Research Laboratories, General Motors Corporation, Warren, Michigan
(Received February 15, 1960)

It has been observed in this laboratory that the physical acoustical properties of CdS crystals are influenced by photon irradiation. Upon illumination with white light from an incandescent lamp, the ultrasonic wave propagation measured by the change in ultrasonic attenuation was found to be changed in large single crystal of CdS. Each crystal was prepared for the attenuation measurements by lapping two parallel (within 0.000020 in./in.) faces normal to the c axis (within $\pm 0.5°$). Electroplated indium electrical contacts were attached to opposite sides of the crystals halfway between the lapped faces so that bulk photoconductance measurements could be made simultaneously.

Using the technique of Roderick and Truell[1] the ultrasonic attenuation in CdS was measured as a function of light intensity and wavelength. The effect of light intensity on the ultrasonic attenuation (measured at 5800 A) proved to be linear but of opposite direction in two crystals examined. In crystal A the ultrasonic attenuation of compressional waves was decreased by illumination with white light. In crystal B the attenuation was increased. The attenuation effect in crystal B was about an order of magnitude greater than the opposite effect in crystal A. (See Table I.)

These effects on the ultrasonic attenuation were noted for compressional waves propagated along the c axis over the ultrasonic frequency range from 10 Mc/sec to 200 Mc/sec. No effect was noted for shear waves along the c axis over the same frequency range. In addition, qualitative measurements indicate that the effect is different for waves propagated normal to the c axis. (See Table I.)

The ultrasonic attenuation and the photoconductance were simultaneously measured as a function of wavelength. Figures 1 and 2 show the spectral responses of the ultrasonic attenuation

Table I. The ultrasonic attenuation characteristics for incandescent white light and the physical properties of the CdS crystals used.[a]

Crystal	Attenuation effect: c axis Compressional	c axis Shear	Normal to $\{1,\bar{1},0,0\}$ plane Compressional	Normal to $\{1,\bar{1},0,0\}$ plane Shear	Impurity content: Zn	Mg	Si	Cu	Thickness along c axis and (area of face)	Natural color	Room temperature luminescence (3650A irradiation)
A	Decrease	NE	NE	Small decrease	0.04	0.0001	0.001	0.0004	1.04 cm (2.3 cm²)	Med. amber	Red
B	Increase	NE	NM	NM	0.01	0.0001	0.001	0.0004	0.63 cm (1.4 cm²)	Dark amber	Dull red
C	Decrease	NE	NM	NM	ND	0.0001	0.001	0.0002	1 cm (1.2 cm²)	Light amber	Red-green

[a]ND—not detected; NE—no effect; NM—not measured.

and the photoconductances for the CdS crystals. In both the attenuation and photoconductance measurements, long response times from point to point (as much as a day) were noted. The crystals exhibit the ultrasonic attenuation effect over the same range of light wavelengths as the response region of the photoconductance effect—from the band edge for CdS at about 5100 A up to about 8000 A in the infrared.

In both crystals the phenomenon of infrared quenching of the photoconductance was observed. Similarly the ultrasonic attenuation effect in

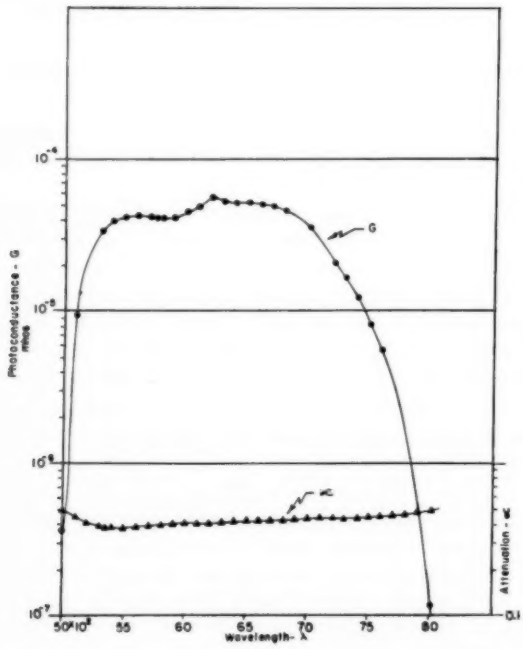

FIG. 1. Photoconductance G and ultrasonic attenuation constant α vs light wavelength in angstroms for CdS crystal A. The ultrasonic attenuation is of the form $I=I_0e^{-\alpha l}$ and was measured at 30 Mc/sec.

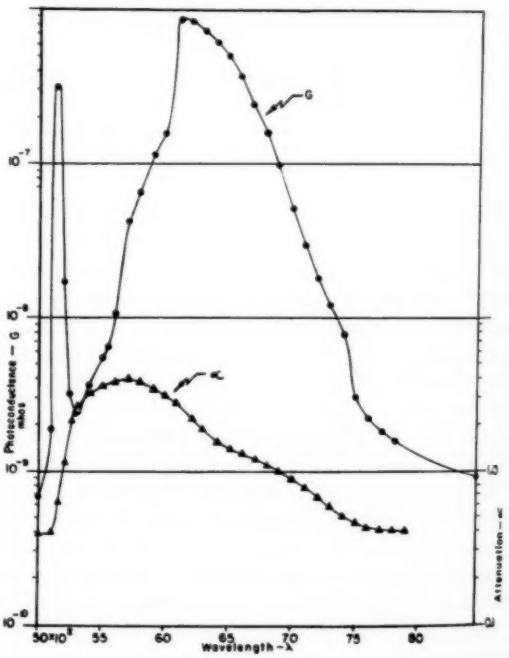

FIG. 2. Photoconductance and ultrasonic attenuation measured at 45 Mc/sec vs light wavelength in angstroms for CdS crystal B.

crystal B was quenched to the dark value by infrared but the attenuation effect in crystal A was unaffected by infrared.

A semiquantitative spectrographic analysis revealed little difference between the two crystals. In Table I are included some properties of the two crystals A and B and also those of a third crystal, C, upon which qualitative measurements have been made.

Two types of mechanisms are being considered as possible explanations of the ultrasonic attenuation changes: (1) relaxation associated with electron or hole trapping at impurity or vacancy sites, or with electron transitions at sulfur photoactivation sites, and (2) changes in thermoelastic attenuation losses due to heat conduction by photoactivated electrons. It is believed that the ultrasonic attenuation effect may be found in other photosensitive crystals and may be a useful tool for solid state investigation of photoconductors.

The author wishes to thank Norman W. Schubring of this laboratory for many valuable discussions relating to this study. The author also expresses his gratitude to Y. T. Sihvonen and D. R. Boyd of this laboratory who grew the CdS crystals[2] and through whose cooperation the photoconductance measurements were made. The advice of Professor R. Truell and his associates of Brown University in the technique of ultrasonic attenuation measurements is gratefully acknowledged.

[1]R. Roderick and R. Truell, J. Appl. Phys. 23, 267 (1952).

[2]D. R. Boyd and Y. T. Sihvonen, J. Appl. Phys. 30, 176 (1959).

EXPERIMENTAL PROOF OF THE EXISTENCE OF A NEW ELECTRONIC COMPLEX IN SILICON

J. R. Haynes
Bell Telephone Laboratories, Murray Hill, New Jersey
(Received February 18, 1960)

Recombination radiation from silicon crystals containing one of the group III or group V elements as an added impurity has recently been examined using a spectroscope of high resolution. Extremely sharp lines appear at low temperatures. It will be shown that these lines can only be interpreted as the radiation produced by the recombination of an electron and a hole both of which are bound in an immobile four-particle complex consisting of an impurity ion and three electronic particles.

Excess electrons and holes were produced in silicon single crystals by illumination with a high-intensity light beam.[1] These carriers recombine in thermal equilibrium with the crystal lattice giving recombination radiation. The intensity of this radiation as a function of photon energy is shown in Fig. 1 for two different silicon specimens at 25°K: (1) a crystal containing a negligible amount of impurity, shown by the dashed line; (2) a crystal containing arsenic added to the melt in the crystal growing process, shown by the solid line.

The dashed trace is essentially all intrinsic recombination radiation produced by the recombination of excitons with simultaneous photon and phonon emission. The energy of the exciton, E_0,

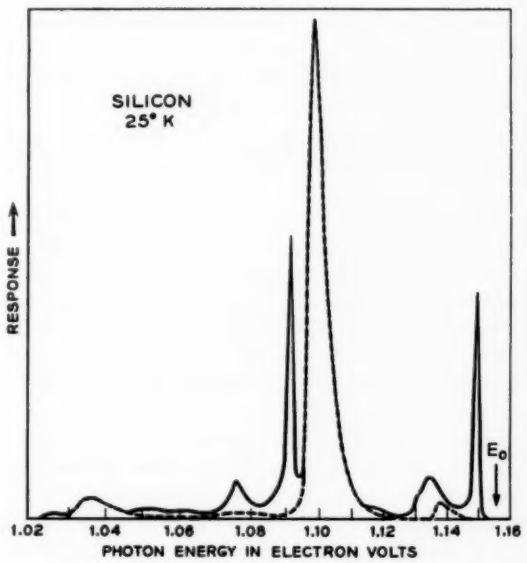

FIG. 1. Spectrometer response (nearly proportional to the number of photons/unit energy interval) as a function of the energy of the photons for two silicon crystals: (1) A specimen containing a negligible amount of impurity, shown by the dashed trace. (2) A specimen containing 8×10^{16} cm^{-3} arsenic atoms, shown by the solid trace.

is shown at 1.156 ev which is less than the energy gap by an amount equal to the exciton binding energy. The principal line is produced by the recombination of excitons that conserve crystal momentum by the emission of a transverse optical (TO) phonon. The line width is primarily due to differences in thermal velocities of the excitons. The line shape is given by a Boltzmann energy distribution with a small amount of broadening produced by exciton collisions with the crystal lattice.

The result of adding 8×10^{16} cm^{-3} arsenic atoms to the silicon in the crystal-growing process is shown in Fig. 1 by the solid trace. The prominent change produced by adding the arsenic is to introduce two new sharp lines at 1.091 and 1.149 ev. These lines are actually much narrower than shown in Fig. 1 since their half-intensity width, W, is the effective slit width of the spectrometer. By narrowing the spectrometer slit, at the expense of signal to noise ratio, it has been found that $W<0.0005$ ev. Evidently the lines are produced by the recombination of an electron and hole both of which are immobilized, since if either were free to move the lines would have the width of a Boltzmann energy distribution.

The ratio of the integrated intensity in the sharp lines to that in the principal exciton line is found to be proportional to the amount of arsenic added. Therefore, the recombining hole and electron responsible for the sharp lines are bound in some kind of complex to single arsenic atoms.

The energy difference of the two sharp lines is the energy of the TO phonon. Evidently recombination proceeds both with and without phonon emission. In the latter case the crystal momentum is conserved with negligible energy loss by giving it to the crystal as a whole via the arsenic atom with which the hole and electron are associated.

The energy, E_D, required to free the bound electron and hole as an exciton from the complex has been measured from the energy displacement of the lines. Since the sharp line at 1.091 ev and the main exciton line are both produced by emission of the same phonon, E_D is the energy difference between the center of the sharp line and the radiation produced by recombining excitons having zero thermal energy (obtained by a Boltzmann energy curve fit to the exciton line). This energy has also been calculated from measurements of the amount that the sharp lines shrink with respect to the exciton line as the temperature of the silicon crystal is increased.[2] Both ways of obtaining E_D give values very close to 0.0065 ev.

These same sharp lines appear when other group V donors are substituted for arsenic as an impurity. The lines, however, are displaced in energy in a regular way. The dissociation energies of the complex produced by adding donors are shown in Fig. 2 plotted as a function of the ionization energy of the donor, E_i (open circles). To a good approximation $E_D=0.1E_i$.

This energy relationship identifies the complex as a hole bound to a positive donor ion by an electron pair bond, since the other two possibilities are eliminated as follows: (1) It cannot be a hole bound by a single electron to the donor ion since then $E_D=E_i-E_x+E_h$, where E_h is the binding energy of the hole, and the binding energy of the exciton, $E_x\approx0.007$ ev.[3] Therefore, $E_D\gtrsim E_i$ for this model. (2) It cannot be an exciton trapped at a neutral donor by mutual polarization since then E_D would decrease as E_i increases.

These sharp lines are also produced by adding group III acceptors to silicon. The dissociation energies of the complex responsible for the lines are also shown in Fig. 2 as a function of the ionization energy of the acceptor introduced (solid circles). Again it is found that $E_D=0.1E_i$. Therefore, this complex is identified by iden-

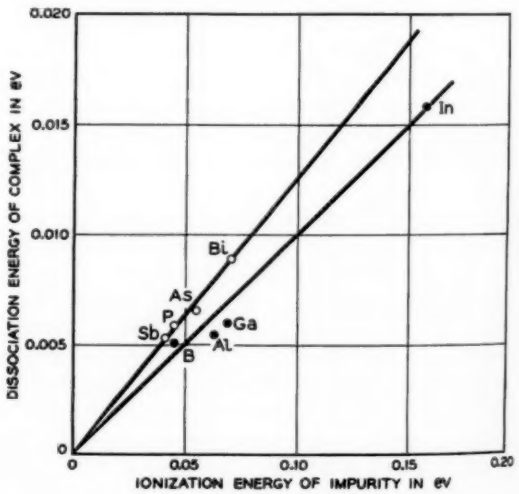

FIG. 2. Energy required to remove an exciton from the complex as a function of the ionization energy of the impurity involved.

tical reasoning as the same complex that was obtained by adding donors, except for complete charge sign reversal. It is an electron bound to a negative acceptor ion by a hole pair bond.

The existence of this complex was pointed out by Lampert[4] who estimated its dissociation energy for equal masses of electrons and holes from Ore's calculation[5] of the minimum dissociation energy of a positron bound to a negative hydrogen ion. However, since Ore's calculated value is more than an order of magnitude too low,[6] Lampert's estimate of E_D is correspondingly in error. This is shown by a simple argument by Kohn[7] who is able to place E_D between $0.055E_i$ and $0.35E_i$ in satisfactory agreement with experiment.

It is a pleasure to thank M. Lax for helpful discussions and W. F. Flood for the specimens and data.

[1]J. R. Haynes, Methods of Experimental Physics, edited by K. Lark-Horovitz and V. A. Johnson (Academic Press, Inc., New York, 1959), Vol. 6, Part B, p. 322.

[2]The equation used is $R_1/R_2=(T_2^{3/2}/T_1^{3/2})\exp(E_D/kT_1-E_D/kT_2)$, where R is the ratio of the area under the sharp lines to that under the exciton line at temperature T. A factor N_1/N_2 should be included if the neutral donor population changes significantly between T_1 and T_2.

[3]G. G. Macfarlane, T. P. McLean, J. E. Quarrington, and V. Roberts, Phys. Rev. 111, 1245 (1958).

[4]M. A. Lampert, Phys. Rev. Letters 1, 450 (1958).

[5]A. Ore, Phys. Rev. 83, 665 (1951).

[6]Using the experimentally determined value of $E_D=0.1E_i$ and reversing Lampert's argument, we obtain a value for the dissociation energy of a positron bound to a negative hydrogen ion (or an electron bound to an antiproton by two positrons) of $0.1(13.6)=1.4$ ev. This is 20 times as large as Ore's calculated value.

[7]Walter Kohn (personal communication). His reasoning follows: For donor impurities the minimum energy of the complex will occur when the effective mass of the hole, $m_h \ll m_e$, the effective mass of the electron. For this condition the "Bohr radius" of the hole is so much larger than that of the two electrons that the system can be considered as consisting of a hole bound to a single negative electronic charge of relatively infinite mass. The dissociation energy $E_D=E_1+E_2-E_\chi$, where E_1 is the energy required to remove the hole, E_2 is the energy required to remove one of the electrons, and E_χ is the energy gained in forming an exciton out of the freed electron and hole. But $E_1=E_\chi$ so that $E_D/E_i=E_2/E_i$, where E_2 is the energy required to remove an electron from a negative hydrogen ion (0.75 ev) and E_i is the ionization energy of hydrogen (13.6 ev). Thus, the minimum energy of $E_D/E_i=0.055$. The value of E_D/E_i will increase monotonically with m_h/m_e, reaching (when $m_h \gg m_e$) the asymptotic value $E_D/E_i=$(dissociation energy of a hydrogen molecule)$/E_i=4.5/13.6=0.33$.

SEARCH FOR DOUBLE-QUANTUM EMISSION IN THE DECAY OF Xe^{131m}

Torsten Alväger and Hans Ryde
Nobel Institute of Physics, Stockholm, Sweden
(Received March 14, 1960)

As a competing process to the single-quantum decay of an excited nuclear state there is a double-quantum transition in which two gamma rays or conversion electrons are emitted simultaneously.[1,2,3] This second order process gives rise to a continuous distribution of the emitted gamma rays. The structure of this distribution depends mainly on the multipolarity of the two transitions. To date no experimental evidence has been found for the existence of two-quantum emission.

The possibility for detecting two-quantum emission should be largest when the single quantum transition is suppressed. This is, for example, the case in the 0+→0+ transition in Zr^{90}, where a single gamma transition is forbidden. The intense bremsstrahlung from the decay of Y^{90} seems, however, to make the observation of the double-quantum emission difficult. Another possibility for studying the double-quantum emission is in connection with a transition of high multipolarity. In this case the de-excitation can occur also by the emission of two quanta of lower multipolarities. This should be the situation in the decay of the isomeric $h_{11/2}$ level in Xe^{131} to the ground state by the 164-kev $M4$ transition. The relative intensity of any other gamma ray in this decay is estimated to be very low. Using an harmonic oscillator potential, Eichler and Jacob[3] have calculated the ratio between the transition probabilities for double- and single-quantum emission in the decay of Xe^{131m}. They obtained the ratio 5×10^{-5}. The weak, two-quantum distribution is very difficult to observe di-

rectly as it is usually masked by other processes giving similar distributions (i.e., Compton processes and bremsstrahlung). However, it would be possible to investigate the double-quantum emission by studying coincidences with the x rays from the internal conversion. Transitions of all energies are then detected in a narrow region (as x rays), which makes the observation more favorable compared with a distribution measurement.

The source, used in this investigation of the decay of Xe^{131m}, was prepared by an electromagnetic isotope separation of Xe, which was previously isolated as the daughter product of I^{131}. The strength of the Xe source was about 0.1 μC. The sample was placed between two NaI(Tl) crystals with 180° geometry. The backscattering from one crystal to the other was hindered by a lead and copper shield between the crystals. The source was surrounded by a thin Al foil stopping the conversion electrons. The pulses from one crystal were fed to a multichannel pulse-height analyzer, while the pulses from the other one were introduced into a single-channel analyzer. The position of this was varied in steps over the whole energy region up to 165 kev, while the multichannel analyzer in all cases recorded pulses corresponding to the x-ray region. Figure 1 shows the coincidence counting rate for the x-ray peak for different positions of the single channel. The points are corrected for the decay of the sample ($T_{1/2} = 12$ days), and also for the change in coincidence efficiency when both channels accept pulses due to x rays.

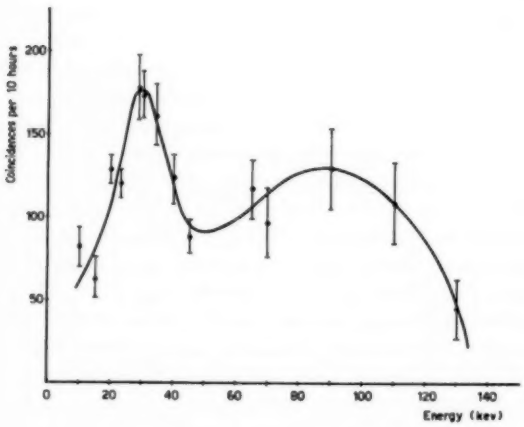

FIG. 1. Coincidence measurements between γ and x rays in the decay of Xe^{131m}.

For each position of the single channel, the pulses obtained which are in coincidence with the x-ray pulses detected in the multichannel analyzer can be due to different processes. No genuine coincidences with x rays occur to a first approximation with the Xe^{131m} sample, but a small I^{131} impurity gives rise to real coincidences. The correction due to the admixture of I^{131} is, however, very small. The rate of accidental coincidences is measured to be less than 2% of the observed counting rate. Other events that may contribute to the observed effect are:

(1) Scattering from one crystal to the other, especially of iodine x-ray escape photons. These effects are suppressed to a negligible value by the lead shield between the crystals.

(2) Internal Compton effect, which should be small for this transition energy.

(3) External bremsstrahlung from the conversion electrons, which is measured to be negligible.

(4) Compton scattering by K electrons (negligible).

(5) K-electron ionization of Xe (about 1 μg carrier in the sample), by the emitted K conversion electrons. This has been checked to be negligible.

(6) An intermediate level.

(7) Double-quantum emission.

Among these effects, only the last three are able to give rise to the observed peak in Fig. 1. As No. 5 is negligible and No. 6 is very improbable, the two-quantum emission is the most probable possibility. This is also supported by the measured distribution in Fig. 1.

From the peak in Fig. 1 it is possible to estimate the ratio between the double- and single-quantum emission. Assuming transitions of $E2M2$ type, a ratio of about 2×10^{-3} is obtained after correction for internal K conversion. This ratio, however, contains a large uncertainty, mainly due to the fact that the conversion coefficients used are those calculated for emission of only one electron, while in the present case there is an emission of two K conversion electrons simultaneously.

[1]M. Göppert-Mayer, Ann. Physik 9, 273 (1931).
[2]R. G. Sachs, Phys. Rev. 57, 194 (1940).
[3]J. Eichler and G. Jacob, Z. Physik 157, 286 (1959).

RESONANT ELASTIC SCATTERING OF C^{12} BY CARBON

D. A. Bromley, J. A. Kuehner, and E. Almqvist
Atomic Energy of Canada Limited, Chalk River, Ontario, Canada
(Received February 29, 1960)

The elastic scattering of C^{12} by carbon has been studied in the range $6 \leq E_{lab}{}^{C} \leq 29$ Mev, using high-resolution Au-Si surface barrier detectors[1] and carbon ion beams of precisely defined energy from the Chalk River tandem accelerator. Excitation curves have been measured for $\theta_{lab} = 45°$, 28.8°, and 19.5°; at energies above the Coulomb barrier, those at 45° and 28.8° show pronounced resonance structure corresponding to excitations in $Mg^{24} \geq 24$ Mev while that at 19.5° shows only very weak residual structure. This is believed to be the first reported example of such resonant phenomena in heavy-ion reactions. In marked contrast to these results for the C+C system, similar measurements for O^{16} ions on oxygen targets show no such resonant behavior corresponding to similar excitations in S^{32}. The binding energies in Mg^{24} and S^{32} are 14.08 and 16.54 Mev, respectively; the calculated[2] Q values for nucleon and alpha emitting reactions are equal to within ~2 Mev for the two systems.

Figure 1 shows the 45° ($\phi_{c.m.} = 90°$) excitation curves for the C+C and O+O systems. The dashed curves show the E^{-2} dependence predicted for pure Coulomb scattering. In view of the agreement between the predicted and measured energy dependence (Fig. 1) and angular dependence (to be discussed later), the cross-section scale in Fig. 1 was obtained by normalizing to the Mott predictions at low energies. In the C+C case, there is no apparent correlation between the structural features of the excitation curves at the different angles studied suggesting that interference effects may be important.

A typical heavy-ion spectrum is inset in Fig. 1. The system energy resolution made it possible to use pulse-height analysis to eliminate contributions from elastic scattering of the incident ions on target contaminants and from inelastic processes without the use of coincidence techniques. With ~50 $\mu g/cm^2$ carbon targets and 2×2 mm detector areas, system resolutions $\lesssim 2\%$ have been obtained using very simple transistorized current preamplifiers.

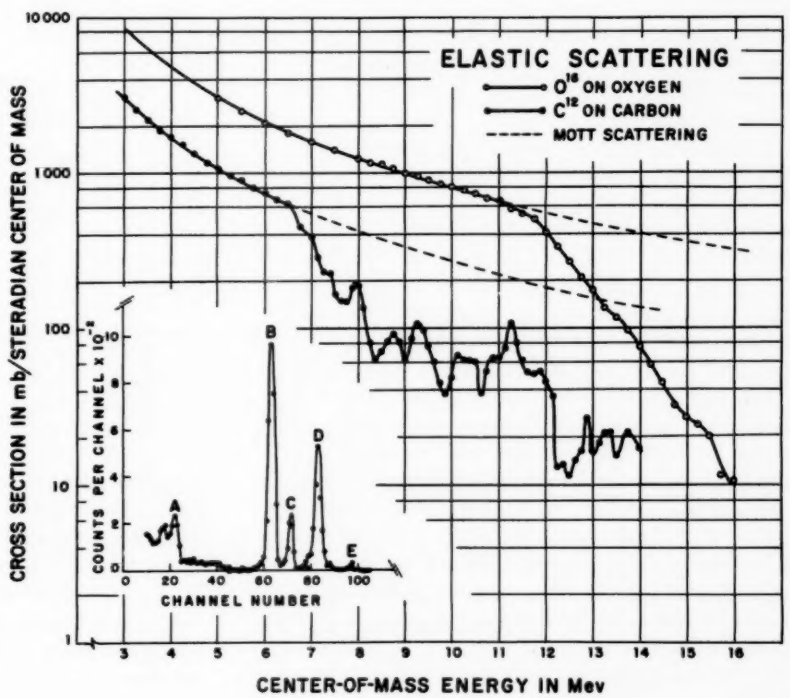

FIG. 1. Excitation curves for the elastic scattering of C^{12} by carbon and of O^{16} by oxygen. Self-supporting targets of carbon (~50 $\mu g/cm^2$) and of SiO (~70 $\mu g/cm^2$) and 5×5 mm Au-Si detectors, have been used in these measurements. The inset figure is a typical spectrum at $\theta_{lab} = 45°$ obtained for 21.0-Mev carbon ions on carbon. The peak legend is as follows: the double peak at A arises from alpha particles and protons from the reaction which completely traverse the junction and thus provide a measure of its thickness. B is from C^{12} elastically scattered by carbon; C is for C^{12} elastically scattered by oxygen; D is from C^{12} elastically scattered by a residual phosphorous contaminant from the stripping compound used in preparing the target, and E is from C^{12} elastically scattered from traces of heavier target contaminants.

Using, as a first approximation, the "quarter point" analysis suggested by Blair,[3] interaction radii of 7.8 and 8.8 f are obtained for the C+C and O+O systems, respectively; these are to be compared to the value of 8.0 f reported previously for the N+N system.[4] Assuming these interaction radii, the classical Coulomb barriers are 6.6 and 10.5 Mev, respectively. As shown in Fig. 1, the shapes of the excitation curves are in good accord with the Mott scattering predictions for energies below the barriers; however, with increasing energy the experimental cross sections are smaller than those predicted. For the O+O system, the almost exponential decrease with very weak superposed structure, is characteristic of essentially all of the previously reported elastic scattering of deuterons,[5] alpha particles,[6] and heavy ions.[7] The results for the C+C system are anomalous not only in that marked resonance structure appears, in some cases with $\Gamma \leq 200$ kev, but also in that the cross section averaged over this resonance structure decreases much less rapidly with increasing energy than in the other cases.

In order to gain further information on this resonance behavior, angular distributions of the elastically scattered carbon ions have been measured at several energies in the range studied; three typical distributions are shown in Fig. 2. As anticipated from the excitation curves, at energies below the barrier, the Mott predictions for the Coulomb scattering of identical, spin-zero Bosons is in excellent agreement with the experimental data.

As the energy is increased above the barrier, however, the shape of the angular distributions changes rapidly with energy as shown. This change is not monotonic; the distribution measured at 13.34 Mev, for example, is very similar to that at 11.25 Mev while that at 12.25 Mev is significantly different. Of particular interest is the fact that the experimental minima at $\phi_{c.m.} \simeq 78°$ and 102° do not shift in angle with changing energy as predicted for Mott scattering. Such stationary minima are, however, characteristic of the Blair model[3] predictions. In the case of the 11.25-Mev distribution, for example, the predicted shape of the angular distribution agrees well with that observed for $\phi_{c.m.} \geq 65°$ assuming total absorption of all incident waves up to and including $l_{max} = 6$; however, the predicted cross sections are a factor ~2 less than those observed in this range. This fit is superior to that obtained with $l_{max} \sim 8$, which corresponds classically to the interaction radius quoted.

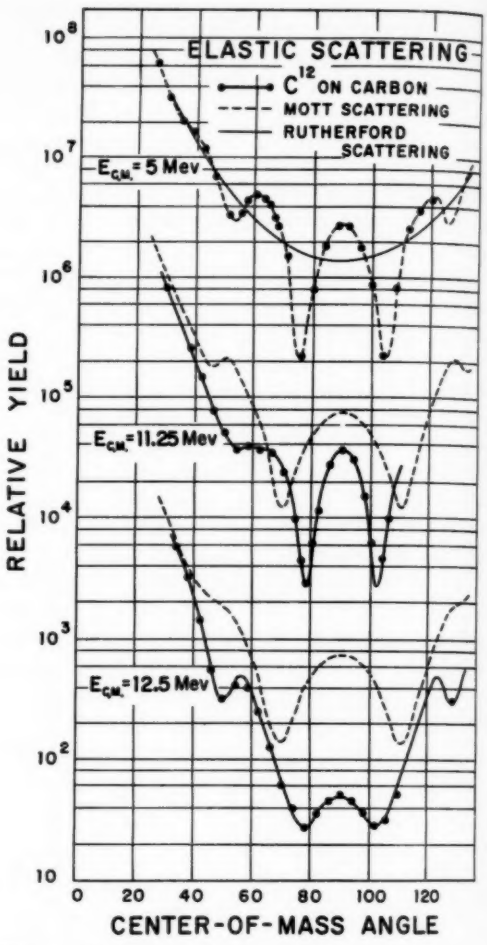

FIG. 2. Typical angular distributions for C^{12} elastically scattered from carbon. The Rutherford and Mott scattering predictions differ only in that the latter includes the quantum mechanical interference term arising from the identity of the incident and target nuclei. The three distributions have been displaced arbitrarily for presentation; however, the corresponding experimental and theoretical curves have been normalized in each case using the data of Fig. 1. An experimental angular resolution ~0.5° has been used in these measurements.

In the case of the 12.5-Mev data there is essentially no agreement for any assumed $l_{max} \leq 10$ since the predicted ratio of the cross section at $\phi_{c.m.} = 90°$ to that at $\phi_{c.m.} = 80°$ is ≥ 10. Significant improvement is obtained by assuming $l_{max} = 6$ and in addition total absorption of $l = 10$ without absorption of $l = 8$, in that the above ratio is

reduced to ~3. More sophisticated analyses of these data are clearly required to produce acceptable fits; such analyses are now in progress using an optical model. The preliminary results obtained with the Blair model do suggest, however, that the resonance structure in the carbon excitation curve reflects the selective absorption of particular incident partial waves to form high-spin states of Mg^{24}.

Any successful explanation of the C+C resonance structure must also include the lack of such structure in the O+O data at corresponding excitations. While the gross structure of the C+C curve ($\Gamma \sim$ few Mev) above the barrier may well reflect size resonances in the effective optical potential, the fine structure ($\Gamma \lesssim 200$ kev) implies the formation of high-spin, quasi-molecular states with $\tau \sim 10^{-21}$ sec. A number of different mechanisms are consistent with these results and while it is not possible to preclude any of these, that which appears most attractive involves the binding of the carbon nuclei into high-spin, dumbbell states through virtual nucleon transfer. On this basis, differentiation between the C+C and O+O systems would reflect the fact that in the energy range accessible, nucleon transfer reactions are energetically forbidden in the former and allowed in the latter, for energies above the Coulomb barrier ($Q \sim -11.5$ Mev). It should be noted however that in the latter case, the transfer reaction products must penetrate much of the Coulomb barrier for the energies involved here. Moreover, in the O+O system both virtual and real transfer reactions involve the transfer of a nucleon between the p and d shells and are thus expected to be inhibited relative to those in the C+C system which are within the p shell.

If it is assumed that the fine structure in the C+C data of Fig. 1 reflects interference between the shape-elastic amplitudes and compound-elastic amplitudes corresponding to the quasi-molecular states (i.e., $\Gamma_{C^{12}} \sim \Gamma_{\text{total}}$ for the latter), the reaction excitation curve would not be expected to show comparable structure (nucleon and alpha emission from such states is inhibited by the changes in shape and angular momentum required). Measurement of this excitation curve is in progress to further elucidate the mechanisms involved.

The results reported herein are part of a program of study of heavy-ion interactions now in progress. Later, more complete publications will present excitation curves at other angles, angular distributions at other energies, and similar measurements for other systems.

We are indebted to Dr. E. Vogt for discussions concerning these results.

[1]J. M. McKenzie and D. A. Bromley, Bull. Am. Phys. Soc. 4, 422 (1959).

[2]V. A. Kravtsov, Uspekhi Fiz. Nauk 65, 451 (1958).

[3]J. S. Blair, Phys. Rev. 95, 1218 (1954).

[4]H. L. Reynolds and A. Zucker, Phys. Rev. (to be published).

[5]J. B. A. England, R. McKeague, and P. E. Hodgson, Proc. Phys. Soc. (London) (to be published). G. W. Greenlees and J. Lowe, Proc. Phys. Soc. (London) (to be published). H. E. Gove, Phys. Rev. 99, 1353 (1955).

[6]D. D. Kerlee, J. S. Blair, and G. W. Farwell, Phys. Rev. 107, 1343 (1957).

[7]M. L. Halbert and A. Zucker, Phys. Rev. 115, 1635 (1959). A. Zucker and M. L. Halbert, Bull. Am. Phys. Soc. 5, 67 (1960). J. A. McIntyre, S. D. Baker, and T. L. Watts, Phys. Rev. 116, 1212 (1959).

QUESTION OF NUCLEON CLUSTERS IN THE NUCLEAR SURFACE*

I. E. McCarthy and D. J. Prowse
University of California, Los Angeles, California
(Received January 25, 1960; revised manuscript received February 23, 1960)

It has been suggested by Wilkinson[1] that strong evidence for the existence of nucleon clusters in the region of the nucleus where the density is less than 20% of its central value (defined as the periphery) is provided by the absorption of K^- mesons by nuclei in photographic emulsions. The ratio of two-nucleon to one-nucleon reactions as determined from the hyperon energy spectra is appreciable—about 20%.[2]

There is strong evidence that the K^- meson reacts with the nucleus in the periphery. The mechanism has been described by Jones.[3] The K^- meson is captured in a Bohr orbit, and cascades electromagnetically into a 5g orbit for heavy emulsion nuclei. (Light nuclei will not be considered here; the same considerations apply.)

In this orbit the probability of capture by the nucleus is comparable with the probability for the next electromagnetic transition. This is not sensitive to any nuclear model since the K^- meson remains in the $5g$ orbit for 10^{-17} second in which time it is practically certain to encounter a nucleon.

Wilkinson's argument is that the two-nucleon reaction occurs in the periphery. Hence there must be a high probability of finding two nucleons closely correlated in momentum in this region to account for the appreciable probability of the two-nucleon reaction. If this is the case the many-body problem of the finite nucleus would be extremely difficult. The approximation made by Brueckner et al.,[4] that the correlations in nuclear matter of low density are similar to those in infinite nuclear matter of that density, would be invalid. On Wilkinson's model, the correlations would be more like those in saturated nuclear matter. Fortunately, however, it is possible to construct a model for the explanation of the K^- meson results which does not require peripheral clusters. Wilkinson assumes that the mechanism for the absorption of the K^- meson is a reaction with the first nucleon or cluster that it encounters. However, it is known from the interaction of K^- mesons in a hydrogen bubble chamber[5] that the cross section for elastic scattering (at appreciable angles) is roughly equal to that for the catastrophic reaction producing a Σ hyperon.

A mechanism which reconciles the above experimental facts is as follows. In many cases, the K^- meson is elastically scattered by the first nucleon it encounters. That is, it transfers momentum and angular momentum to the nucleon. According to the Pauli principle the angular momentum of the nucleon must be increased (low angular momentum states are occupied), so the K^- meson drops into a part of the nuclear surface where the density is comparable with that of saturated nuclear matter. (Only hyperons originating near the surface will escape from the nucleus. The distinction between the periphery and the denser part of the surface is important.)

The cross section for such an elastic scattering will be inhibited by the Pauli principle. If the momenta of the K^- meson and the struck nucleon are comparable, the cross section will be reduced by a factor of about 2. Clearly the momenta are at least comparable; in fact, to the extent that the uncertainty principle allows one to speak of localized momenta[6] the K^- meson has higher momentum since its wave function is less smooth in the region in question.

We would expect most of the one-nucleon events to take place in the periphery, but all of the two-nucleon events to take place in a region where the density of nuclear matter is an appreciable fraction of its maximum value, where a small number of one-nucleon reactions would also be expected. Confirmation that this is the case comes from recent measurements at Livermore and UCLA[7] of the charged pion spectrum from the absorption events; positive pions are observed with energies in excess of 100 Mev whereas the spectrum would be expected to cut off at 90 Mev if a reasonable proton momentum distribution is used. The only possible explanation for these events which was first suggested by Gilbert, Violet, and White[8] is that the reactions take place in a region where the Σ hyperons can be produced in negative energy states (i.e., deep in the nuclear surface) thus enabling the pion to carry away more energy than would be possible for a collision taking place in the periphery. This experimental result is good evidence for the model explained above which provides the required mechanism, introducing the K mesons deep into the nuclear surface.

There is evidence[9] that (p,α) reactions are direct, and because of the short mean free path of α particles in nuclei, are predominantly of a surface nature. There is, however, a strong distinction regarding clustering which must be drawn between the denser part of the surface ($\rho > 20\%$), into which protons are quite capable of penetrating and from which α particles are capable of emerging, and the periphery where the K^- mesons must be removed from the entrance channel.

---

*Partially supported by the U. S. Atomic Energy Commission and the National Science Foundation.

[1]D. H. Wilkinson, Phil. Mag. 4, 215 (1959).

[2]B. Bhowmik et al., Nuovo cimento 14, 315 (1959).

[3]P. B. Jones, Phil. Mag. 3, 33 (1958).

[4]K. A. Brueckner, Proceedings of the International Conference on the Nuclear Optical Model, Florida State University Studies, No. 32 (The Florida State University, Florida, 1959).

[5]M. F. Kaplon, 1958 Annual International Conference on High-Energy Physics at CERN, edited by B. Ferretti (CERN Scientific Information Service, Geneva, 1958), p. 171.

[6]See the work of G. A. Baker, Jr., I. E. McCarthy, and C. E. Porter (to be published) on the distribution

of momentum in localized regions of the nucleus.

[7]R. S. White, D. J. Prowse, and D. H. Stork (private communications).

[8]F. C. Gilbert, C. E. Violet, and R. S. White, Phys. Rev. 107, 228 (1957).

[9]P. E. Hodgson, Phil. Mag. 44, 113 (1953).

COLLISIONAL DE-EXCITATION OF (π^-, p) ATOMS*

J. E. Russell and G. L. Shaw
Department of Physics, Indiana University, Bloomington, Indiana
(Received February 26, 1960)

Preliminary results of a recent experiment by Fields et al.[1] to determine the time t_a required by a π^- to be slowed down from an initial velocity of $0.05c$ and absorbed in a hydrogen bubble chamber yield $t_a = (4 \pm 2) \times 10^{-12}$ sec. This result is based on two $\pi^- \to \mu^- + \bar{\nu}$ decays found among 70 000 stopped pions.

The purpose of this note is to suggest that this result lends added support to the conclusion of Day, Snow, and Sucher[2] that absorption from P states is suppressed in (K^-, p) atoms.

It will be shown that the experimental value of t_a indicates that π^- mesons are absorbed predominantly from atomic S states with $n \geq 3$. Two arguments will be offered in support of this conjecture. (1) An improved calculation of collisional de-excitation rates indicates that the minimum time required for a π^- to reach a state with $n = 1$ or 2 exceeds t_a. (2) Absorption from the states $3S$ and $4S$ is consistent with calculated de-excitation rates and may be accounted for by the Stark effect reshuffling of l values discussed recently by Day et al. in connection with the absorption of K^- mesons in hydrogen.

In Wightman's[3] theoretical investigation of the moderation of negative mesons in liquid hydrogen, it was concluded that a π^- is slowed down from a velocity of $\sim 0.05c$ and captured by a hydrogen molecule to form a highly excited (π^-, H_2^+) system in $\sim 10^{-12}$ sec. The (π^-, H_2^+) was expected to break up in a time $< 10^{-13}$ sec yielding a (π^-, p) atom in a state of high excitation $(13 \lesssim n \lesssim 29)$. Three processes were discussed in connection with the subsequent de-excitation of the (π^-, p) atom. (1) For $n \gtrsim 13$ a (π^-, p) is of molecular dimensions, and it was argued that the reaction $(\pi^-, p) + H_2 \to (\pi^-, p) + H_1 + H_1$ proceeds with a total cross section that is, from qualitative considerations, approximately geometrical. Since the dissociation energy of a hydrogen molecule is 4.7 ev, Wightman estimated that the mesonic atom would emerge from the collision with ~ 1 ev recoil kinetic energy. (2) Ejection of an Auger electron from an H_2 molecule was found to be most important for $4 \lesssim n \lesssim 13$, the mesonic atom acquiring essentially no recoil energy. Wightman's calculation of the Auger effect was semiclassical: a hydrogen atom and a (π^-, p) were held a fixed distance apart, and the motion of the meson was described by a Bohr-Sommerfeld orbit. Probabilities were calculated for Auger transitions induced by the oscillating electric dipole field of the mesonic atom, and the cross sections inferred from them were appreciable (much larger than geometrical for large n and small Δn), indicating that de-excitation was rapid. (3) The dipole moment of the (π^-, p) decreases quadratically with n, and it was estimated that radiative transitions would predominate for $n \lesssim 4$.

A reliable knowledge of de-excitation rates would indicate a lower limit to the time necessary for a π^- to reach an atomic state with principal quantum number n. Since the lifetime for the fastest radiative process, the $2P - 1S$ transition, is 6.8×10^{-12} sec, the results of Fields et al. indicate the need for an improved calculation of the Auger effect, the classical atomic orbits employed by Wightman being inappropriate for low quantum numbers. It is also necessary to ascertain that modes of de-excitation other than those discussed by Wightman are negligible.

Using the Born approximation, numerical values of the total cross section $\sigma_A(n, l; n', l')$ for Auger de-excitation from the state (n, l) to the state (n', l') were computed for various values of the velocity v of the mesonic atom. It was assumed, as Wightman had also assumed in his calculations, that the liquid hydrogen existed in atomic rather than in molecular form. The entire system was treated quantum mechanically: the relative motion of the (π^-, p) and the H_1 atom was described by plane waves, and hydrogenic wave functions were used for the initial and final

states of both atoms. It was found that for $v \leq 10^6$ cm sec^{-1} the σ_A were very nearly proportional to $(1/v)$, and that for $v \sim 10^8$ cm sec^{-1} and $n \leq 4$ they were less than geometrical (i.e., $< \pi a_0^2$).

Mesonic atoms can, in principle, also be de-excited by being scattered inelastically without ejecting an Auger electron. This was also investigated in Born approximation. For given values of (n, l) and (n', l') the sum of the de-excitation cross sections involving excitation of discrete levels of a hydrogen atom was negligible ($\lesssim 0.01\sigma_A$). On the other hand, the cross section for the process in which the H_1 atom remains unchanged was found to be comparable with σ_A. However, this latter process, which is due entirely to the interaction between the mesonic atom and the proton, involves a large momentum change and can occur only when the two are quite close to one another. The Born approximation did not take into account the distortion of the wave function for the relative motion of the two atoms which occurs at small distances. The kinetic energy of the (π^-, p) is, at most, several ev, while for low values of n the potential energy of a proton at a distance $R = \langle n, l | r | n, l \rangle$ from the center of a (π^-, p) is several hundred ev. The calculation was repeated inserting an infinite repulsive potential of radius R between the two atoms. In the low-energy limit, where only incident S waves need be considered, it was found that this cross section was reduced by a factor $> 10^3$.

The transition rate $\gamma_A(n, l; n', l')$ for Auger de-excitation is given by $\gamma_A = Nv\sigma_A$, where $N = 3.5 \times 10^{22}$ cm^{-3} is the number of hydrogen atoms per unit volume in an H_2 bubble chamber. The Auger transition rate γ_A, the radiative transition rate γ_R, and the lifetime $\tau_{n,l}$ are listed for low values of (n, l) and (n', l') in Table I. Since the first Born approximation does not take into account any damping processes, it is reasonable to expect that the computed values of σ_A overestimate the Auger cross sections and that, consequently, the resulting values of $\tau_{n,l}$ underestimate the de-excitation lifetimes. Therefore, Table I indicates that it is unlikely that a π^- could reach a state with $n = 1$ or 2 in a time less than t_a.

Day, Snow, and Sucher[2] have adduced reasons for believing that K^- mesons captured by protons in liquid hydrogen should be absorbed predominantly from high S states. They argue that an excited (K^-, p) atom colliding with a hydrogen molecule experiences an intense electric field and, due to the Stark effect, may readily transfer some of its orbital angular momentum to the motion of its center of mass. Consequently, the populations of the high S states, from which a K^- is quickly absorbed, are continually being replenished, and very few mesons reach states with $n = 1$ or 2.

Table I. Radiative and Auger transition rates γ_R and γ_A and the resulting lifetimes $\tau_{n,l}$.

(n, l)	(n', l')	γ_R (10^{10} sec^{-1})	γ_A (10^{10} sec^{-1})	$\tau_{n,l}$ (10^{-12} sec)
$2P$	$1S$	14.9	0.3	6.6
$3D$	$2P$	1.5	8.4	10.1
$3P$	$2S$	0.5	2.9	13.5
	$1S$	3.9	0.1	
$4F$	$3D$	0.3	83.8	1.2
$4D$	$3P$	0.2	42.7	2.2
	$2P$	0.5	1.1	
$4P$	$3D$	0.0	2.1	4.3
	$3S$	0.1	18.6	
	$2S$	0.2	0.5	
	$1S$	1.6	0.0	

This same mechanism may be expected to be operative during the de-excitation of (π^-, p) atoms, the only difference being that absorption is restricted to lower values of n, since the S-wave πp interaction is much weaker than that of the $\bar{K}p$ system. The absorption rate γ_{nS} of a π^- in the nS state is[4] $1.1 \times 10^{15}/n^3$ sec^{-1}. The rapid absorption found by Fields et al. may be accounted for if t_c, the time elapsing between close collisions, is short enough to assure that the S states are quickly refilled. If, following Day et al.,[2] it is assumed that a (π^-, p) atom with principal quantum number n emerges from each Stark effect collision with its S state populated statistically, the resulting average absorption rate $\bar{\gamma}_n$ is given by

$$\bar{\gamma}_n = (n^2 t_c)^{-1}(1 - e^{-\gamma_{nS} t_c}).$$

To account for the experimental results it is required that $(\bar{\gamma}_n)^{-1} < t_a$, a condition which is satisfied for $n \lesssim 5$ and $t_c \sim 10^{-13}$ sec.

Two points should be noted in connection with this scheme.

(1) The values of $(\bar{\gamma}_n)^{-1}$ and t_a require that the (π^-, p) atom be brought from the state in which it is initially formed to a low state $(3 \leq n \leq 5)$ in a very short time ($\sim 10^{-12}$ sec). Although this allows time for only a few collisions, it would not be inconsistent with Wightman's calculations,

which indicated that for large values of n the de-excitation rates would be exceedingly high, thus making possible appreciable changes of n during a single collision. In fact, Wightman had pointed out that an Auger transition, in spite of its selection rule $\Delta l = 1$, could effect large changes of n and l if it were preceded by a virtual Stark effect transition.

(2) If the initial de-excitation proceeds very quickly, it is unlikely that the (π^-, p) could be moderated to thermal velocities ($\sim 10^5$ cm sec^{-1}) in the course of a few collisions. Since a mesonic atom travels $\sim 10^{-7}$ cm between close collisions,[2] a value of $t_C \sim 10^{-13}$ sec indicates that the (π^-, p) has a velocity of $v \sim 10^8$ cm sec^{-1}, corresponding to the kinetic energy of about 1 ev which Wightman had estimated it would have after breaking up an H_2 molecule. Although the πp interaction shifts the binding energy of the nS state[5] ($6/n^3$) ev below that of the other states with the same n, a large kinetic energy would tend to suppress any tendency for the population of the S states with $3 \leq n \leq 5$ to be appreciably different from statistical following a close collision. Moreover, the small wavelength ($\lambda\!\!\!^{-} \sim 5 \times 10^{-10}$ cm) associated with this velocity would facilitate the transfer of orbital angular momentum during Stark effect collisions, thereby eliminating Adair's[6] objections [at least for the case of (π^-, p) atoms] to the original arguments of Day et al., who had assumed a velocity of $\sim 10^5$ cm sec^{-1}.

It should not be supposed that the collisional de-excitation of a (K^-, p) atom necessarily proceeds as quickly as that of a (π^-, p), since the cross sections for energetically allowed Auger transitions decrease rapidly for $n \gtrsim 12$, while the size of the (K^-, p) is still less than molecular dimensions for $n \lesssim 25$. However, despite the somewhat increased likelihood of a (K^-, p) being moderated to thermal velocities by the time it reaches low n values, the very intense S-wave $\bar{K}p$ interaction makes it possible, as Day et al.[7] have pointed out, to avoid Adair's objections by only considering the absorption of K^- mesons via virtual Stark effect transitions during the actual collision processes. Nevertheless, without regard to the details of Stark effect reshuffling, the de-excitation of a (K^-, p) should not differ in any very significant way from that of a (π^-, p), and, consequently, the experimental value of t_a would appear to give evidence that there is some mechanism whereby K^- mesons are absorbed predominantly from S states.

The authors wish to thank Dr. M. H. Ross for several helpful discussions and the Indiana University Research Computing Center for the use of their facilities.

---

*Supported by the National Science Foundation.

[1]T. Fields, G. B. Yodh, M. Derrick, and J. Fetkovich, Bull. Am. Phys. Soc. 4, 402 (1959), and private communication. Grateful acknowledgment is made for permission to quote these data in advance of publication.

[2]T. B. Day, G. A. Snow, and J. Sucher, Phys. Rev. Letters 3, 61 (1959).

[3]A. S. Wightman, thesis, Princeton University, 1949 (unpublished); Phys. Rev. 77, 521 (1950).

[4]J. A. Kuehner, A. W. Merrison, and S. Tornabene, Proc. Phys. Soc. (London) 73, 545 (1959).

[5]S. Deser, M. L. Goldberger, K. Baumann, and W. Thirring, Phys. Rev. 96, 774 (1954).

[6]R. K. Adair, Phys. Rev. Letters 3, 438 (1959).

[7]T. B. Day, G. A. Snow, and J. Sucher (to be published).

ANALYSIS OF THE SCATTERING OF K^+ MESONS IN EMULSION*

L. S. Rodberg†
Los Alamos Scientific Laboratory, Los Alamos, New Mexico
and Physics Department, University of Maryland, College Park, Maryland

and

R. M. Thaler‡
Los Alamos Scientific Laboratory, Los Alamos, New Mexico
and Physics Department, Case Institute of Technology, Cleveland, Ohio
(Received March 11, 1960)

Using data on the scattering of K^+ mesons in emulsion,[1] together with data on the scattering of K^+ mesons by hydrogen[2] ($T=1$), we have investigated the K^+-nucleon interaction in the $T=0$ state. The method used requires only simple hand calculations and is believed to be quite accurate at high energies. The emulsion data of Zorn[1] are summarized in Table I. The K^+-p data may be summarized in terms of the S-wave effective range expansion as follows[3]:

$$k_{\text{c.m.}}\cot\delta_1 = -\frac{1}{a_1}+\tfrac{1}{2}k_{\text{c.m.}}{}^2 r_1, \qquad (1)$$

with $a_1=0.34$ f, $r_1=0.50$ f, where a_1 and r_1 are accurate to about 10%.[4] For the energy region under consideration here (incoming kinetic energy less than 350 Mev), the K^+-p angular distribution indicates that the $T=1$ phase shifts for $L\geq 1$ may be neglected.

If we assume that the elastic scattering of K^+ on nuclei is given by a complex square well potential of depth $V+iW$, then in the WKB approximation one finds[5] for the total inelastic scattering cross section:

$$\sigma_{\text{inel}} = \pi R^2 - \frac{2\pi}{\lambda^2}[1-e^{-\lambda R}(1+\lambda R)]. \qquad (2)$$

Here R is the radius of the nucleus with $R=1.2A^{1/3}\times 10^{-13}$ cm and $\lambda=-4E_K W/(k_{\text{lab}}\hbar^2)$. Equation (2) is valid when $(V+iW)/E_K \ll 1$ and $k_{\text{lab}}R \gg 1$. Equation (2) is, of course, averaged over the representative elements of the emulsion. The total inelastic cross section then determines λ and hence W. The values of λ de-

Table I. The emulsion data of Zorn,[a] the quantities X and λ, the K^+-nucleon phase shift parameters, and the optical potentials derived from these data. T_K is the average laboratory kinetic energy of the K meson in each energy interval.

	$T_K=180$ Mev	$T_K=255$ Mev	$T_K=340$ Mev
σ_{inel} (mb)	357 ± 27	412 ± 32	406 ± 35
$P=\left(\frac{\sigma_{\text{c.x.}}^{\text{emulsion}}}{\sigma_{\text{inel}}-\sigma_{\text{c.x.}}^{\text{emulsion}}}\right)$	0.24 ± 0.04	0.51 ± 0.08	0.70 ± 0.12
$\sigma_{\text{c.x.}}^{\text{emulsion}}$ (mb)	70 ± 14	139 ± 25	167 ± 31
λ (f^{-1})	0.36 ± 0.06	0.51 ± 0.10	0.49 ± 0.11
X (f^2)	0.038 ± 0.011	0.089 ± 0.023	0.106 ± 0.029
δ_1 (rad)	-0.52	-0.64	-0.76
δ_0 (rad)	-0.035 ± 0.087	0.14 ± 0.31	0.26 ± 0.12
μ_0	0.03 ± 0.03	0.16 ± 0.13	0.37 ± 0.09
V_S (Mev)	17.3	14.5	12.1
W (Mev)	-12.1 ± 2.0	-19.0 ± 3.7	-19.5 ± 4.4

[a]See reference 1.

termined from the experimental data are given in Table I. In the impulse approximation the optical model potential is[6]

$$V+iW=-2\pi A\bar{f}(0)\frac{k_{\text{lab}}}{k_{\text{c.m.}}}\frac{\hbar^2}{E_K}\frac{1}{(\frac{4}{3}\pi R^3)}, \tag{3}$$

for a square well, where A is the mass number of the nucleus, k_{lab} is the wave number in the laboratory system, $k_{\text{c.m.}}$ is the wave number in the K^+-nucleon center-of-mass system, E_K is the total laboratory energy of the K meson (including rest energy), and $\bar{f}(0)$ is the forward scattering amplitude in the K^+-nucleon center-of-mass system averaged over isotopic spin. [Note that for $R\sim A^{1/3}$ Eq. (3) is independent of A.] Thus

$$\bar{f}(0)=\alpha_1 f_1(0)+\alpha_0 f_0(0), \tag{4}$$

where the subscript denotes the isotopic spin state, and $\alpha_1=(A+Z)/2A$, $\alpha_0=(A-Z)/2A$. If only the S-wave phase shifts need be considered for $T=1$, and only the S- and P-wave phase shifts for $T=0$,

$$f_1(0)=\frac{1}{k_{\text{c.m.}}}e^{i\delta_1}\sin\delta_1,$$

$$f_0(0)=\frac{1}{k_{\text{c.m.}}}\{e^{i\delta_0}\sin\delta_0+e^{i\delta_{01}}\sin\delta_{01}+2e^{i\delta_{03}}\sin\delta_{03}\}. \tag{5}$$

Here δ_1 and δ_0 are the S-wave phase shifts in the $T=1$ and 0 states, respectively, and $\delta_{0,2J}$ are the $T=0$, $L=1$ phase shifts for states of total angular momentum J. In terms of these phase shifts λ is

$$\lambda=\frac{6A}{k_{\text{c.m.}}^{\ 2}R^3}\{\alpha_1\sin^2\delta_1+\alpha_0\sin^2\delta_0+3\alpha_0\mu_0\}, \tag{6}$$

where

$$\mu_0=\tfrac{1}{3}\sin^2\delta_{01}+\tfrac{2}{3}\sin^2\delta_{03}. \tag{7}$$

If we assume that phase shifts for $L\geq 2$ may be neglected in the $T=0$ state, we may write the total cross section for the charge-exchange reaction, $K^+ + n \rightarrow K^0 + p$, as

$$\frac{\sigma_{\text{c.x.}}}{4\pi}=X=\frac{1}{4k_{\text{c.m.}}^{\ 2}}[\sin^2(\delta_1-\delta_0)+3\mu_0]. \tag{8}$$

A good approximation to the total charge-exchange cross section in emulsion at high energy is

$$\sigma_{\text{c.x.}}^{\text{emulsion}}=\bar{N}'\sigma_{\text{c.x.}}, \tag{9}$$

where $\bar{N}'$ is the average number of neutrons with which the K meson may interact per emulsion nucleus. If there were no attenuation of the incident beam, we would have $\bar{N}'=\bar{N}$, the average number of neutrons per emulsion nucleus. (In the usual way we treat the nuclear emulsion as a mixture of N:Br:Ag in the ratio 56:22:22, so that $\bar{N}=27.2$.) In general N' can be obtained by multiplying the density of neutrons at position $\vec{r}$ by the probability that the meson reaches $\vec{r}$ without being scattered inelastically, and integrating over all $\vec{r}$. For a uniform medium this gives

$$N'=\frac{3N}{2\pi\lambda R^3}\sigma_{\text{inel}}, \tag{10}$$

with σ_{inel} given by Eq. (2). The average value of N'/N is about $\frac{1}{2}$ at these energies. Values of X determined from the emulsion data are given in Table I.

Equations (9) and (10) may be used because of: (a) the incoherence of charge exchange scattering in nuclei; (b) the high incident kinetic energy; and (c) the very small probability of multiple charge exchange collisions. It turns out that the mean free path for a charge exchange collision in nuclear matter at the energies considered here is greater than ~10 f. There is also only a very small probability that an inelastic non-charge-exchange collision (involving a large energy loss) will be followed by a charge exchange collision because of the very rapid decrease of the charge exchange cross section with decreasing energy. Attenuation due to inelastic scattering may, of course, not be neglected. Comparison with the geometric cross section of the total inelastic cross section and the charge exchange cross section indicates readily why this is to be expected, since $0.1\leq\sigma_{\text{c.x.}}^{\text{emulsion}}/\pi R^2\leq 0.3$ whereas $0.6\leq\sigma_{\text{inel}}/\pi R^2\leq 0.8$, in the energy region under consideration. For the geometric cross section we have used

$$\pi R^2=\pi(1.2\text{ f})^2[0.22(108)^{2/3}+0.22(80)^{2/3}+0.56(14)^{2/3}]=556\text{ mb}. \tag{11}$$

By inserting in Eqs. (6) and (8) the values of λ and X determined from experiment (Table I), we

may solve for δ_0 in terms of δ_1. The result is

$$\sin(2\delta_0 - \delta_1) = \frac{k_{\text{c.m.}}^2[(R^3/6A)\lambda - 4\alpha_0 X] - \alpha_1 \sin^2\delta_1}{\alpha_0 \sin\delta_1} \tag{12}$$

This gives the values for δ_0 quoted in Table I. These values for δ_0 are consistent with the form

$$\delta_0 = -k_{\text{c.m.}} a_0, \text{ with } a_0 = -0.080 \pm 0.068 \text{ f}, \tag{13}$$

where a_0 has been obtained by a least-squares fit. We may then solve Eqs. (6) and (8) for μ_0. These values also appear in Table I. It should be noted that the errors in δ_0 and μ_0 are correlated. The independent experimental parameters are σ_{inel} and P (Table I), so that λ and X are correlated; these depend on both δ_0 and μ_0. The result is a strong correlation between the errors in δ_0 and μ_0 so that a small value of μ_0 will be associated with a large value of δ_0, and vice versa.

To get some idea of the magnitude of the P-wave phase shifts, we may write $\mu_0 = \sin^2\bar{\delta}_{0P}$, where $\bar{\delta}_{0P}$ is an "average" P-wave phase shift. (In the absence of spin-orbit splitting, $\bar{\delta}_{0P}$ is the P-wave phase shift.) If we fit $\bar{\delta}_{0P}$ to the form

$$k_{\text{c.m.}}^3 \cot\bar{\delta}_{0P} = -(1/\bar{a}_{0P})^3, \tag{14}$$

we find

$$|\bar{a}_{0P}| = 0.44 \pm 0.03 \text{ f}.$$

To determine the individual P-wave phase shifts, one can use the real part of the optical potential, which can be written as the sum of an S-wave and a P-wave part. Thus

$$V = V_S + V_P,$$

with

$$V_S = \Gamma[\alpha_1 \sin 2\delta_1 + \alpha_0 \sin 2\delta_0],$$

$$V_P = \Gamma\alpha_0[\sin 2\delta_{01} + 2\sin 2\delta_{03}],$$

$$\Gamma = -\frac{3A}{4R^3}\frac{\hbar^2}{\bar{E}_K}\frac{k_L}{k_{\text{c.m.}}^2}. \tag{15}$$

The values of V_S obtained using Eqs. (1) and (13) are given in Table I. If the optical model potential were known, V_P could be found and the two P-wave phase shifts determined by solving Eqs. (7) and (15) simultaneously. From the present experimental values,[7]

$$V + iW = [20.7 \pm 2.3 - (7.9 \pm 1.2)i] \text{ Mev}$$

at $T_K = 150$ Mev and[8]

$$V + iW = [22 \pm 6 - (19.3 \pm 2.0)i] \text{ Mev}$$

at $T_K = 260$ Mev, we would conclude that V_P is small (indicating a large spin-orbit splitting) and repulsive. However, there is great uncertainty in the value of the optical model potential determined from experiment, so that these conclusions are subject to considerable doubt. Further, there is some indication from a comparison of inelastic scattering at low energies with Monte Carlo calculations [see, for instance, M. Grilli et al., Nuovo cimento 10, 205 (1958)] that the K^+-nucleon cross section has a significant backward peaking, implying an attractive P-wave amplitude. Future improvements in the elastic scattering data, with consequent improvement in the optical model parameters, and improvements in the analysis of low-energy data, may help to resolve this disagreement.

*Work performed under the auspices of the U. S. Atomic Energy Commission.

†Now at the University of Maryland, College Park, Maryland.

‡Now at the Case Institute of Technology, Cleveland, Ohio.

[1]Although much emulsion data exist, in this analysis we have used only those supplied to us by Dr. Gus T. Zorn (private communication). We are very grateful to Dr. and Mrs. Zorn for making their data available to us prior to publication.

[2]T. F. Kycia, L. T. Kerth, and R. G. Baender, Phys. Rev. (to be published).

[3]The angular distribution[2] at 225 Mev may be fit using a large P-wave phase shift in the $J = \frac{1}{2}$ state with a negligible S-wave phase shift. However, the total $K^+ - p$ cross section is nearly constant from low energies up to 275 Mev; this energy dependence is not compatible with a dominant P-wave interaction.

[4]These values are obtained if it is assumed that the data can be fit by an expression of the form of Eq. (1); the results of this Letter do not depend on this assumption, since δ_1 is used only in an energy region where it is known from experimental measurements.[2]

[5]S. Fernbach, R. Serber, and T. B. Taylor, Phys. Rev. 75, 1352 (1949).

[6]This equation and the conditions under which its use is justified have been written down in many places, see, for example, W. Riesenfeld and K. Watson, Phys. Rev. 102, 1157 (1956); H. A. Bethe, Ann. Phys. 3, 190 (1958); A. K. Kerman, H. McManus, and R. M. Thaler, Ann. Phys. 8, 551 (1959).

[7]G. Igo, D. G. Ravenhall, J. J. Tiemann, W. W. Chupp, G. Goldhaber, S. Goldhaber, J. E. Lannutti,

and R. M. Thaler, Phys. Rev. 109, 2133 (1958). These authors treat the potential nonrelativistically; to convert the potential to the conventional relativistic form, as the fourth component of a four-vector, we have multiplied their result by M_K/E_K.

[8]M. A. Melkanoff, O. R. Price, D. J. Prowse, D. H. Stork, and H. K. Ticho, Proceedings of the International Conference on the Nuclear Optical Model, Florida State University Studies, No. 32 (The Florida State University, Tallahassee, 1959).

FINITE SELF-ENERGY OF CLASSICAL POINT PARTICLES

R. Arnowitt*
Department of Physics, Syracuse University, Syracuse, New York

S. Deser*
Department of Physics, Brandeis University, Waltham, Massachusetts

and

C. W. Misner†
Palmer Physical Laboratory, Princeton University, Princeton, New Jersey

(Received February 10, 1960)

The infinite mass self-energy difficulties of quantum field theory already occur, as is well-known, in the corresponding classical theories. Although cutoffs may be introduced to effect renormalization in both the classical and quantum cases, such procedures are physically unsatisfactory. We wish to point out in this note that at least for the static (Coulomb-type) contribution, one obtains finite results for the classical self-energies if the gravitational contribution to the total energy is included. Furthermore, it will be shown rigorously (in the static case) that the natural cutoff furnished by general relativity implies that all the mass of a point charge arises from its total self-field and that a neutral particle has no mass.

It has previously been shown[1] that the energy of the gravitational field is given by[2]

$$E=\int(g_{ij,j}-g_{jj,i})\,dS_i, \tag{1}$$

where dS_i is a two-dimensional surface element at spatial infinity. When point particles or other fields (such as the electromagnetic field) are coupled to the gravitational field, Eq. (1) represents the total energy of the combined system.[3] We begin by considering the metric field arising from the coupling of a neutral static point particle. In isotropic coordinates $[g_{ij}=\chi^4(r)\delta_{ij}]$ the relevant field equation is

$$-2(R^0_0-\tfrac{1}{2}R)({}^3g)^{1/2}\equiv-8\chi\nabla^2\chi$$
$$=-T^0_0({}^3g)^{1/2}=m_0\delta^3(\vec{\mathbf{r}}), \tag{2}$$

where m_0 is the bare mass of the particle and $\delta^3(\vec{\mathbf{r}})$ is invariantly defined in three-space as a scalar density,[4] i.e., $\int\delta^3(\vec{\mathbf{r}})d^3r=1$. The solution of Eq. (2) which is asymptotically flat is seen to be

$$\chi(r)=1+m_0/[32\pi r\chi(0)]. \tag{3}$$

The parameter $m\equiv m_0/\chi(0)$ is given in terms of m_0 by

$$m=\lim_{\epsilon\to0}2m_0[1+(1+m_0/8\pi\epsilon)^{1/2}]^{-1}. \tag{4}$$

In Eq. (4), ϵ is essentially the "radius" of the δ^3 function. This relation between m and m_0 is a consequence of explicitly considering the source term in Eq. (2). From Eq. (1) one sees that $E=m$. That this energy is to be correctly interpreted as the total mass of the particle follows from the fact that an isotropic time-symmetric metric possesses no dynamical gravitational modes.[5] Thus E represents the mass of a gravitationally clothed one-particle system (and no dynamical gravitational excitations). From Eq. (4) then, this total mass approaches zero as $(32\pi m_0\epsilon)^{1/2}$. The gravitational self-mass for a neutral particle therefore cancels the bare mass m_0. The physical origin of this result ($m=0$) is connected to the well-known fact that there is an upper limit, in general relativity, to the amount of energy that can reside in a given region. As the size of the particle (here ϵ) goes to zero its mechanical energy content must vanish. We may note that the (incorrect) weak-field result for the self-mass could be obtained from Eq. (4) by taking the limit m_0 small before letting ϵ tend to zero. Here one would find $m=m_0-\frac{1}{2}m_0^2/\epsilon+O(1/\epsilon^2)$, the standard linearly infinite Coulomb-type self-

energy. Higher terms in this perturbation expansion are more and more divergent. The correct result, $m=0$, thus indicates the lack of validity of the perturbation approach.

If a particle is coupled to another field of nonzero range, it may be expected to have nonvanishing total mass due to the interaction with the other field. In flat space, one has, for electromagnetic interactions, the infinite Coulomb self-energy $\frac{1}{2}e^2/(4\pi\epsilon)$. We shall now show that this infinite result is made finite when gravitational coupling is taken into account. The coupling of the electromagnetic field to the gravitational field is included in the generally covariant electromagnetic Lagrangian,

$$\mathfrak{L}_{\rm em}=A_{\nu}\,\mathfrak{F}^{\mu\nu}{}_{,\mu}+\tfrac{1}{4}(-g)^{-1/2}\,\mathfrak{F}^{\mu\nu}\mathfrak{F}^{\alpha\beta}g_{\mu\alpha}g_{\nu\beta}, \quad (5)$$

where A_μ is the vector potential and $\mathfrak{F}^{\mu\nu}$ is the field strength tensor density. We are here employing that formulation of the electromagnetic field in which A_μ and $\mathfrak{F}^{\mu\nu}$ are to be varied independently. This gives rise to the usual Maxwell equations as well as to the relations between potentials and field strengths. The analysis for finding the independent dynamical variables of the Maxwell field proceeds just as in Lorentz covariant electrodynamics.[6] One finds that the canonical variables are $A_i{}^T$ and $\mathcal{E}^{iT}\equiv\mathfrak{F}^{0iT}$, the transverse parts of $A_i,\mathcal{E}^i$ $(A_i{}^T{}_{,i}=0=\mathcal{E}^{iT}{}_{,i})$. The longitudinal part of $\mathcal{E}^i$ is determined by the differential constraint equation $\mathcal{E}^i{}_{,i}=\rho$ where ρ is the charge density.

In order to investigate the self-energy of a point charge, one must consider the coupled Einstein-Maxwell equations. For the static case these are

$$-8\chi\nabla^2\chi=m_0\delta^3(\vec{\mathbf{r}})+\tfrac{1}{2}\chi^{-2}\mathcal{E}^i\mathcal{E}^i, \quad (6a)$$

$$\mathcal{E}^i{}_{,i}=e\,\delta^3(\vec{\mathbf{r}}). \quad (6b)$$

The term $\frac{1}{2}\chi^{-2}\mathcal{E}^i\mathcal{E}^i$ in Eq. (6a) is the electromagnetic energy density. The solution for $\chi(r)$ is

$$\chi^2(r)=(1+m/32\pi r)^2-(e/16\pi r)^2, \quad (7)$$

where m is related to the particle's bare mass m_0 and its charge e by

$$m=\lim_{\epsilon\to 0}16\pi\{-\epsilon+[\epsilon^2+(e/8\pi)^2+m_0\epsilon/8\pi]^{1/2}\}. \quad (8)$$

From Eq. (1), we again have $E=m$. As in the neutral case there are no dynamical gravitational modes excited, nor are there any transverse canonical electromagnetic modes present since the solution of Eq. (6b) we have taken, $\vec{\mathcal{E}}=(e/4\pi)\vec{\nabla}r$, is purely longitudinal. Thus m is simply the total mass of the charged particle. The mass is finite and equals $2|e|$, or in conventional units,

$$m=\gamma^{-1/2}|e|/(4\pi)^{1/2}. \quad (9)$$

It should be stressed that this finite result has been obtained entirely within the framework of standard Einstein-Maxwell theory. The possibility of a finite combined gravitational-electrostatic self-energy can be seen already in Newtonian physics where $-\frac{1}{2}\gamma m^2/\epsilon$ would compensate $e^2/4\pi\epsilon$ if Eq. (9) held. Of course, the relation (9) between m and e was <u>not</u> chosen just to achieve this compensation, but was forced in order that solutions of the general relativistic Eqs. (6) exist. That the total mass here is not zero, unlike the neutral case, arises from the fact that the electric energy term in Eq. (6a) is spread out in a nonzero region. Similarly, an electrically uncharged particle coupled to a Yukawa field, for example, will possess a nonvanishing finite self-mass independent of m_0. As in the neutral case, the weak-field limit can be obtained by expanding in e and m_0 before letting $\epsilon\to 0$. One would get then $m=m_0-\frac{1}{2}\gamma m_0{}^2/\epsilon+\frac{1}{2}e^2/4\pi\epsilon+O(1/\epsilon^2)$, and no compensation occurs since e and m_0 are independent parameters, which shows again the lack of validity of the perturbation expansion.

The solutions derived here for the neutral and charged one-particle states differ from the conventional Schwarzschild and Reissner-Nordstrom metrics in two ways. First, these usual metrics can be seen not to satisfy Eqs. (2) and (6), respectively, for any finite mass m_0 and in fact only solve the field equations for $r>0$. Hence the correct relation between the parameter m and the bare mass m_0 and charge e cannot be made for these solutions, i.e., one would fail to discover that, for a <u>point</u> particle, m is determined by e. Second, the way in which the metric enters into the matter stress tensor is uniquely determined by the canonical formalism; this is not the case for the usual discussion of coupling in which there is still ambiguity.[7]

The extension of the above results for the mass of a single point source to two-body solutions is (aside from its intrinsic interest) necessary to see whether these masses enter properly into the interaction energy. We have been able to carry out the analysis for the case of two charges of the same sign. For simplicity, we consider here the situation of equal bare masses and equal

charges. In Eqs. (6), the term $m_0\delta^3(\vec{r})$ is replaced by $m_0[\delta^3(\vec{r}-\vec{r}_1)+\delta^3(\vec{r}-\vec{r}_2)]$ and $e\delta^3(\vec{r})$ by $e[\delta^3(\vec{r}-\vec{r}_1)+\delta^3(\vec{r}-\vec{r}_2)]$, where $\vec{r}_1$ and $\vec{r}_2$ are the positions of the point charges. The solution corresponding to Eq. (7) generalizes to the form[8] $\chi^2(\vec{r})=\psi^2(\vec{r})-\varphi^2(\vec{r})$ where $\psi=1+(a/32\pi)(|\vec{r}-\vec{r}_1|^{-1}+|\vec{r}-\vec{r}_2|^{-1})$ and $\varphi=(e/16\pi)(|\vec{r}-\vec{r}_1|^{-1}+|\vec{r}-\vec{r}_2|^{-1})$. Here the total energy $E=2a$ and the field equations give

$$E=32\pi\{-\epsilon+[\epsilon^2+(e/8\pi)^2(1+x)^2+(m_0\epsilon/8\pi)(1+x)]^{1/2}\}[1+x]^{-1}, \quad (10)$$

where $x=\epsilon/|\vec{r}_1-\vec{r}_2|$. In the limit $\epsilon=0$, one obtains $E=4|e|=2m$. Since the dynamical modes of both the Einstein and Maxwell fields again vanish, E here represents the total energy of the two particles. For two neutral particles ($e=0$), one has $E=0$ in accord with the one-particle result. When $e\neq 0$, one would have expected for large $r_{12}\equiv|\vec{r}_1-\vec{r}_2|$ that $E-2m=[(e^2/4\pi)-\gamma m^2]/r_{12}$. However, this interaction energy vanishes on account of Eq. (9). The rigorous result above ($E=2m$) shows that the cancellation between the electrostatic and gravitational interaction energies holds[9] even for small r_{12}. While these results are consistent with those for one body, it would be of interest to examine the case of opposite charges where the cancellation would not be expected. This case cannot be obtained merely by changing the sign of the $|\vec{r}-\vec{r}_2|^{-1}$ term in $\varphi(\vec{r})$, since the electric field $\vec{\mathcal{E}}$ corresponding to such a metric has a transverse part, $\vec{\mathcal{E}}^T$, so that the total energy now includes a contribution from these pure electric dynamical modes. We have not been able to solve Eq. (6a) with $\vec{\mathcal{E}}=e\nabla(|\vec{r}-\vec{r}_1|^{-1}-|\vec{r}-\vec{r}_2|^{-1})$ for an asymptotically flat g_{ij}.

The compensation of the usual infinite static self-energies obtained here arises due to the distinctive nature of the gravitational coupling which modifies the free Lagrangians of all fields rather than introducing an additive interaction Lagrangian. Ultimately, the interest of these classical results rests on their extension to quantum theory. Of course, the criteria for the usefulness of a gravitational cutoff in that domain would depend not merely on finiteness but on the numerical values it would yield.

*Supported in part by a National Science Foundation Research Grant.

†Alfred P. Sloan Research Fellow.

[1]R. Arnowitt, S. Deser, and C. W. Misner, Nuovo cimento (to be published); Phys. Rev. 116, 1322 (1959); Phys. Rev. (to be published); Phys. Rev. (to be published); which will be referred to as I, II, III, and IV, respectively.

[2]We use units such that $\kappa=16\pi\gamma c^{-4}=c=1$, where γ is the Newtonian gravitational constant. Latin indices run from 1 to 3, Greek from 0 to 3. The summation convention holds even if repeated indices are both covariant. A comma represents ordinary differentiation. It should be mentioned that the energy of Eq. (1) depends only on the spatial part of the metric which constitutes the initial Cauchy data. Thus, to calculate the energy of the system one does not have to know g_{00} or any time development of the system. The same expression for the energy may also be obtained from the usual surface integral forms of the energy [see for example L. Landau and E. Lifshitz, Classical Theory of Fields (Addison-Wesley Publishing Company, Inc., Reading, Massachusetts, 1951), Eq. (11-88), where $g_{0\mu}$ cancels out in the linearized asymptotic form valid at spatial infinity.

[3]That this is reasonable follows from the fact that the energy of a system is the coefficient of $1/r$ in the asymptotic expansion of g_{ij}; see also IV.

[4]The $({}^3g)^{1/2}$ factor on the left-hand side of Eq. (2) is uniquely determined when one puts the Lagrangian including matter variables into canonical form (see IV). That it must be present follows obviously from the scalar density nature of the $\delta^3(r)$ function.

[5]If one chooses the coordinate conditions $x^i=2g_{ij}{}_{,j}-(1/2\nabla^2)g^T{}_{ij,j}$, $t=-(1/2\nabla^2)(\pi^T+\nabla^2\pi^L)$ (in the notation of reference 1), the analysis of the Nuovo cimento Letter would show that the canonical variables are $g_{ij}{}^{TT}$ and π^{ijTT}. These dynamical modes vanish everywhere when the spatial metric is isotropic and $\pi^{ij}=0$ (initially static situation).

[6]R. Arnowitt and S. Deser, Phys. Rev. 113, 745 (1959).

[7]Thus, in the usual treatment of the interior Schwarzschild solution, the bare rest-mass density is never even introduced. The standard "proper rest-mass density" parameter includes clothing effects in its definition in an unanalyzed manner.

[8]See C. W. Misner and J. A. Wheeler, Ann. Phys. 2, 594 (1957).

[9]A corroboration of the absence of interaction energy and therefore of forces between the particles is furnished by the fact that in the case $m=2|e|$, the initial value metric described by ψ and φ determines a static solution of the Einstein equations [A. Papapetrou, Proc. Roy. Irish Acad. A51, 191 (1947)].

POSSIBLE RESONANCES IN WEAK INTERACTIONS AND TEST OF THE INTERMEDIATE BOSON HYPOTHESIS OF TANIKAWA AND WATANABE*

Toichiro Kinoshita
Laboratory of Nuclear Studies, Cornell University, Ithaca, New York
(Received March 11, 1960)

Weak interactions are described satisfactorily at low energies by the universal $V-A$ theory,[1] at least when no change of strangeness is involved. Up to now, however, no information has been available concerning the properties of weak interactions at higher energies. Recently Lee, Yang, and Schwartz[2] have pointed out that the neutrinos from the decay of high-energy mesons can be used to study weak interactions. In this Letter, we shall discuss possible deviations of the weak interactions at high energies from their low-energy behavior, identity of the neutrinos emitted in the $\pi-\mu$ decay and β decay,[3] and whether the weak interaction is basically of the Fermi type or Yukawa type.[4]

Recently Glashow[5] has pointed out that if the weak interaction is mediated by a boson, the cross section for the process

$$\bar{\nu}+e^- \to (b) \to \bar{\nu}+\mu^- \qquad (1)$$

exhibits a resonance at $\sim 2.5\times 10^{11}$ ev (assuming that the boson has the K-meson mass) where (b) denotes an intermediate state consisting of all self-energy diagrams of the boson. Resonance of this kind takes place whenever the particle in the one-particle intermediate state has a mass greater than the sum of masses of incident particles. As is well known, the cross section at resonance is very large, and is independent of the strength of interaction. The width is related to the lifetime of the intermediate particle. Thus, the widths for the processes caused by the known weak interactions such as

$$\bar{\nu}+e^- \to (\pi^-) \to \bar{\nu}+e^- \text{ (or } \bar{\nu}+\mu^-),$$
$$\pi^-+p \to (\Lambda) \to \pi^-+p \text{ (or } \pi^0+n), \qquad (2)$$

are $10^{-5}-10^{-7}$ ev, too narrow to be of immediate interest. On the other hand, if the weak interaction is mediated by a boson as in the case (1), the width becomes of the order of 100 ev. This means that, even for an incident beam with energy spread of 100 Mev, the effective cross section is still about $10^{-6}\times\sigma_{\text{resonance}}$, which is quite enormous for processes involving weak interactions.

Thus, the resonance scattering will be a very important tool for studying weak interactions at high energies provided, of course, that weak processes actually occur through intermediate bosons. At least, it enables us to test the intermediate-boson hypotheses experimentally. Unfortunately, the advantage of the resonance is partially lost in the case (1) because of the very high resonance energy in the laboratory system. Thus, resonance scattering is not a practical method to test an intermediate-boson hypothesis of this kind.[6] However, there is another kind of intermediate-boson theory proposed by Tanikawa and Watanabe[7,8] which gives, as is shown below, resonance energies of only several hundred Mev for some processes. The validity of such a theory can therefore be tested without extreme difficulty using some of the existing accelerators.

In the theory of Tanikawa and Watanabe, β decay is assumed to be a second order effect of the basic interaction

$$H_1 = g_1\bar{p}(1-\gamma_5)e_C B_1 + g_1\bar{n}(1-\gamma_5)\nu_C B_1 + \text{H.c.}, \qquad (3)$$

where e_C denotes the charge conjugate operator of e and B_1 is a complex field describing a particle with no spin and no electric charge. The B_1 particle is assumed to carry nucleonic and leptonic charges so that the interaction (3) conserves these charges. In order to reproduce the shape of the β-decay spectrum, the mass of the boson must be greater than $\sim 2300 m_e$; such a mass also guarantees the stability of the nucleon.[7]

Similarly, the basic interaction for the μ capture is

$$H_2 = g_2\bar{p}(1-\gamma_5)\mu_C B_2 + g_2\bar{n}(1-\gamma_5)\omega_C B_2 + \text{H.c.}, \qquad (4)$$

where ω denotes the neutrino produced in the $\pi-\mu$ decay which may or may not be identical with ν.[3] In the rest of this Letter we will assume for simplicity that the masses of B_1 and B_2 are equal to $m_B = 2300 m_e$, and that g_1 and g_2 are equal to g, where

$$g^2/4\pi = 6.4\times 10^{-7}, \qquad (5)$$

corresponding to the usual Fermi coupling constant $G = 10^{-5} m_p^{-2}$. In this theory, the μ capture

occurs through a one-boson intermediate state:

$$\mu^- + p \to (B) \to \omega + n, \tag{6}$$

which shows a resonance for some incident muons. Since the reverse process,

$$\omega + n \to (B) \to \mu^- + p, \tag{7}$$

is more interesting from the experimental point of view, we shall consider this in the following paragraphs.

The total cross section for the process (7) is

$$\sigma = \frac{g^2 m_B \tau_\mu^{-1}}{[(p_n + p_\nu)^2 - m_B^2]^2 + m_B^2(\tau_\mu^{-1} + \tau_\nu^{-1})^2} \tag{8}$$

near the resonance energy, where τ_μ and τ_ν are the partial lifetimes for the decays $B \to p + \mu^-$ and $B \to n + \omega$, given by

$$\tau_\mu^{-1} = \frac{g^2}{4\pi} \frac{(m_B^2 - m_p^2 - m_\mu^2)}{m_B^3} \times [(m_B^2 - m_p^2 + m_\mu^2)^2 - 4m_\mu^2 m_B^2]^{1/2},$$

$$\tau_\nu^{-1} = \frac{g^2}{4\pi} \frac{(m_B^2 - m_n^2)^2}{m_B^3}. \tag{9}$$

In the rest system of the neutron, (8) is reduced to

$$\sigma = \frac{g^2}{4m_n} \frac{\Gamma_\mu}{(E - E_0)^2 + \frac{1}{4}(\Gamma_\mu + \Gamma_\nu)^2}, \tag{10}$$

where

$$E_0 = (m_B^2 - m_n^2)/2m_n = 265 \text{ Mev},$$

$$\Gamma_\nu = m_B/(m_n \tau_\nu) = 120 \text{ ev},$$

$$\Gamma_\mu = 0.88\Gamma_\nu. \tag{11}$$

At resonance, the cross section reaches 6.8×10^{-27} cm^2, which is independent of g.

Of course, no neutron target at rest is available, so neutrons in a nucleus must be used. Because of neutron motion, neutrinos within the energy range 210–330 Mev may be scattered resonantly by some neutrons. Therefore, we shall see a smeared-out effect of the process (7), with an effective cross section $\sim 2 \times 10^{-32}$ cm^2, rather than a sharp resonance. If the intensity of the neutrino beam were 10^6/sec and the neutron density of the target were 3×10^{23}/cm^3, the process (7) would occur once every 170 seconds for a target 1 cm thick. The background for the neutrino beam may be eliminated in the usual way by making use of a very thick absorber.

The above estimate is based on the assumption that $m_B = 2300 m_e$. Since nothing is actually known about m_B, however, it is necessary to measure the cross section of (7) at various neutrino energies. Although the neutrinos from the pion beam have a continuous spectrum, the resonance energy E_0, and hence the mass m_B, may be measured without very much trouble. If one fails to observe the process (7) for a wide range of neutrino energies, one can determine a lower limit for the mass of the B particle.

Since the neutrino beam considered above contains neutrinos resulting from μ-e decay, the process

$$\nu + n \to (B) \to e^- + p \tag{12}$$

will take place in addition to (7). If the neutrinos ν and ω are identical, all neutrinos will contribute to (12).[9] Thus, the identity of ν and ω may be tested by examining the observed ratio of the processes (7) and (12).[3]

We note that the resonance feature of the intermediate boson theory is not restricted to neutrino reactions. For instance, the process

$$e^- + p \to (B) \to e^- + p \tag{13}$$

would contribute to electron-proton scattering. This contribution is isotropic in the center-of-mass system, and is about 5×10^{-28} cm^2/steradian at resonance, the resonance energy and the width being given approximately by (11). It will thus dominate the Coulomb scattering at the resonance energy, except in the extreme forward direction. Since the energy resolution of the electron beam is ~1% at present, this contribution to the cross section is actually smeared out and becomes effectively $\sim 5 \times 10^{-32}$ cm^2, which is still larger at large angles than the scattering due to the electromagnetic interaction.[10] Therefore, the process (13) may be tested experimentally. For this purpose we have only to observe the scattering (at a large angle) by increasing the incident energy continuously from about 250 Mev up to the maximum available energy. This is necessary since the width is very narrow and the exact resonance energy is not known, being a function of the unknown mass m_B.

If either the process (7) or (13) were not detected, it would be sufficient to disprove the intermediate-boson theory of Tanikawa and

Watanabe.[7] It should be noted, however, that some variants of their theory may be found which cannot be disproved by one negative experiment alone. Therefore, it is desirable that both of these experiments be performed. It seems to be rather difficult to invent a theory of the Tanikawa type which does not give a resonance in any of the processes $\nu+p$, $\nu+n$, $e+p$, and $e+n$, where ν and e denote either particles or antiparticles.

We conclude that it is probably worthwhile to search for possible anomalies in electron and neutrino reactions over the energy range which may be covered with the present accelerators before looking into weak processes at higher energies.

I should like to thank C. R. Schumacher for checking some of the calculations.

---

*Supported in part by the joint program of the Office of Naval Research and the U. S. Atomic Energy Commission.

[1]R. P. Feynman and M. Gell-Mann, Phys. Rev. 109, 193 (1958); E. C. G. Sudarshan and R. E. Marshak, Phys. Rev. 109, 1860 (1958).

[2]M. Schwartz, Phys. Rev. Letters 4, 360 (1960); T. D. Lee and C. N. Yang, Phys. Rev. Letters 4, 307 (1960). Similar considerations have recently been made by Y. Yamaguchi (to be published), and N. Cabbibo and R. Gatto (to be published).

[3]It is usually assumed that neutrinos emitted in the $\pi-\mu$ decay and β decay are of the same kind. There is no positive proof for this, however. Obviously, it is desirable that this be examined experimentally.

[4]The possibility that weak interactions are mediated by a boson has been considered by many authors: H. Yukawa, Proc. Phys.-Math. Soc. Japan 17, 48 (1935); J. Schwinger, Ann. Phys. 2, 407 (1957); T. D. Lee and C. N. Yang, Phys. Rev. 108, 1611 (1957); R. P. Feynman and M. Gell-Mann, Phys. Rev. 109, 193 (1958); Y. Tanikawa, Progr. Theoret. Phys. (Kyoto) 3, 338 (1948); Y. Tanikawa and S. Watanabe, Phys. Rev. 113, 1344 (1959).

[5]S. L. Glashow, Phys. Rev. (to be published).

[6]Lee and Yang (reference 2) showed that the production cross section of such a boson in the neutrino-nucleus collision is about 10^{-35} cm^2 for an incident neutrino energy much greater than 2 Bev. This is more practical than the resonance scattering method as a direct test of the intermediate boson hypothesis. It should be noted that the absence of $\mu\rightarrow e+\gamma$ is not conclusive evidence against the intermediate-boson hypothesis. See G. Feinberg, Phys. Rev. 110, 1482 (1958).

[7]Y. Tanikawa and S. Watanabe, Phys. Rev. 113, 1344 (1959).

[8]The theory of Tanikawa and Watanabe leads to the $V-A$ theory only after spinors are rearranged by the Fierz transformation. In this theory, therefore, it is not easy (if not impossible) to find a natural explanation for the conservation of the vector current part of the weak interaction, if it is in fact conserved (R. P. Feynman and M. Gell-Mann, reference 1). If the presence of the weak magnetism [M. Gell-Mann, Phys. Rev. 111, 362 (1958)] is established experimentally, it may again be hard to explain by Tanikawa's theory. The experimental result is not conclusive yet.

[9]In this case, formulas (8) and (10) must be modified slightly to take account of an additional decay mode of the B particle.

[10]R. Hofstadter, F. Bumiller, and M. R. Yearian, Revs. Modern Phys. 30, 482 (1958).

AXIAL VECTOR CURRENT CONSERVATION IN WEAK INTERACTIONS*

Yoichiro Nambu
Enrico Fermi Institute for Nuclear Studies and Department of Physics
University of Chicago, Chicago, Illinois
(Received February 23, 1960)

In analogy to the conserved vector current interaction in the beta decay suggested by Feynman and Gell-Mann, some speculations have been made about a possible conserved axial vector current.[1-3] One can formally construct an axial vector nucleon current, which satisfies a continuity equation,

$$\Gamma_\mu^A(p',p)=i\gamma_5\gamma_\mu-2M\gamma_5 q_\mu/q^2,\quad q=p'-p, \qquad (1)$$

where p and p' are the initial and final nucleon momenta. Such an attempt has some appeal in view of the apparently modest renormalization effect on the axial vector beta decay constant ($g_A/g_V\approx 1.25$), although the second appealing point,[1] namely, the possible forbidding of $\pi\rightarrow e+\nu$, has now lost its relevance.

The expression (1), unfortunately, can be easily ruled out experimentally, as was pointed out by Goldberger and Treiman,[3] since it introduces a large admixture of pseudoscalar interaction.

On the other hand, Eq. (1) arouses theoretical curiosity as to the origin of the second term if it really exists; according to our conventional field theory, we would have to interpret the denominator q^2 as implying a massless, pseudoscalar, and charged quantum bridging the nucleon and lepton currents.

We would like to suggest that there may not be a strict pseudovector current conservation, but that we may have an approximate conservation which becomes rigorous in the limit $q^2 \gg m_\pi^2$, m_π being the pion mass. Specifically, we propose that the axial vector part of the nucleon beta decay vertex has the following form and properties:

$$g_A \Gamma_\mu^A(p',p) = g_V\left[i\gamma_5\gamma_\mu F_1(q^2) - \frac{2M\gamma_5 q_\mu}{q^2+m_\pi^2} F_2(q^2)\right],$$

$$F_1(0) = g_A/g_V \approx F_2(0),$$

$$F_1(q^2) \sim F_2(q^2) \quad \text{for} \quad q^2 \gg m_\pi^2. \tag{2}$$

The pion is then the analog of the massless quantum mentioned above. This is consistent with the dispersion relations expected for Γ_μ^A. Namely, F_1 and F_2 should have in general the form

$$F_i(q^2) = F_i(-m_\pi^2) - (q^2+m_\pi^2)\int_{m_0^2}^{\infty} \frac{\rho_i(m^2)dm^2}{(q^2+m^2)(m^2-m_\pi^2)} \qquad (i=1,2), \tag{3}$$

where $m_0 = 3m_\pi$ unless there are new particles of low mass. Thus the F's will be slowly varying for $|q^2| \ll m_0^2$. The conditions in Eq. (2) imply that $F_1/F_2 \approx 1$ for all q^2. If $m_\pi = 0$ and $F_1/F_2 \equiv 1$, then we restore exact current conservation,[2] and we also expect $F_1(0) = g_A/g_V = 1$.

If we adopt Eq. (2), the second term of Γ_μ^A immediately gives a relation between g_A, the pion decay (pseudovector) constant g_π, and the pion-nucleon (pseudoscalar) coupling G_π:

$$2Mg_A \approx 2Mg_V F_2(-m_\pi^2) = \sqrt{2}\, G_\pi g_\pi. \tag{4}$$

With $g_A = 1.25\, g_V = 1.75\times10^{-49}$ erg cm^3,[4] $G_\pi^2/4\pi = 13.5$, this gives a π-μ decay life of 2.7×10^{-8} sec as compared with the observed value 2.56×10^{-8} sec.

Goldberger and Treiman[5] have arrived at the same relation Eq. (4) (in the limit of their self-energy integral $J \to \infty$) from an entirely different approach. In our opinion, this is not a coincidence, as will be explained elsewhere.

We are tempted to extend this approximate conservation of the axial vector (and naturally also the vector current) to the strangeness-nonconserving beta decays. We take, for example, the ΛN axial vector in the form

$$\Gamma_\mu^A(p_N', P_\Lambda) \approx i\gamma_5\gamma_\mu - \frac{(M_\Lambda + M_N)\gamma_5 q_\mu}{q^2+m_K^2}, \tag{5}$$

and attribute the second term to the pseudoscalar K meson.[6] The degree of accuracy of the relation (5) will be poorer than in the previous case in view of the Λ-N mass difference (which destroys vector conservation) and the large K-meson mass. At any rate, we obtain an analog of Eq. (4):

$$(M_\Lambda + M_N)\, g_A' \approx G_K g_K, \tag{6}$$

which relates the Λ beta decay axial vector coupling g_A', the ΛNK coupling G_K, and the $K_{\mu 2}$ decay coupling g_K.

With the observed $K_{\mu 2}$ lifetime 2.1×10^{-8} sec and a tentative value $G_K^2/4\pi = \frac{1}{4}G_\pi^2/4\pi$, we get

$$g_A'/g_A \approx 1/10. \tag{7}$$

This is not inconsistent with the observed beta decay of Λ which seems an order of magnitude less than predicted from a universal coupling scheme $g_V' = g_A' = g_V$.[7]

We can still go further, though the argument becomes more arbitrary. Let us assume that a fundamental weak coupling $(\bar{N}N\bar{N}\Lambda)$ gives rise to an effective V-A interaction (or at least part of it) of the form

$$g''(\Gamma_\mu^V - \Gamma_\mu^A)_{\bar{N}N}(\Gamma_\mu^V - \Gamma_\mu^A)_{\bar{N}\Lambda}. \tag{8}$$

Here $\Gamma_\mu^V = i\gamma_\mu$ which is approximately conserved by itself, and Γ_μ^A stands for Eq. (2) or (5). We see easily that Eq. (8) contains information about the $\Lambda \to N + \pi$ decay matrix element:

$$(2M_N g''/\sqrt{2}\, G_\pi) q_\mu (\Gamma_\mu^V - \Gamma_\mu^A)_{\bar{N}\Lambda}. \tag{9}$$

Combined with the assumption of $\Delta T = \frac{1}{2}$ selection rule, this gives a lifetime of 2.5×10^{-10} sec

for $g'' = g_V$ as compared with the observed value 2.8×10^{-10} sec.

It is possible to apply this kind of consideration to other hyperons. Moreover, if the Feynman–Gell-Mann coupling scheme such as $(\pi\pi e\nu)$ is formally extended to $(K\pi e\nu)$, etc. as has been tried by some people, all the observed decay processes may be covered. Here we would like to point out that if all baryons should satisfy Eqs. (4) and (6), the ratios g_A/G_π and g_A'/G_K must be approximately common constants.

Our final remark concerns the theoretical basis for the assumptions made here. If the baryons are derived from some fundamental field ψ which possesses an invariance under a transformation of the type $\psi \to \exp(i\vec{\alpha}\cdot\vec{\tau}\gamma_5)\psi$,[8] then there will be a conservation of the pseudovector charge-current. A finite observed mass can be compatible with the conservation if the particle is coupled with a boson as was noted in Eq. (1).

This situation may be understood by making an analogy to the theory of superconductivity originated by Bardeen, Cooper, and Schrieffer,[9] and refined by Bogoliubov.[10] There gauge invariance, the energy gap, and the collective excitations are logically related to each other as was shown by the author.[11] In the present case we have only to replace them by γ_5 invariance, baryon mass, and the mesons. In fact, the mathematical method used in superconductivity may be taken over to study the self-energy problem of elementary particles. It is interesting that pseudoscalar mesons automatically emerge in this theory as bound states of baryon pairs. The nonzero meson masses and baryon mass splitting would indicate that the γ_5 invariance of the bare baryon field is not rigorous, possibly because of a small bare mass of the order of the pion mass.

The above-mentioned model of elementary particles will be studied in a separate paper.

*This work was supported by the U. S. Atomic Energy Commission.

[1]J. C. Taylor, Phys. Rev. 110, 1216 (1958).

[2]J. C. Polkinghorne, Nuovo cimento 8, 179 and 781 (1958).

[3]M. L. Goldberger and S. B. Treiman, Phys. Rev. 110, 1478 (1958).

[4]A. I. Alikhanov, Ninth Annual International Conference on High-Energy Physics, Kiev, 1959 (unpublished).

[5]M. L. Goldberger and S. B. Treiman, Phys. Rev. 110, 1178 (1958); M. L. Goldberger, Revs. Modern Phys. 31, 797 (1959).

[6]It is also possible to associate a scalar K meson with the ΛN vector current conservation, while leaving the axial vector unaccounted for.

[7]Again Eq. (5) and the subsequent conclusions are essentially the same as those of C. H. Albright, Phys. Rev. 114, 1648 (1959) and B. Sakita, Phys. Rev. 114, 1650 (1959), which are based on the Goldberger-Treiman method. For the Λ-decay case below, see L. Tenaglia, Nuovo cimento 14, 499 (1959).

[8]F. Gürsey (private communication) has recently obtained similar results on the π decay based on this γ_5 invariance. We do not here specify the interaction of the ψ field, which may be of the nonlinear Heisenberg type, or due to an intermediate boson (different from π or K).

[9]J. Bardeen, L. N. Cooper, and J. R. Schrieffer, Phys. Rev. 106, 162 (1957).

[10]N. N. Bogoliubov, V. V. Tolmachev, and D. V. Shirkov, A New Method in the Theory of Superconductivity (Academy of Sciences of USSR, Moscow, 1958).

[11]Y. Nambu, Phys. Rev. 117, 648 (1960).

ERRATUM

HELICITY OF NEGATIVE MUONS FROM PION DECAY. W. A. Love, S. Marder, I. Nadelhaft, and R. T. Siegel [Phys. Rev. Letters 2, 107 (1959)].

In this Letter we presented preliminary results of an experiment designed to measure the forward-backward asymmetry of β rays emitted from B^{12}, which has been produced by absorption of polarized muons in carbon (in C_5H_{12}). Continuing measurements have yielded an amended result for the asymmetry parameter a, as defined in this Letter, of $a = (0.64 \pm 0.58)\%$. It thus appears that in pentane the B^{12} is depolarized by one of the various interactions (quadrupole coupling, multiple electron capture and loss, etc.) which might cause spin reorientation. Therefore, a definite conclusion about the helicity of the negative muon cannot be drawn from our results to date.

ABSTRACTS

In this section are printed the abstracts of Articles that have been forwarded to The American Institute of Physics for publication in THE PHYSICAL REVIEW. In quoting information obtained from this section before the appearance of the corresponding Article, reference should be made to "Physical Review (to be published)" rather than to this Journal.

NUCLEAR MAGNETIC RESONANCE IN PARAMAGNETIC FeF_2. J. W. Stout, Institute for the Study of Metals, University of Chicago, Chicago, Illinois, and R. G. Shulman, Bell Telephone Laboratories, Murray Hill, New Jersey (Received January 7, 1960).

A nuclear magnetic resonance study of the F^{19} resonance in paramagnetic FeF_2 is reported. The hyperfine interactions with the magnetic electrons are measured and shown to be important in determining the resonance properties. The isotropic hyperfine interaction indicates the presence of $(0.46 \pm 0.03)\%$ unpaired 2s spins in F^- orbitals from each Fe^{++} ion neighbor.

THEORY OF SUPERCONDUCTING CONTACTS. R. H. Parmenter, RCA Laboratories, Princeton, New Jersey (Received January 6, 1960).

The Bardeen-Cooper-Schrieffer (BCS) theory of superconductivity is generalized to the case of a position-dependent energy gap (at the absolute zero of temperature and in the absence of magnetic fields). The BCS integral equation for the energy gap goes over into an integro-differential equation. The latter has nontrivial solutions (i.e., finite energy gap) even for the case of normal material ($V = 0$). Expressions are obtained for the energy gap, for the volume energy density, and for the surface energy density at an interface, for both normal and superconducting material. These results are applied to a number of problems involving superconducting contacts. When a thin slice of normal material is sandwiched between bulk superconductors, it is found that the slice acts superconducting for thicknesses less than about 10^{-5} cm. When a thin slice of superconductor is sandwiched between bulk normal material, the slice acts like normal material for thicknesses less than about 10^{-5} cm. The energy gap at the free surface of a bulk superconductor may differ by as much as 30% from its constant value deep inside the material, the former being either larger or smaller than the latter, depending on the value of $N(0)V$, where $N(0)$ is the density of one-electron states at the Fermi level in the normal metal.

BAND STRUCTURE OF ALUMINUM. Walter A. Harrison, General Electric Research Laboratory, Schenectady, New York (Received January 4, 1960).

Calculations of the band energies at symmetry points in aluminum by Heine are extended into the zone using the pseudopotential interpolation scheme in order to obtain constant-energy curves in the neighborhood of the Fermi surface. In conjunction with this calculation, the lines of contact between various bands are found in detail. The de Haas–van Alphen effect, cyclotron resonance effect, anomalous skin effect, and low-temperature specific heat are discussed in terms of these constant-energy curves and the results compared with experiment. It appears from this comparison that the geometry of the Fermi surface is given quite well by the band calculations, but that there is a discrepancy of a factor of order two between the derived and measured effective masses. A "single-orthogonalized-plane-wave approximation" is compared with the more exact treatment and found to be a good starting approximation, suitable for semiquantitative treatment of the electronic structure.

ELECTRONIC STRUCTURE OF POLYVALENT METALS. Walter A. Harrison, General Electric Research Laboratory, Schenectady, New York (Received January 4, 1960).

A single-orthogonalized-plane-wave approximation is defined and used to construct the Fermi surfaces for face-centered cubic and body-centered cubic metals of valence one through four and for hexagonal close-packed metals of valence one through three. The de Haas–van Alphen effect, cyclotron resonance effect, and anomalous skin effect are discussed in detail in terms of these surfaces and the deduced properties are compared with experiment where suitable experiments exist. In particular, earlier

and equivalent comparisons for lead and for aluminum are reviewed, and detailed comparisons with existing experimental data on zinc and cadmium are made. It is found that the single-orthogonalized-plane-wave approximation is in semiquantitative agreement with experiment in all of these cases, both as to the form of the Fermi surface and its associated effective masses. In conjunction with these studies, detailed descriptions of the apparent Fermi surfaces in zinc and cadmium are given. An extension of the method to allow experimental determination of a more precise description of the band structure is discussed, and the generalization of the method to studies of alloys is outlined.

THEORY OF DIELECTRIC CONSTANTS OF LiF. E. R. Levin, Pitman-Dunn Laboratories, Frankford Arsenal, Philadelphia, Pennsylvania, and E. L. Offenbacher, Temple University, Philadelphia, Pennsylvania (Received January 8, 1960).

The static and high-frequency dielectric constants and the effective charge of LiF are calculated on the basis of a simplified model in which the polarizability of the positive ion is neglected and that of the negative ion is attributed entirely to perturbations in the outermost subshell ($2p$) of electrons. The present calculation differs from the variational treatment of Yamashita mainly in the inclusion of perturbed wave functions for the $2p$ electrons which are orthogonal to the core-electron wave functions. Also, different methods are employed in evaluating portions of the energy of the crystal in a field and in deducing the effective charge ratio e^*/e from the calculated energy. It is found that the use of trial wave functions which preserve the orthogonality within individual ions is of prime importance, and leads to results in generally better agreement with observation than the previously used nonorthogonal functions.

COLLOIDS IN ADDITIVELY COLORED SODIUM CHLORIDE. H. W. Etzel, U. S. Naval Research Laboratory, Washington, D. C. (Received January 7, 1960).

A study has been made of the formation of colloids in additively colored sodium chloride. Both natural and synthetic single crystals were additively colored by heating in a vapor of sodium and by injecting electrons from a point cathode. Subsequent irradiation with ultraviolet light and heating of the synthetic crystals produced an absorbing type colloid throughout the crystal. The same treatment applied to the natural crystals produced F centers throughout the bulk of the crystal and absorbing-type colloid specks at localized points in the crystal. In the synthetic crystals the formation of these colloids is shown to be related to the presence of hydroxyl ions in the crystals prior to coloration. In the natural crystal the formation of such colloids is dependent upon the presence of small occlusions of water distributed randomly in the crystal prior to coloration.

THEORY OF THE TEMPERATURE DEPENDENCE OF THE MAGNETOELASTIC CONSTANTS OF CUBIC CRYSTALS. C. Kittel, Miller Institute for Basic Research in Science, University of California, Berkeley, California, and J. H. Van Vleck, Harvard University, Cambridge, Massachusetts (Received January 6, 1960).

The conventional theory of the variation with temperature of the anisotropy of cubic crystals is extended to include the magnetoelastic constants.

EFFECT OF HIGH PRESSURE ON SOME HOT ELECTRON PHENOMENA IN n-TYPE GERMANIUM. S. H. Koenig, International Business Machines Watson Laboratory, New York, New York, Marshall I. Nathan, International Business Machines Research Laboratory, Poughkeepsie, New York, and William Paul and Arthur C. Smith,* Gordon McKay Laboratory, Harvard University, Cambridge, Massachusetts (Received January 8, 1960).

The pressure dependence of the current density vs electric field characteristic for n-type germanium at 297°K has been measured to a maximum pressure of 30 000 kg/cm^2, and to a maximum field of 10 000 v/cm. It is concluded that the electrons are "heated" by the field sufficiently to cause the conduction band valleys along the ⟨100⟩ direction in reduced momentum space to be appreciably populated with electrons at atmospheric pressure. The pressure dependence of the angle ϵ between current and

field at 77°K has been measured to a maximum field of 3000 v/cm and a maximum pressure of 5000 kg/cm^2. ϵ is independent of pressure except for a small increase for applied fields of ~3000 v/cm. Suggested interpretations for the data are given.

*Present address: Department of Electrical Engineering, Massachusetts Institute of Technology, Cambridge, Massachusetts.

EFFECT OF CRYSTALLINE FIELDS ON CHARGE DENSITIES AND MAGNETIC FORM FACTORS. A. J. Freeman, Materials Research Laboratory, Ordnance Materials Research Office, Watertown, Massachusetts, and Solid-State and Molecular Theory Group, Massachusetts Institute of Technology, Cambridge, Massachusetts, and R. E. Watson, Solid-State and Molecular Theory Group, Massachusetts Institute of Technology, Cambridge, Massachusetts (Received January 14, 1960).

The effects of crystalline fields on 3d charge densities and magnetic form factors for transition metal ions are discussed on the basis of recent theoretical investigations augmented by an analysis of optical absorption data. It is shown that the crystalline field has two effects on the free-ion 3d wave functions and hence on their form factors as well: (1) a differentiation or "splitting" of the two types of cubic 3d functions by an expansion of the t_{2g} (e_g) orbitals and a contraction of the e_g (t_{2g}) orbitals resulting in two different radial charge densities, and (2) a net expansion of the charge distribution from the free-ion value. The magnetic form factors due to this "splitting" effect when calculated according to the methods of Weiss and Freeman show measurable deviations from the free-atom results. A form factor for Mn^{+2} based on optical absorption data shows a large expansion of the 3d charge density, in agreement with the magnetic form factor measurements of Hastings, Elliott, and Corliss. This agreement, based on the use of theoretical $F^k(3d, 3d)$ integrals, indicates that the well-known discrepancy between theoretical and experimental values of these integrals arises from the fact that the quantities obtained experimentally are not true $F^k(3d, 3d)$ integrals. The crystalline potential due to an array of negative-ion charge densities has been employed to discuss these various effects and their meaning with respect to a proper (essentially molecular) treatment.

CRYSTAL POTENTIAL AND ENERGY BANDS OF SEMICONDUCTORS. III. SELF-CONSISTENT CALCULATIONS FOR SILICON. Leonard Kleinman and James C. Phillips,* Department of Physics, University of California, Berkeley, California (Received December 11, 1959).

An approximately self-consistent crystal potential is constructed for Si from a superposition of free-atom core and a sampling of crystal valence-band charge densities. Valence-core exchange is calculated directly from core wave functions while valence-valence exchange is included using momentum-independent and momentum-dependent approximations taken from the results for a free-electron gas. The resulting crystal potential is surprisingly similar to one previously obtained by Woodruff from a superposition of free-atom charge densities. The calculated valence wave functions in the core region differ substantially from those of Woodruff because of the variational method used by him to calculate wave functions in that region. As a result the calculated energy gap is changed from Woodruff's value of 4 ev to about 1.5 ev, in substantially better agreement with the experimental value (1.1 ev). The various uncertainties in the calculation are listed; it is concluded that the relative position of levels near the band gap should be correct to within about 1 ev. Effective masses are also calculated and compared with experiment; the agreement is quite good.

*Present address: Royal Society Mond Laboratory, Cambridge, England.

SURFACE MAGNETOSTATIC MODES AND SURFACE SPIN WAVES. J. R. Eshbach and R. W. Damon, General Electric Research Laboratory, Schenectady, New York (Received January 6, 1960).

Examination of the spatial configuration of the magnetostatic modes of a ferromagnetic body shows that those modes whose frequency lies between $\omega = \gamma(B_i H_i)^{1/2}$ and $\omega = \gamma(H_i + 2\pi M)$ are surface modes. It is also found that the complete spin wave spectrum consists of a set of surface spin waves in addition to the spin wave band usually considered. The magnetostatic mode spectrum thus merges smoothly into the spin wave spectrum.

The characteristic equation for the surface

modes on a plane surface at an arbitrary angle to the applied dc field is given. The properties of the surface modes on plane surfaces and on spheroidal bodies are discussed.

TRANSITION PROBABILITIES FOR THE EXCITED STATE $d\epsilon^3\ ^2\Gamma_3$ OF Cr^{3+}. A. M. Clogston, Bell Telephone Laboratories, Murray Hill, New Jersey (Received January 11, 1960).

In recent experiments Geschwind has observed transitions between the Zeeman components of the excited metastable state $d\epsilon^3\ ^2\Gamma_3$ of trivalent chromium present as a dilute impurity in Al_2O_3. In first order the transitions are forbidden. In third order a number of processes give rise to a transition probability and predict $g_\perp = 0.1$, consistent with the experimental observations. The magnetic moment associated with the transition is shown to rotate opposite to the usual sense.

EXPERIMENTAL FUSION CURVES OF INDIUM AND TIN TO 105 000 ATMOSPHERES. J. Duane Dudley* and H. Tracy Hall, Brigham Young University, Provo, Utah (Received December 18, 1959).

The experimental fusion curves of indium and tin have been determined to a pressure of 105 000 atmospheres. The melting point was detected at various pressures by means of a sharp increase in the electrical resistance of the sample, which gave rise to a sudden increase in the sample temperature. The melting temperature of indium was found to rise smoothly from a normal value of 156°C to a value of 417°C at 105 000 atm. The experimental data are fitted very well by the Simon equation $P/a = (T/T_0)^c - 1$, with $a = 15\,000$ atm, $c = 4.34$, and $T_0 = 429$°K. No evidence of polymorphism is observed. A phase transition is found for tin, with a triple-point on the fusion curve at 38 000 atm, 318°C. The melting temperature for the first phase rises smoothly from its normal value of 232°C to the triple-point, and the data are fitted very well by the Simon equation with $a = 7400$ atm, $c = 11.3$, $T_0 = 505$°K. The melting temperature for the second phase rises smoothly from the triple-point to a value of 500°C at 105 000 atm, and the data are fitted very well by the Simon-type equation $(P - 38\,000)/21\,800 = (T/591)^{5.25} - 1$. The uncertainty is estimated to be approximately ±5% in the measured melting temperature, ±5% in the pressure calibration, ±20% in the Simon coefficient a, and ±2% in the Simon exponent c.

*Present address: Applied Research Division, Sandia Corporation, Albuquerque, New Mexico.

ELECTRICAL CONDUCTIVITY OF X-IRRADIATED KCl. R. W. Christy and E. Fukushima, Dartmouth College, Hanover, New Hampshire (Received January 13, 1960).

The conductivity of Harshaw KCl crystals has been measured isothermally as a function of time in the temperature range 150-200°C, after exposing the crystals at room temperature to x-ray doses sufficient to produce about 10^{16} F centers/cm^3. Besides the F band, a V band at about 5.75 ev is produced. If the F band is eliminated by optical bleaching before the measurement but the V band remains, the conductivity increases monotonically to an asymptotic value, which is equal to the conductivity of the unirradiated crystal for virgin samples but is lower for samples which have been annealed in air at 260°C beforehand. If both the F band and the V band are present, the conductivity increases more rapidly at first, and then decreases to an asymptotic value. The behavior is qualitatively similar to that previously observed in NaCl, though there are significant differences in the optical absorption spectrum and temperature dependence of the conductivity changes.

ELECTRON CAPTURE AND LOSS BY HYDROGEN ATOMS IN MOLECULAR HYDROGEN. R. Curran* and T. M. Donahue, University of Pittsburgh, Pittsburgh, Pennsylvania (Received November 20, 1959).

Measurements of the single electron capture and loss cross sections for atomic hydrogen in molecular hydrogen are reported for atoms of energies 4 to 35 kev. Peaks in the loss cross section are found which appear to be associated with the formation of negative ions in the target gas.

*Present address: Westinghouse Research Laboratories, Pittsburgh, Pennsylvania.

GROUND-STATE Q VALUES FOR THE $Si^{30}(p,\alpha)Al^{27}$ AND $O^{16}(p,\alpha)N^{13}$ REACTIONS. R. E. White and W. W. Buechner, Department of Physics and Laboratory for Nuclear Science, Massachusetts Institute of Technology, Cambridge, Massachusetts (Received December 4, 1959).

Alpha-particle groups observed during the magnetic analysis of charged particles produced in the bombardment of silicon-dioxide targets with 8- and 8.59-Mev protons have been identified as arising from the reactions $Si^{30}(p,\alpha)Al^{27}$ and $O^{16}(p,\alpha)N^{13}$. The corresponding Q values are -2.366 ± 0.010 Mev and -5.206 ± 0.010 Mev, respectively.

DECAY OF RUTHENIUM-105. Babulal Saraf, P. Harihar, and R. Jambunathan, Atomic Energy Establishment, Trombay, Bombay, India (Received June 9, 1959).

The decay of Ru^{105} has been studied employing two scintillation spectrometers in coincidence. It is found that Ru^{105} decays to the excited levels of Rh^{105} with the emission of six β groups, with end-point energies of ~125, 525, 915, 1080, 1150, and ~1800 kev, the branching ratios being approximately ~0.002, 0.068, 0.11, 0.30, 0.51, and ~0.01, respectively. The subsequent γ rays have the energies of 130, 265, 320, 400, 475, 485, 665, 725, 875, 960, 1350, and 1750 kev. From γ-γ and β-γ coincidence measurements, a level scheme of Ru^{105} has been worked out, showing the excited states at 130, 395 (or 530), 475, 725, 795, 960, 1350, and 1750 kev.

BETA- AND GAMMA-RAY SPECTRA OF Pd^{111}. William W. Pratt, Department of Physics, The Pennsylvania State University, University Park, Pennsylvania, and Robert G. Cochran,* College of Engineering and Architecture, The Pennsylvania State University, University Park, Pennsylvania (Received January 6, 1960).

Beta rays of 2.18 Mev and gamma rays of 0.377, 0.580, 0.620, 0.810, 1.380, and 1.450 Mev were found in the decay of the 22-minute isomer of Pd^{111}. Beta rays of 2.02 Mev and gamma rays of 0.170 and 1.690 Mev were found associated with the 5.5-hour isomer. Although the beta-ray groups may both represent the decay of the 22-minute state, the dissimilarity of the gamma-ray spectra implies some degree of beta-ray branching from the 5.5-hour state.

*Present address: Department of Nuclear Engineering, The Texas Agricultural and Mechanical College, College Station, Texas.

EFFECTS OF A NUCLEAR OCTUPOLE MOMENT ON NEUTRON SCATTERING. Kirk W. McVoy,* Brookhaven National Laboratory, Upton, New York (Received December 9, 1959).

Recent applications of the nuclear optical model to the description of neutron scattering by spheroidal nuclei have shown that "shape effects" are very important for highly deformed nuclei. It has also been found that the "adiabatic approximation," which assumes the nucleus to be rigidly fixed in orientation throughout the scattering, is remarkably accurate for very low-energy (S-wave) neutrons.

The first part of the present paper is devoted to a detailed investigation of this approximation, showing that the major factor determining its validity for the heavy nuclei to which it has been applied is the large size of the "effective rotating mass" of the nucleus in comparison to the neutron mass. This is analogous to the Born-Oppenheimer approximation in molecular physics, where the large ratio of nuclear to electronic mass enables one to calculate electronic wave functions by considering the slower nuclear motion to be "frozen" completely.

The second purpose of the paper is to investigate the effect of a "pear-shaped" deformation, or octupole moment, of the nuclear optical potential on the S-wave neutron strength function. (A square-edged potential well is used, which is somewhat similar in its effect to a rounded-edge well with a smaller imaginary potential.) This is done for the very heavy nuclei, $225 < A < 240$, where the possibility of octupole deformations has been suggested by other data. The effect of a small octupole moment for these particular nuclei is found to be largely masked by the nearly indistinguishable effect of their large quadrupole moments, and, in view of the uncertainty in their measured quadrupole moments, neutron scattering at this time cannot be said to provide any positive evidence of octupole moments. On the contrary, if the quadrupole moments reported from Coulomb excitation measurements are employed, the measured neutron

strength function puts an upper limit on the octupole moments of about one-third the quadrupole moment. More accurate data, both on the neutron strength function (as well as R') and on the quadrupole moments, would permit a more accurate estimate of the octupole moments.

*Present address: Brandeis University, Waltham, Massachusetts.

CONVERSION, K-AUGER, AND L-AUGER SPECTRA OF Hg^{199}. J. C. Nall, Q. L. Baird,* and S. K. Haynes,† Department of Physics, Vanderbilt University, Nashville, Tennessee (Received December 17, 1959).

The high resolution of the spectrometer made possible the detailed study of K, L, M, $N+O$ conversion lines and the K- and L-Auger spectra of Au^{199} with the following results (here ω and a are the fluorescence and Auger yields and f_{ij} is the Coster-Kronig transfer probability): K-Auger lines, $\omega_K = 0.952 \pm 0.003$, $KLL:KLX:KXY = 1.00:0.496 \pm 0.015:0.094 \pm 0.003$, and $KL_IL_I:KL_IL_{II}:KL_IL_{III}:KL_{II}L_{II}:KL_{II}L_{III}:KL_{III}L_{III} = 1.00:1.32 \pm 0.1:0.85 \pm 0.06:0.40 \pm 0.03:1.28 \pm 0.08:0.76 \pm 0.05$; L-Auger lines, $LMM:LMX:LXY = 1.00:0.30 \pm 0.03:0.015 \pm 0.004$, and $a_L = 0.590 \pm 0.04$, $\omega_L = 0.410 \pm 0.04$, $a(L_I) = 0.16 \pm 0.02$, $a(L_{II}) = 0.46 \pm 0.04$, $\omega(L_{II}) = 0.32 \pm 0.03$, and Coster-Kronig yields, $f(L_{II}L_{III}X) = 0.22 \pm 0.04$, $f(L_IL_{II}X) + f(L_IL_{III}X) = 0.74 \pm 0.04$. In addition considerable detail was obtained on the KLX and L-Auger fine structure. The results of all of the known L-Auger yield work since 1952 have been tabulated in this paper.

The conversion line results are compared and combined with those of two other groups to give an optimum set of relative intensities.

From these are obtained for the 51-kev transition, $\alpha(L_I):\alpha(L_{II}):\alpha(L_{III}):\alpha(M):\alpha(N):\alpha(O) = 1.00:0.087 \pm 0.010:0.012 \pm 0.007:0.212 \pm 0.04:0.068 \pm 0.005:0.016 \pm 0.001$; 156-kev transition, $\alpha(K):\alpha(L_I):\alpha(L_{II}):\alpha(L_{III}):\alpha(M):\alpha(N+O) = 1.00:0.144 \pm 0.015:0.830 \pm 0.028:0.586 \pm 0.018:0.418 \pm 0.017:0.107 \pm 0.005$; 209-kev transition, $\alpha(K):\alpha(L_I):\alpha(L_{II}):\alpha(L_{III}):\alpha(M):\alpha(N+O) = 1.00:0.155 \pm 0.005:0.029 \pm 0.003:0.0085 \pm 0.0003:0.050 \pm 0.008:0.0130 \pm 0.004$, where α is the internal conversion coefficient. efficient.

In addition, by use of Rose's Tables the 51-kev transition was determined to be $(3.3 \pm 1) \times 10^{-4}$ $E2$, and the 209-kev transition (0.113 ± 0.01) $E2$, and the $E2$ assignment of the 158-kev transition was confirmed to better than 1%. The relative gamma-ray intensities are 209 kev:51 kev:158 kev = $1.000:0.045 \pm 0.002:4.59 \pm 0.23$.

*Now at Argonne National Laboratory, Lemont, Illinois.

†Now at Michigan State University, East Lansing, Michigan.

He-ION INDUCED REACTIONS OF ALUMINUM AND MAGNESIUM. Richard H. Lindsay, Department of Physics, Washington State University, Pullman, Washington, and Robert J. Carr, Department of Chemistry, Washington State University, Pullman, Washington (Received December 14, 1959; revised manuscript received March 1, 1960).

The $Al^{27}(\alpha, 3p)Mg^{28}$ and $Mg^{26}(\alpha, 2p)Mg^{28}$ reactions produced by the bombardment of aluminum and magnesium targets with 42-Mev He ions have been studied. The excitation functions for these reactions are presented. At 40-Mev He-ion bombarding energy, the cross section for the $(\alpha, 3p)$ is about 80 microbarns and the peak yield of the $(\alpha, 2p)$ reaction observed at 34 Mev is 1.65 mb. Excitation functions are also given for the production of Na^{22} from the bombardment of aluminum with 30-42 Mev He-ions, which proceeds chiefly through the reaction $Al^{27}(\alpha, 2\alpha n)Na^{22}$, and of Na^{24} from the bombardment of natural magnesium, primarily through the $Mg^{25}(\alpha, \alpha p)Na^{24}$ reaction.

BETA DECAY OF Y^{91}. O. E. Johnson and W. G. Smith, Physics Department, Purdue University, Lafayette, Indiana (Received January 11, 1960).

The decay of Y^{91} was studied using NaI(Tl) scintillation counters and a 4π beta-ray scintillation spectrometer. A single gamma ray with a measured energy of 1.208 ± 0.010 Mev was observed. The shape and end-point energy of the weak ($\sim 0.3\%$) beta group in coincidence with the 1.208-Mev gamma ray was measured. The end-point energy was determined to be 0.319 ± 0.010 Mev. The experimental shape factor is clearly in disagreement with that predicted for a once-forbidden unique transition, $\Delta I = 2$ (yes). The 0.319-Mev beta spectrum yields a shape factor which may, within experimental accuracy, be interpreted as a statistical shape. These measurements yield a Y^{91} - Zr^{91} mass difference of 1.527 ± 0.014 Mev.

LEVELS IN Bi^{210} FROM THE $Bi^{209}(d,p)$ REACTION. G. B. Holm,* J. R. Burwell,† and D. W. Miller, Department of Physics, Indiana University, Bloomington, Indiana (Received December 21, 1959).

Q values and differential cross sections have been measured for nuclear states in Bi^{210} excited by the $Bi^{209}(d,p)$ reaction. A previously unobserved group with $Q = 2.35 \pm 0.03$ Mev has been found, corresponding to a state with probable proton-neutron assignment $(h_{9/2}g_{9/2})$. The observed Q value for this state is in good agreement with the Q value expected for the 1- ground state of RaE. Groups of states with mean excitation of 0.41, 0.88, and 1.4, 2.02, 2.56, 2.81, 3.15, and 4.03 Mev have been found, and neutron assignments of $g_{9/2}$, $i_{11/2}$, $d_{5/2}$, $s_{1/2}$, $g_{7/2}$, $d_{3/2}$, and $h_{11/2}$ have been suggested. A comparison with theoretical calculations by Newby and Konopinski for the $(h_{9/2}g_{9/2})$ group of states gives further support to their observation that a calculation of levels in the neighborhood of Pb^{208} is far less accurate when the extra-core interaction type is proton-neutron than when it is neutron-neutron or proton-proton.

*On leave from the Nobel Institute of Physics, Stockholm, Sweden.

†Now at the University of Oklahoma, Norman, Oklahoma.

$(p,p'\gamma)$ ANGULAR CORRELATIONS AT LOW ENERGY. H. J. Hausman, G. F. Dell, and H. F. Bowsher, Department of Physics, The Ohio State University, Columbus, Ohio (Received December 4, 1959).

At an incident proton bombarding energy of 6.5 Mev, angular correlations have been measured between protons scattered inelastically from various even-even nuclei and the decay gamma rays from the first excited states of these nuclei. Among the angular correlation experiments reported are $C^{12}(p,p'\gamma)$ 4.4 Mev, $Ne^{20}(p,p'\gamma)$ 1.63 Mev, $Si^{28}(p,p'\gamma)$ 1.78 Mev, and $S^{32}(p,p'\gamma)$ 2.25 Mev, which were done for proton detector angles of 60°, 90°, and 120°. The measured angular correlation functions are all of the form $A + B[\sin^2 2(\theta_\gamma - \theta_0)]$, where θ_0 is the axis of symmetry. None of the symmetry directions agreed with predictions of the simple direct-reaction theories. However, the symmetry directions for the correlation functions changed with proton detector angle for the experiments on C^{12}, Ne^{20}, and S^{32}; for the experiment on Si^{28} the angular correlation functions were symmetric about 90°, independent of proton detector angle. The results of the angular correlation experiments appear to be consistent with a collective interaction involved in these direct-type reactions rather than a nucleon-nucleon type collision at the nuclear surface.

SYSTEMATICS OF NEUTRON SEPARATION ENERGIES. K. N. Geller, J. Halpern, and E. G. Muirhead,* Physics Department, University of Pennsylvania, Philadelphia, Pennsylvania (Received December 14, 1959).

Photoneutron thresholds for 73 isotopes have been measured by radioactivity and neutron detection methods using a 25-Mev betatron. The neutron separation energies inferred from the observed thresholds are in general agreement with the values predicted from mass data and reaction energies. Several discrepancies are observed between threshold and neutron binding energies where ground-state transitions require a spin change $\geq 7/2$. For these nuclei, the threshold energies are consistent with neutron emission leaving the residual nucleus in an excited state.

*Permanent address: University of Melbourne, Melbourne, Australia.

ANALYSIS OF (d,t) PICK-UP REACTIONS. Amélia Império Hamburger, Sarah Mellon Scaife Radiation Laboratory, University of Pittsburgh, Pittsburgh, Pennsylvania (Received December 10, 1959).

A comparison is made between (p,d) [or (d,p)] and (d,t) pick-up reactions involving transitions between the same nuclear levels. Eleven cases are studied, having transfer orbital angular momentum $l = 0$, 1 or 2, for nuclei from Li^6 to Mg^{25} (also Sn^{117}), and for incident energies of the order of 15 Mev. It is found that if the differential cross sections of the corresponding (d,p) and (d,t) reactions are plotted as functions of momentum transfer the curves differ by a factor independent of angle. This property holds primarily in the region of the first peak of the angular distribution. Towards larger angles the curves differ in shape. Because of the

proportionality between the curves in the forward direction, it is possible to obtain an expression for extracting the stripping reduced width of (d,t) reactions. This reduced width corresponds to the reduced width of the same transition when studied by a (d,p) process. No emphasis is placed on the interpretation of the results in terms of the structure of the triton.

An attempt is made to determine the triton momentum transform directly from an analysis of the $d+d \rightarrow p+t$ experiments, considering these as stripping reactions. It was not possible to apply the curves thus obtained to the (d,t) reactions in the heavier nuclei.

The experiment $F^{19}(d,t)F^{18}$ ground state was performed with 14.8-Mev deuterons, for angles θ_{lab} between 5° and 45°. The results extend the information about transitions with $l=0$.

ENERGY SPECTRA AND ANGULAR DISTRIBUTION OF PHOTONEUTRONS FROM CARBON. V. Emma, C. Milone, and A. Rubbino, Istituto di Fisica dell' Universitâ, Centro Siciliano di Fisica Nucleare, Catania, Italy (Received January 5, 1960).

Energy spectra and angular distribution of photoneutrons from carbon are studied by irradiation with a 30-Mev bremsstrahlung beam. The spectra exhibit a fine structure from which the following levels in C^{12} may be distinguished: 21.4, 22.2, 22.9, 23.6, (24.3), 24.8, and 25.6 Mev. Many of these coincide with levels found in the $C^{12}(\gamma,p)$ and $C^{12}(\gamma,3\alpha)$ reactions.

Photoneutron emission occurs predominantly by transition to the ground state of C^{11}.

The angular distribution is of the form $1+1.5\sin^2\theta$ for all neutrons having energy $E_n > 3$ Mev. This distribution agrees with that expected according to Wilkinson's independent-particle model for ejection from the $l=1$ orbit.

DEPENDENCE OF THE In^{116} ACTIVATION RATIO ON NEUTRON ENERGY. Fahri Domanic* and Vance L. Sailor, Brookhaven National Laboratory, Upton, New York (Received December 4, 1959).

Indium was irradiated with monochromatic neutrons of various energies, and a measurement was made of the ratio of the 54-minute to the 13-second activities of In^{116} produced by neutron capture in In^{115}. Such a ratio expresses the relative probability for populating the ground state or the isomeric state from the initial compound state. The irradiations were made with monochromatic neutrons from a crystal spectrometer at the resonance energies 1.456 ev and 3.86 ev, in regions between resonances at 0.1 and 2.66 ev, and with "pile neutrons." The results show that the activation ratio differs for the two resonances by a factor of approximately 3.5, with relatively more of the 13-second activity being associated with the 3.86-ev resonance. The half-lives of the two In^{116} activities were redetermined and the values 13.4 ± 0.4 seconds and 53.9 ± 0.2 minutes were obtained.

*On leave from the University of Ankara, Ankara, Turkey.

LOW-ENERGY PHOTODISINTEGRATION OF H^3 AND He^3 AND NEUTRON-DEUTERON SCATTERING. L. M. Delves,* Clarendon Laboratory, Oxford, England (Received December 11, 1959; revised manuscript received January 4, 1960).

The cross sections for electric dipole photodisintegration of H^3 and He^3 at low energies are expressed in terms of the effective range parameters of the doublet n-d scattering matrix. Agreement with the experimental results is possible for either set of n-d scattering lengths.

*Now at Massachusetts Institute of Technology, Laboratory for Nuclear Science, Cambridge, Massachusetts.

TOTAL GAMMA ABSORPTION IN C^{12}, N^{14}, O^{16}, AND Al^{27} AT 20 Mev. E. E. Carroll, Jr.* and W. E. Stephens, Department of Physics, University of Pennsylvania, Philadelphia, Pennsylvania (Received December 21, 1959).

Total gamma absorption cross sections were measured of C^{12} from 20.0 to 21.2 Mev, and of N^{14}, O^{16}, and Al^{27} from 20.0 to 20.5 Mev using monochromatic gamma rays. A direct absorption technique was used, utilizing $T^3(p,\gamma)He^4$ photons, varied in energy by changing the energy of the incident protons. The C^{12} cross section showed structure with possible resonances at 20.15 Mev, 20.46 Mev, and 20.92 Mev, with integrated cross sections of 1.1, 1.0, and 6.6 Mev millibarns, respectively. O^{16} showed a sharply rising cross section suggesting a strong resonance above about 20.3 Mev. The cross

sections of N^{14} and Al^{27} were smooth over the energy interval investigated.

*Now with the Westinghouse Electric Corporation, Bettis Atomic Power Laboratory, Pittsburgh, Pennsylvania.

PION PRODUCTION BY PIONS. Walton A. Perkins, III, John C. Caris, Robert W. Kenney, and Victor Perez-Mendez, Lawrence Radiation Laboratory, University of California, Berkeley, California (Received October 7, 1959).

A liquid hydrogen target was bombarded by negative pions of energies 260, 317, 371, and 427 Mev. Positive pions from the reaction $\pi^- + p \rightarrow \pi^+ + \pi^- + n$ were detected by the use of a counter telescope, that selected the π^+ by its characteristic $\pi - \mu$ decay. With the 260-Mev beam, π^+ mesons were counted at 90° in the laboratory system. At 317, 371, and 427 Mev, the differential cross section was measured for π^+ mesons emitted at 60°, 90°, 125°, and 160° in the center-of-mass system. The angular distributions are nearly isotropic at 317 and 371 Mev but are peaked forward at 427 Mev. The total cross sections are 0.14 ± 0.10 mb at 260 Mev, 0.71 ± 0.17 mb at 317 Mev, 1.93 ± 0.37 mb at 371 Mev, and 3.36 ± 0.74 mb at 427 Mev. These results indicate a much larger cross section than the theoretical prediction based on the static model. Reasonable agreement can be obtained by the inclusion of a pion-pion interaction in the production mechanism.

INTERACTIONS OF FAST μ MESONS IN LEAD WITH SMALL-ENERGY TRANSFER. J. de Pagter* and R. D. Sard, Department of Physics, Washington University, St. Louis, Missouri (Received September 25, 1959).

With the Pb target material divided into 1.27-cm slabs between hodoscoped Geiger tubes and surmounted by a magnet cloud chamber, a study has been made of the interactions of fast μ mesons in which at least one evaporation neutron is produced and no additional charged particles emerge from the slab. The cross section-average neutron multiplicity, $\sigma\bar{m}$, is $(15.2 \pm 2.1) \times 10^{-29}$ cm^2 per nucleon. From hodoscope observations without neutron coincidence it is found that for an electron-initiated shower to stay concealed in a 1.27-cm Pb plate its energy must be less than about 100 Mev. With the help of "approximation B" track length theory and experimental photonuclear neutron yields, we calculate that hidden knock-on showers contribute $(5.8 \pm 1.2) \times 10^{-29}$ to the total $\sigma\bar{m}$, leaving $(9.4 \pm 2.4) \times 10^{-29}$ cm^2 per nucleon as the result for the direct μ-meson nuclear interaction. This analysis is supported by the agreement between the number of visible showers observed and calculated. The neutron yield in the direct interaction is found to increase with μ-meson momentum. The Weizsäcker-Williams approximation is used to calculate the effect expected from the interaction between the electric charge of the μ meson and the nucleons. Within the rather large uncertainties involved in the use of this approximation, there is excellent agreement with the experimental results.

*Now at the Cambridge Electron Accelerator, Harvard University, Cambridge, Massachusetts.

HIGH-ENERGY NEUTRON BEAM OF 45% POLARIZATION. Douglas Miller and Russell K. Hobbie, Cyclotron Laboratory, Harvard University, Cambridge, Massachusetts (Received January 11, 1960).

A beam of polarized neutrons has been produced by allowing the 164-Mev internal proton beam of the Harvard synchrocyclotron to strike a beryllium target. The neutrons produced in the forward direction are then polarized by scattering from carbon at 15°. When neutrons of energy greater than 110 Mev are selected by the detection process, an average beam energy of 124 Mev results. An intensity of 2.9×10^5 neutrons/in.^{2} min through a 2-in. by 6-in. collimator has been obtained, with a polarization 0.447 ± 0.020. The shielding techniques are also discussed.

ELECTROMAGNETIC CORRECTIONS TO THE RATIO $\sigma(p+d \rightarrow H^3 + \pi^+)/\sigma(p+d \rightarrow He^3 + \pi^0)$. H. S. Köhler,* CERN, Geneva, Switzerland (Received December 11, 1959).

Electromagnetic corrections to the ratio between charged and uncharged pions produced along with either a triton or helium-3 from 600-Mev protons incident on deuterium have been estimated. It was found that the main correction

comes from the difference in triton and helium-3 wave functions. It was not found possible to correct unambiguously for the effects of mass difference between charged and uncharged pions. An enhancement of around 10% of positive pions was obtained with an estimated uncertainty of ±3%. The result agrees with experiments at CERN.

*Now at Laboratory of Nuclear Studies, Cornell University, Ithaca, New York.

ANTIPROTON INTERACTIONS IN HYDROGEN AND CARBON BELOW 200 Mev. Lewis E. Agnew, Jr.,* Tom Elioff, William B. Fowler,† Richard L. Lander, Wilson M. Powell, Emilio Segrè, Herbert M. Steiner, Howard S. White, Clyde Wiegand, and Tom Ypsilantis, Lawrence Radiation Laboratory, University of California, Berkeley, California (Received December 18, 1959).

About 500 antiprotons in a partially purified antiproton beam have been observed to enter the 30-in. propane bubble chamber. An arrangement of counters identified the antiproton events, thus reducing scanning to a minimum and also providing a sample of antiprotons free of scanning bias. The antiprotons entered the propane at a kinetic energy of 220 Mev and were brought to rest. Scattering and annihilation interactions in both hydrogen and carbon have been observed as a function of antiproton energy. Differential scattering cross sections have been obtained, and the following total cross sections have been measured for antiproton kinetic energies, T, in the ranges 75 to 137.5 Mev and 137.5 to 200 Mev:

Interaction	Cross section, σ (mb) $75 \leq T \leq 137.5$	$137.5 \leq T \leq 200$
$(\bar{p}$-$p)$ elastic	66 ± 17	56 ± 14
$(\bar{p}$-$p)$ annihilation	112 ± 23	60 ± 18
$(\bar{p}$-C) elastic [5 deg (lab) cutoff]	345 ± 60	255 ± 45
$(\bar{p}$-C) annihilation	474 ± 76	360 ± 65

The above results show satisfactory agreement with the Ball-Chew theory where comparison can be made.

The details of the annihilation process in hydrogen and carbon have been observed. One feature of the experiment is that, in contrast to previous studies of annihilation products, we are able to make a direct observation of the neutral pions through pair production by π^0 decay photons. The significant results for carbon and hydrogen annihilations at an average antiproton kinetic energy $\cong$100 Mev are:

Annihilation product	Hydrogen annihilations Multiplicity	Hydrogen annihilations Average total energy (Mev)	Carbon annihilations Multiplicity	Carbon annihilations Average total energy (Mev)
π^-	1.53 ± 0.08	402 ± 21	1.58 ± 0.07	366 ± 13
π^+	1.53 ± 0.08	379 ± 19	1.33 ± 0.08	371 ± 13
π^0	1.60 ± 0.50	356 ± 110	1.15 ± 0.30	342 ± 90

In addition to the above-listed annihilation products, the carbon stars contained nucleons that carried off more than 188 Mev per star. When pion absorption is considered, the carbon result of 4.1 ± 0.3 pions per annihilation is consistent with the observed hydrogen multiplicity of 4.7 ± 0.5 pions. Pion energy spectra and frequency distributions, as well as other details, have been obtained.

Seventeen strange particles have been identified among the products of all the annihilations. This indicates that the production of a pair of K mesons occurs in (4.0 ± 1.0)% of all annihilations. The average total energy per K pair is greater than 1200 Mev.

The charge-exchange process $\bar{p} + p \rightarrow \bar{n} + n$ has been observed and, based on six possible events, we obtain the result $\lambda \geq 630$ g/cm^2 for the mean free path in propane ($50 \leq T_{\bar{p}} \leq 150$ Mev).

*Now at Los Alamos Scientific Laboratory, Los Alamos, New Mexico.

†Now at Brookhaven National Laboratory, Upton, New York.

COMPLETE DETERMINATION OF POLARIZATION FOR A HIGH-ENERGY DEUTERON BEAM. Janice Button, Lawrence Radiation Laboratory, Berkeley, California, and Ronald Mermod, CERN, Geneva, Switzerland (Received December 2, 1959).

Double-scattering measurements have been made which yielded all parameters necessary to describe completely the interaction of the deuteron with complex nuclei. Deuterons of 410 and 420 Mev were scattered from beryllium and carbon, respectively. Tensor components of polarization, which should appear in the scattering of spin-1 particles and which were unobservable at low energies, were determined to be appreciably different from zero. The usual vector spin polarization normal to the plane of scattering was found to reach a maximum of about 70%. The impulse approximation was employed to obtain estimates of deuteron cross section and polarization on the basis of nucleon scattering data.

ANGULAR MOMENTUM EXPANSIONS IN RELATIVISTIC FIELD THEORY. Robert Lee Warnock,* Harvard University, Cambridge, Massachusetts (Received October 30, 1959).

As a step toward more general applications of angular momentum expansions in quantum field theory, the expansion of the scattering matrix is examined in the case of scattering of spin 0 by spin $\frac{1}{2}$ particles. The matrix is represented in terms of its eigenvalues and eigenvectors, the latter being eigenstates of total angular momentum. Using eigenstates of helicity to simplify the discussion, the eigenvectors may sometimes be obtained from the conservation laws alone. The eigenvalues are computed only to second order in a Yukawa interaction, but the results are more useful than the usual second order matrix elements. Since angular momentum expansions lead effectively to solutions of operator equations, the expressions derived facilitate the relativistic application of Heitler's unitary approximation (with an exact solution of the equation relating the transition operator T and the Hermitian reaction operator K) or the determinantal method of Schwinger and Baker.

*Present address: Department of Physics, Boston University, Boston, Massachusetts.

PION PRODUCTION IN MUON-NUCLEON COLLISIONS. G. von Gehlen,* Instituto di Fisica dell'Università di Roma, Rome, Italy (Received November 2, 1959).

A relation between the differential cross sections for certain angles and energies of inelastic electron scattering and inelastic muon scattering is given. The asymmetry of the pion production by longitudinal polarized muons has been calculated using Fubini-Nambu-Wataghin matrix elements.

*On leave of absence from University of Marburg/Lahn, Germany.

QUANTIZED MESON FIELD IN A CLASSICAL GRAVITATIONAL FIELD. Tsutomu Imamura,* Department of Physics, University of North Carolina, Chapel Hill, North Carolina (Received January 4, 1960).

The behavior of a quantized meson field in a classical gravitational field is examined. Physical quantities such as the expectation value for the number of created mesons are represented in terms of a formal Green's function. They are computed explicitly for the case of a special space-independent gravitational field. The inadequacy of standard iteration procedures is discussed in an Appendix.

*On leave of absence from Osaka University, Osaka, Japan.

ANALYTICITY PROPERTIES OF PRODUCTION AMPLITUDES. R. Ascoli* and A. Minguzzi, CERN, Geneva, Switzerland (Received December 28, 1959).

We study the analytic properties of production amplitudes as functions of the momentum transfer Δ^2 between one of the incoming particles and one of the outgoing particles, when the total energy and the three further parameters determining the relative motion of the three outgoing particles in the center-of-mass system are held fixed. We find that suitable combinations of the amplitudes are analytic functions of Δ^2 regular within an ellipse in the Δ^2 plane. It is also shown that in the same domain the cross section $\partial^2\sigma/\partial\Delta^2\partial w^2$ is an analytic and regular function of Δ^2, w^2 being the total mass of two of the outgoing particles. The poles in Δ^2 con-